POLITECNICO DI MILANO

SCHOOL OF CIVIL, ENVIRONMENTAL AND LAND PLANNING ENGINEERING

Master of Science in Environmental and Land Planning Engineering

POLITECNICO
MILANO 1863

ASSESSING CLIMATE CHANGE IMPACT ON ALPINE HYDROPOWER: A CASE STUDY IN THE ITALIAN ALPS

Supervisor:
Prof. Andrea Castelletti

Co-supervisor:
Ing. Federico Giudici

Master Graduation Thesis by:
Rachele TARANTOLA
Student id 820478

Accademic Year 2016/2017

Milano, 3 October 2017

This thesis experience has taught me much, both on scientific and human aspect.

First of I would like to thank my supervisor, Professor Andrea Castelletti, who stimulated my interest in water resources management and gave me the occasion to deepen it. Moreover, he gave me the opportunity to develop part of my thesis in a stimulating environment like ETH in Zurich and supported my thesis with his valuable advices.

I would sincerely like to thank Federico Giudici for his incessant motivation, enthusiasm, frankness and his constant help and encouragement during difficult times. His presence has been precious in the last months and this work would have not been possible without his help.

I am grateful to Professor Paolo Burlando, who hosted me in Zurich at ETH, giving me the opportunity to get in touch with his brilliant research group. In particular, I would like to thank Daniela Anghileri, who supported me during my visit. It was a pleasure to work with her and she taught me much.

Besides the scientific aspects of the work, the support of my parents and friends has been fundamental in achieve this important goal. I particularly thank my parents, my brother, my granny and my uncles for their unconditional trust, support and love.

I'm thankful to the friends who shared with me the university experience: Federica, Benedetta, Erik, Alice and the many brilliant people I met in the last years. A particular thank to Giulia, who has always been there with the right world and Marianna for the time spent together.

Finally, I would express a loving thank to Alessandro, who shared with me this long journey and has always been close to me with his love and sensibility.

TABLE OF CONTENTS

LIST OF FIGURES

LIST OF TABLES

ACRONYMS

AC	Adaptive capacity
ADA	Adapted policy
AR5	Fifth Assessment Report
ARPA	Agenzia Regionale per la Protezione Ambientale
BAU	Business As Usual
BP	Benchmark Policy
Cdf	Cumulative distribution fuction
CORDEX	COordinated Regional climate Downscaling EXperiment
DDP	Deterministic Dynamic Programming
DMI	Danish Meteorological Institute
DP	Dynamic Programming
GCM	Global Circulation Model
GHG	Green-House Gases
GME	Gestore del Mercato Energetico
IS	Improvement space
IPCC	Intergovernmental Panel of Climate Change
KNMI	Koninklijk Nederland Meteorologish Instituut
PUN	Prezzo Unico Nazionale
QM	Quantile Mapping
RCM	Regional Climate Model
RCP	Radiative Concentration Pathway
SD	Statistical Downscaling
SDP	Stochastic Dynamic Programming

SMHI	Swedish Meteorological and Hydrological Institute
SRES	Special Report on Emission Scenarios
TE	Topkapi-ETH

ABSTRACT

Climate change is severely altering the Alpine environment. Temperature rising and extreme precipitation events are deeply affecting the hydrological regime, reducing water availability and altering inflow seasonality. Moreover, reduced snowfall and warmer climate are accelerating glaciers retreat, causing the permanent loss of the main freshwater source in the Alps. Alpine hydropower systems are operated based upon hydrologic and socio-economic conditions and are thus vulnerable to climate changes. The central role of hydropower as key flexible and renewable source in the energy market is urging the scientific community to search for mitigation measures. The need for adaptation of hydropower operations to future changing conditions requires the generation of realistic information that hydropower decision maker may include in policy design, regarding the future hydrological regimes and long-term impact on catchment components. In this thesis, we assess climate change impact on the Alpine hydropower, focusing on a case study in the Italian Alps. We carry out the assessment on the real case study of Cancano-San Giacomo hydropower system, located in Adda river basin. We apply the traditional, top-down climate change impact study approach, known in the literature as "scenario-based" approach. Local climate change projections are derived from high-resolution EURO-CORDEX scenarios using statistical downscaling technique. Local climate projections are then employed to feed Topkapi-ETH model, a distributed physically based hydrological model that is used to reproduce the Adda river basin response to climate change. This model allows monitoring multiple outputs, both distributed maps and point specific time series, concerning different hydrology aspects. Topkapi-ETH simulations provide us inflow projections and ice pack maps and runoff. Inflow time series are used to assess the historical and future impact of climate change on the hydropower. More precisely, we first evaluate the vulnerability of historical operating policy to new inflow conditions. We then assess the adaptive capacity of the operating policy including inflow projections in policy design. The advantages are estimated by evaluating the enhancement in reservoir operation comparing adaptive policies performances to historical operating policy.

RIASSUNTO

Il cambiamento climatico sta gravemente alterando l'ambiente alpino. Il regime idrologico risente dell'aumento delle temperature e dell'intensificazione degli eventi piovosi estremi, che influiscono sulla disponibilità d'acqua e sulla stagionalità degli afflussi. La riduzione delle precipitazioni nevose e un clima generalmente più caldo accelerano inoltre il ritiro dei ghiacciai, causando la perdita permanente di una delle principali riserve di acqua dolce delle Alpi. I sistemi idroelettrici situati nelle Alpi operano seguendo driver idrologici e socio-economici e sono quindi vulnerabili al cambiamento climatico. L'idroelettrico costituisce una delle principali fonti di energia rinnovabile e la sua flessibilità gli conferisce un ruolo centrale nel mercato energetico: queste considerazioni stimolano la ricerca di misure di mitigazione del cambiamento climatico. La necessità di adattare le politiche di gestione a questi cambiamenti richiede la generazione di informazioni realistiche riguardo il regime idrologico futuro e gli impatti a lungo termine sulle componenti del bacino idrografico. Queste informazioni possono essere interessanti per il gestore idroelettrico e possono essere incluse nel processo di ottimizzazione delle politiche. In questa tesi si valuta l'impatto del cambiamento climatico sull'ambiente alpino e sui sistemi idroelettrici, ponendo l'attenzione agli effetti sulle riserve idriche naturali permanenti presenti nel bacino e alla capacità di adattamento al cambiamento climatico dell'idroelettrico. Analizziamo il caso di studio reale del sistema idroelettrico di A2A, situato nel bacino del Lago di Como nelle Alpi italiane, impiegando l'approccio classico per gli studi d'impatto noto come "scenario-based". Le proiezioni climatiche a scala locale sono generate partendo dagli scenari EURO-CORDEX ad alta risoluzione applicando un downscaling statistico. Le proiezioni climatiche locali sono utilizzate nelle simulazioni di Topkapi-ETH, un modello distribuito fisicamente basato che riproduce la risposta del bacino del lago di Como al cambiamento climatico. Questo modello consente di ottenere diversi output riguardo svariati aspetti dell'idrologia, sia in forma di mappe che di serie temporali. Le simulazioni di Topkapi-ETH forniscono le proiezioni dell'afflusso al serbatoio nel futuro oltre che le mappe di spessore e le serie di deflusso dei ghiacciai. Le serie di afflusso sono utilizzate per modellizzare le operazioni del serbatoio nel contesto storico e nella valutazione degli impatti futuri del cambiamento climatico. Più precisamente, in primo luogo si valuta la vulnerabilità della politica storica alle nuove condizioni di afflusso. In un secondo momento, si valuta la capacità di adattamento della

politica del sistema idroelettrico, includendo le proiezioni future di afflusso nell'ottimizzazione della politica. Il vantaggio dovuto all'informazione d'afflusso futuro viene quantificato valutando il miglioramento delle prestazioni del sistema gestito con le politiche adattative rispetto alle prestazioni della politica storica.

1
INTRODUCTION

1.1 SETTING THE CONTEXT

Climate change is a phenomenon that has been taking place along all the 20th century. According to McCarthy et al. [2001] "Most of the observed warming over the last 50 years is likely to have been due to the increase in greenhouse gas concentrations. […] Human activities [...] are modifying the concentration of atmospheric constituents [...] that absorb or scatter radiant energy." Earth radiation energy accumulates in the oceans and in the atmosphere, causing rising temperatures and extreme precipitation events intensification, which significantly affect natural and human environments. In the recent years scientific community started to show interest in this topic, producing a wide variety of studies to quantify climate change magnitude in terms of main drivers and climatic variables variations and impacts on environment and human activities. In order to monitor the phenomenon the Intergovernmental Panel of Climate Change (IPCC), an international body for assessing the science related to climate change, was instituted. Its scope is "to provide policymakers with regular assessments of the scientific basis of climate change, its impacts and future risks, and options for adaptation and mitigation." [Moss et al., 2008]

The main results of these studies are collected in the Fifth Assessment Report (AR5) and show that climate change affects significantly the entire hydrological cycle. A considerable rise in average temperature has been detected during the 20th century [Hartmann et al., 2013] and is likely to proceed also in the 21st. Moreover, temperature changes are expected to be uneven all over the world: larger warming will occur over land compared to oceans and will be more marked in boreal hemisphere [Collins et al., 2013]. Elevate average temperature causes glacier shrinkage [Kaser et al., 2010], determining

ultimately a sea mean level rise [Marzeion et al., 2012]. Although precipitation average pattern is consistent with temperature ones [Collins et al. 2013], Frei et al. [2006] reports of growth of precipitation extremes in different areas of the globe. Several studies showed that the intensification of heavy precipitation events could occur even in regions that are undergoing to mean precipitation decrease [Katz and Acero, 1994]. Other extreme events, such as floods, droughts, heat wave and hurricanes, were investigated as a reliable climate change indicator [Katz and Brown, 1992]. Although this topic is still under debate, climate change may also cause an intensification of precipitation both in frequency and magnitude increasing inland flood risk [Bindoff et al., 2013, Gao et al., 2006]. In the meanwhile, subtropical dry climates are experiencing severe droughts that will intensify in 21st century, leading to increase displacement of people [Pachauri et al., 2014]. Climate change is also modifying natural environments: Parmesan and Yohe [2003] study on biosphere reveals that ranges of plants and animals are moving in response to recent changes in climate. Allen et al. [2010] research highlights that "increases in the frequency, duration, and/or severity of drought and heat stress associated with climate change could fundamentally alter the composition, structure, and biogeography of forests in many regions".

Giorgi [2006] recognized some regions more sensitive to climate change: among them the Mediterranean region and the Alps. Alpine regions regimes are likely to be affected more then others since they are characterized by a high presence of snow and glaciers and are more sensitive to climate conditions [Zierl and Bugmann, 2005; Beniston, 2003]. In temperate Alpine climate, the hydrological regime is mostly snow-melt dominated and relies on glacier reserves and abundant winter snowing: snow accumulates on the glaciers during the winter and melt in spring constituting the main water contribution to rivers runoff [Huss 2011; Barontini et al., 2009] Main precipitation events mostly concentrate in spring and autumn, while summers are dry. Temperature rising is strongly altering water cycle: temperature at high elevations have increased up to 2°C since 1900, three times the observed global-average in 20th century warming [Beniston, 2003] determining an anticipation of the melting season and decrease in snow cover [Gobiet et al., 2014; Beniston, 2012; Beniston et al., 2011]. High temperature also undermines general ice sheet equilibrium, accelerating glacier retreat [Haeberli and Beniston, 1998] and glaciers are expected to lose form 50% to 90% of their volume in the 21st century [Beniston et al., 2012]. Severe reductions are also affecting precipitation regimes. Alps have been described as the "Water tower of Europe" by Mountain Agenda

in 1998 because Alpine water runoff contributes twice as much to the four major European rivers runoff [Huss, 2011].

During the last century, Alpine territory has been exploited for hydropower purposes. Hydropower is the fist source of clean energy worldwide. It was estimated 20% of the energy produced originate from hydropower [Castelletti et al., 2008] and regulated dams intercept more than 20% of the waters, globally [Giuliani et al., 2016]. Thanks to its flexibility, hydropower storage plays a key role in the integration of intermittent renewable energy sources in the energy network [Schaefli, 2015; Gaudard et al., 2014a].

Hydropower uses water force to produce energy and is thus sensitive to water availability. The modifications of the hydrological regime could impact also on these energy production systems.

Various hydropower system configurations exhibit different weakness [Schaefli, 2015]. Run-of-the-river power plants use natural or diverted water flow to produce energy, exploiting low hydraulic heads. Any change in river flow regime, especially in extreme droughts and decreasing average flow conditions, will have immediate impacts on this power plants. These systems consist of a regulated reservoir, built by barring a stream with a dam, and one or more power plants hydraulically connected to the reservoir. Water released from the reservoir is conveyed to the power plant, where is used to move the turbine and produced energy. After that, water is released to the river without volume losses. Storage power plant move large volumes of water in space and time: they collect catchment runoff in the reservoir during the snow-melting season to release to produce energy when it is more convenient. Water availability and energy prices mainly influence the operational rule of the reservoir. In Alpine environment, the moments of accumulation and exploitation of the resource are out-of-phase on yearly basis, as energy production is shifted to winter when energy demand is high, while reservoir inflow is abundant in spring. The impact of climate change on the water cycle is likely to affect the hydropower systems, mostly in regions largely relying on natural storage as glacier and snowpack. Glacier shrinkage and snow precipitation reduction will lower water availability threatening hydropower interest [Diolaiuti et al., 2012; Huss, 2011]. Van Vliet et al. [2016] estimated 61-74% of worldwide hydropower would experience reduction in power system capacity due to global warming.

1.2 OBJECTIVE OF THE THESIS

The objective of the thesis is to assess the impact of climate change on future hydrology and on hydropower in a power plant in the Italian Alps. As Schaefli [2015] remarks, impact studies need to be case specific, because they refer to peculiar hydrological, technical and socio-economic conditions. We carry out the analysis on the real case study of A2A power system, an Alpine storage hydropower system in the upper Adda river basin in the Italian Alps. We want to answer the main questions:

- How will local Alpine climate change in the hydropower system catchment during the 21st century?
- How will the historical operating rule of the hydropower system behave in a changed climate?
- In case of worsening, can we improve power system operations, adapting management rules to new inflow conditions? What's the value of the new inflow information?

We follow the top-down workflow classically adopted in climate change impact studies. The first stage is the analysis of climate change scenarios, which refers to the EURO-CORDEX project and to the IPCC Fifth Assessment Report. High resolution projections of air temperature, precipitation and cloud cover transmissivity are first downscale to reproduce site-specific climatic features, then fed into the hydrological model of the catchment Topkapi-ETH. We first evaluate the impact of these drivers on the hydrological regime simulating the inflow to the reservoir in future conditions with. Moreover, we exploit the distributed physically based model potential to understand the most relevant changes which the catchment components might undergo in climate change, focusing in particular on glaciers retrain.

We then move to the hydropower system characterization, first modeling the main features of the operating rule of the reservoir under historical inflows and prices. We then force the hydropower historical operating rule with future inflows to assess the impact that climate change could have on the system; in this thesis prices are supposed to remain unchanged in future condition to focus on hydrological impact. This experiment highlights the vulnerability of the power system to climate change. These impacts have already been explored in literature [Maran et al., 2014; Beniston et al., 2011; Gaudard et al., 2014b; Barontini et al., 2009; Schaefli et al., 2007; Alfieri et al., 2006].

A second objective of the thesis is to highlight the fundamental role of hydrological forecasts under future conditions. In a changing context, forecast information, such as inflow, can enhance system operations [Anghileri, 2014; Pianosi and Soncini-Sessa, 2009; Georgakakos and Graham, 2008], both in close and far future. Historical operating rule is designed for a specific hydrological regime and can't adapt when the system deviates from that hydrological conditions. Instead, enlarging the information sets considering inflow forecast in operating rule design, hydropower system may become more adaptive and reliable to future climate [Denaro et al., 2017; Culley et al., 2016; Castelletti et al., 2008; Hobbs et al., 1997]. In other words, the use of new forecast information can improve reservoir operation in future context, adapting the operational rule to climate change. Through operating rules comparison, we can measure the value of the forecast, i.e., how useful forecasts are from the point of view of the decision making process. Adaptive capacity of reservoir power system has been only partially explored in literature. Most of the studies approach compares "no-forecast" situations, usually associated to historical operations, to "perfect forecast" conditions, in which complete information is considered in the operative rule [Anghileri, 2014]. We start from this approach, comparing the historical operational rule (no-forecast) to inflow complete information operational rule, in present and future. The second situation is unrealistic, since the decision-maker might likely know only partial information: in literature, several studies consider this option by degrading perfect inflow information. Instead, we include more realistic inflow scenarios, produced with the hydrological model in the design of operative rule adapted to future conditions. The comparison between adapted rules and historical one in future context allows estimating the value of the information.

1.3 THESIS' STRUCTURE

The thesis is organized as following: in Chapter 2 explain the methodology and precise further the scope of the thesis; we also provide a wide description of the tools we employ in the following. In Chapter 3 the case study on upper Adda river basin and A2A power system is presented. In Chapter 4 and 5 we focus on the implementation and validation of the tools described in Chapter 2: in Chapter 4 we focus on climate change scenarios of the meteorological variables and inflows projection production; in Chapter 5

the implementation of the model of reservoir operations is explained. In Chapter 6 we comment the results concerning climate change in the Alps first and the impacts of climate change on the hydropower system. Eventually, Chapter 7 summarizes the path of this study, the main findings, its limitations and further research opportunities.

2
METHODOLOGY AND TOOLS

Hydropower systems have been proved to be vulnerable to climate change. Storage power plants shift production capacity in space and time, accumulating water in the reservoir, which is then released to produce energy when the situation is more convenient. Reservoir release is defined on according to socio economic drivers (energy demand, energy prices), natural drivers (inflow forecast, glaciers' dynamics) and operational and normative constraints (min/max production, minimum environmental flow). High inflow season and high prices periods occur out of phase on yearly basis: water coming from snow-melting is stored in spring, when prices and demand are low, to use it for energy production in winter, when natural inflow would be low but energy and prices demand are

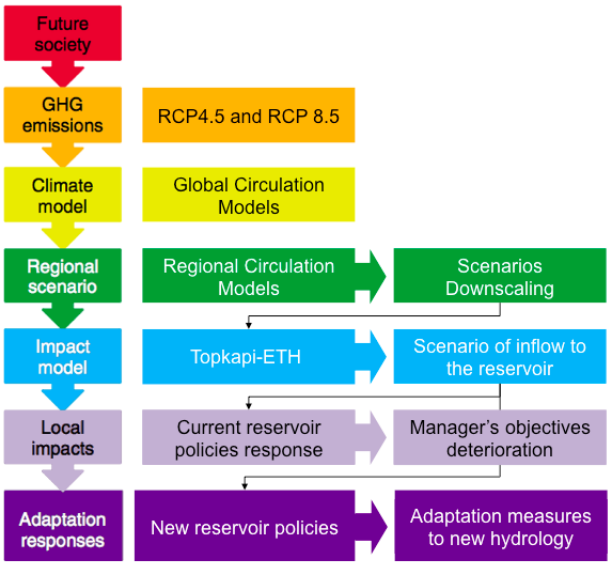

Fig. 2.1 *– Top-down approach framework. On the left: framework of the top-down approach according to [Wilby et Dessay 2010]; on the right: flow chart that will be followed in the thesis.*

at peak. In Alpine region inflows are highly influenced by precipitation and temperatures, which trends are changing due to global warming. As already explained, we follow a top-down approach [Wilby and Dessai, 2010], which moving from global scale to local scale "follows a step-wise approach and quantifies indicators of physical vulnerability based on scenarios of future socio-economic change that are used as inputs to a series of hierarchical models." [Dessai et al., 2004]. Figure 2.1 illustrates its principal phases.

Future society's impact scenarios are used to compute green house gases (GHGs) emission scenarios, which in their turn are fed into climate models to produce global climate change scenarios of the main climatic variables. The scenarios are refined simulating climatic models on the regional scale. We enter the framework at this level ("Scenarios downscaling" box in figure 2.1): we further refine climatic scenario spatial scale and assess their hydrological impact using a hydrological model. We then move to local impact to the object of our research: the storage hydropower system. We assess the historical operational rule response to climate change and we search for adaptation measures for the hydropower system changing the reservoir operational rule.

The framework is further specified in figure 2.2. The figure shows two main working areas: the quantification of the climate change scenarios and the computation of the operating optimal policy for the hydropower system. The quantification of climate change is essentially the estimations of future inflow to the reservoir. We start from high-resolution global scale scenarios of the main meteorological variables, which are provided by EURO-CORDEX project. We downscale the scenario to adapt the scenarios to our case study scale, in order to better describe site-specific phenomena and further enhance spatial resolution. We need a hydrological model of the catchment to reproduce its response to climate change. We use exploit the potential of a physically based spatially distributed model that allows exploring the impacts of climate change on different components of the catchment. Feeding the hydrological model with meteorological variables scenarios we obtain inflow projections that will be used in the next phase. Beside the impact on future inflows, we focus on glacier dynamics. Glaciers retreat is a phenomenon widely accepted in the scientific community. They constitute a key permanent source of freshwater and the evaluation of their volume could be important information for hydropower decision makers, both in present and future.

In the policy design phase, represented in purple box in figure 2.2, we produce a model to describe reservoir operation. We suppose a rational decision-maker, who decides

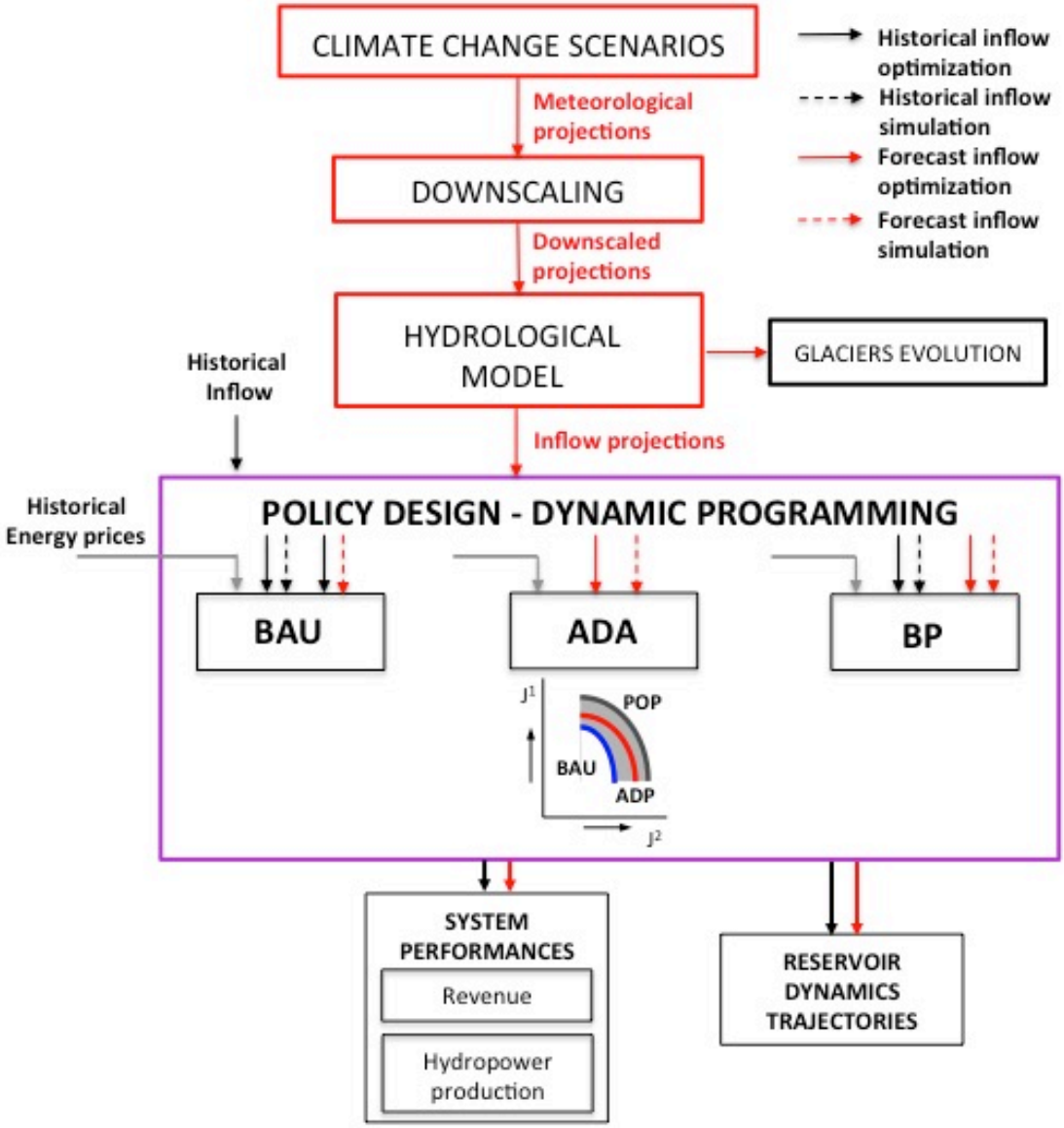

Fig. 2.2 – *The framework adopted in this study. In the red boxes, top-down approach is adopted to quantify climate change in the Alpine environment. Starting from high-resolution meteorological variables scenarios at global scale, we downscale the scenarios to introduce local scale effects that are not described by global climate models. We simulate the hydrological model of the catchment with the climate change scenarios, obtaining projected inflow to the reservoir and glacier thickness and discharge data to monitor their evolution. In purple box, management policies of the reservoir are designed. We design the operating rule of the reservoir in historical conditions (BAU), the operating policies adapted to future inflow condition (ADA) and two benchmark policies, which represent present and future perfect knowledge of the inflow (BP). The performances of the operating policies are evaluated in terms of HP production and revenue from electricity sale. The policies for the systems are computed and compared in present conditions (black arrows) and under future scenarios (red arrows).*

the release from the reservoir at each time-step to maximize his own objectives, regulates the reservoir. In our case, we suppose the decision-maker wants to maximize energy production and the revenue from energy selling: these will also be the indicators with which we can evaluate hydropower system performances. As already explained, the main drivers that force decision-maker decision are water availability and energy prices, but in this thesis we focus only on the hydrological aspect, neglecting energy prices future changes.

Since we consider two objectives for the decision-maker, we set up a Multi-Objective decision problem. In designing policy, the inflow can be characterized in stochastic manner: we suppose the inflow probability density function at each time-step is estimated before taking the decision. This reproduces decision-maker uncertainty towards inflow in a realistic way, and for this reason in this thesis we refer to this policy's class as "operating policies". Further detail on this topic will be given in the dedicated 2.2 section. We use recorded inflow time-series (black solid arrows in figure 2.2) in designing the historical operating policy, called Business As Usual (BAU) now on, since it reproduces the main features of the currently operating rule of the hydropower system. We evaluate historical performances, in terms of revenue and energy productions, feeding BAU policy with observed inflow time-series (black dashed arrows in figure 2.2). We then simulate BAU policy with inflow projections obtained in the previous phase. The comparison between historical and future performances of the BAU allows assessing policy vulnerability to climate change. The daily trajectories of storage and release, which we will also call generically "reservoir dynamics", are computed and compared as well to detail the reason of the performances differences.

In order enhance the hydropower system operations, we introduce inflow projections in policy optimization (red solid arrow in figure 2.1). We thus design operating policies for the reservoir adapted to climate change that will be referred ADA so on. ADA policies are simulated with future inflow compared to BAU policy under climate change conditions (red dashed arrows). This comparison highlights how much advantage the operating policy can take from including the inflow forecasts in the decision making process, thus defining the "adaptive capacity" of the BAU policy.

The operating policies are also compared to Benchmark Policy (BP), both in historical and future conditions. BP policies are computed supposing that the inflow at each time-step is known before taking the decision. These policies constitute an upper bound to BAU adaptive capacity because they represent the best optimal policy that can be

designed for that system representation. The space individuated by non-adaptive BAU policy and the BP policy is the "space of improvement" of the BAU policy.

In order to perform the experiments described we need three main tools: the climate change scenarios, the hydrological model and the model of reservoir operations. They are described in the following sections.

2.1 CLIMATE CHANGE SCENARIOS

Climate change scenarios quantify global warming phenomena and play a central role in impact assessment studies, because they are necessary to quantify future water availability to the reservoir.

Moving from future society's projections in terms of anthropic pressure, economic trends and technology development, Green-House Gases (GHG) emissions are computed. The Representative Concentration Pathways (RCPs) are Green House Gases concentration trajectories introduced by the IPCC [AR5, 2014]. They describe possible climate futures in term of radiative forcing values relative to the pre-industrial period. Radiative forcing is defined as cumulative measure of human emissions of GHGs from all sources expressed in Watts/m^2. The new RCP scenarios describe future changes in balance between incoming and outgoing radiation to the atmosphere, caused by GHGs that compose it. RCPs substitute the Special Report on Emission Scenarios (SRES) projections published in 2000, used in IPCC Third Assessment Report and Fourth Assessment Report. The new scenarios, rather than using storylines of GHGs concentrations linked to unique assumptions about patterns of economic and demographic growth, use radiative forcing trajectories, which may result from a combinations of different demographic, economic and technology future conditions. In principle infinite RCPs scenarios can be produced with this assumption, and a selection process was necessary. The IPCC Working Group III used these criteria in 2007 to identify four main RCPs (figure 2.3). The four RCPs (RCP2.6, RCP4.5, RCP6, RCP8.5) are named after the radiative forcing values relative to pre-industrial values (+2.6, +4.5, +6.0 and +8.5 W/m2) they reach at the end of the century. Since climatic models require data on concentrations of GHGs in the atmosphere, the research community coupled each RCP to a specific GHGs emission scenario. This step was needed to make RCPs suitable for climate modeling and comparable with the old SRES scenarios (see table 2.1).

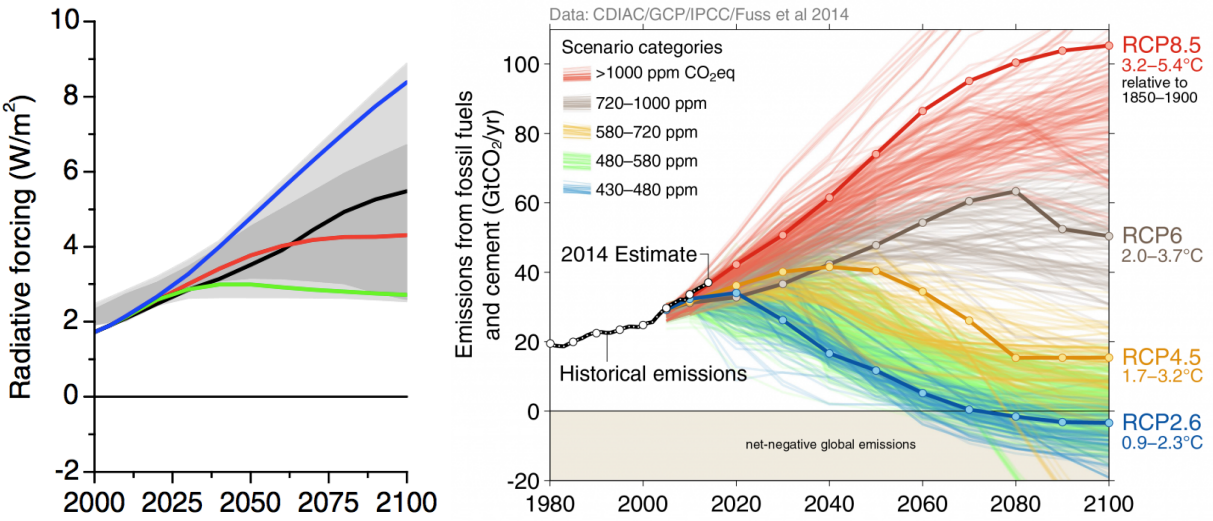

Fig. 2.3 *– On the left radiative forcing trends relative to pre industrial levels. Grey area indicates the 98th and 90th percentiles (light/dark grey) of the literature [Van Vuuren et al., 2011]; on the right, emissions scenarios associated with RCPs according to IPCC AR5 [Fuss et al., 2014]*

Tab. 2.1 *– RCPs features resume table*

	Radiative forcing [W/m²]	**Corresponding SRES**	**Pathway by 2100**	**Reference bibliography**
RCP 2.6	2.6	–	Decline	Van Vuuren et al., 2006, 2007a;
RCP 4.5	4.5	B1	Stabilization	Clarke et al. 2007; Smith and Wigley 2006; Wise et al. 2009;
RCP 6	6	B2	Stabilization	Fujino et al. 2006; Hijioka et al. 2008;
RCP 8.5	8.5	A1F1	Rise	Riahi et al. 2011, 2007;

RCPs are adopted as input to Global Circulation Models (GCMs) to obtain meteorological variables scenarios at global scale for the 21st century. GCMs are mechanistic, spatially distributed models describing the phenomena that take place in the atmosphere. Since their first appearance in 1956, GCM description was enriched with models of the oceans, cryosphere, land surface composition and elevation and anthropic pressure (figure 2.4). GCMs are defined over a broad 3D grid in space, which varies from a model to another, and hourly time resolution (figure 2.5). Starting from measured boundary condition, climatic variables of interest such as temperature, pressure and precipitation are computed in each cell of the grid at each time-step. The uncertainty due

to system complexity requires a frequent update of the boundary conditions to obtain accurate forecasts.

A GCM can provide reliable prediction information on scales of about 100km grid. The coarse resolution of GCMs makes it impossible to use GCMs output for a direct analysis of the impacts. The results need to be downscaled at a finer grid. There are various and complementary techniques of downscaling, mainly grouped in two families: dynamical downscaling and statistical downscaling. Dynamical downscaling techniques are performed nesting a Regional Climate Model (RCM) in a GCM (figure 2.6). Regional Climate Models have the same purpose and structure of GCMs. They work on a finer grid on a relatively small domain, allowing a more accurate description of orography, land use and small-scale phenomena.

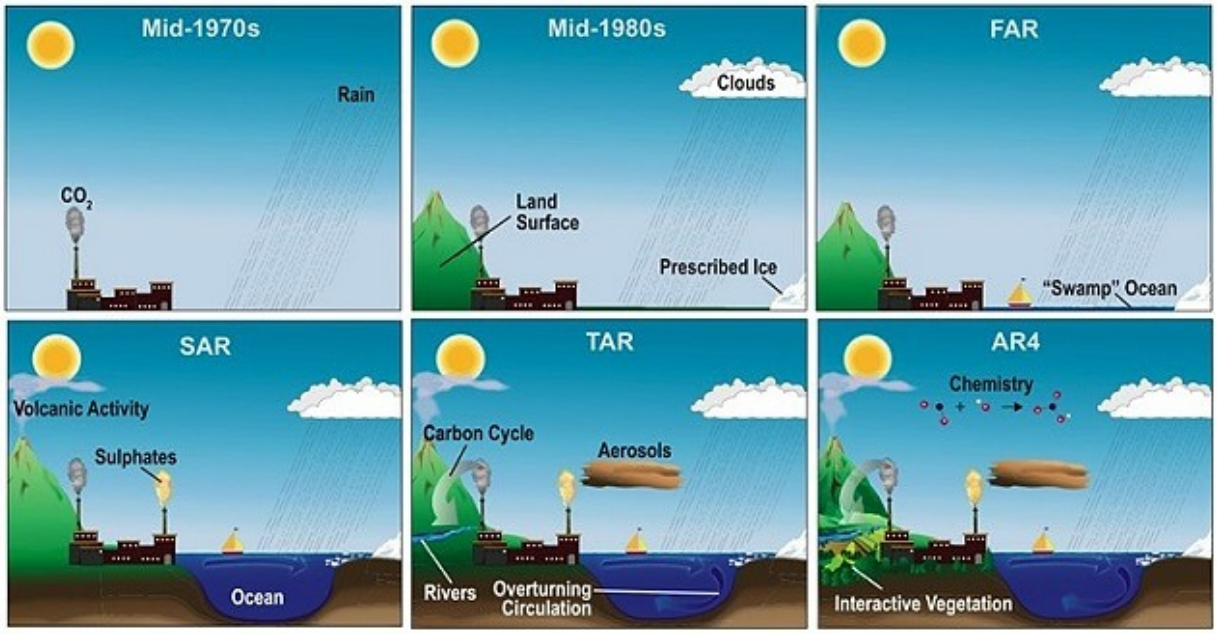

Fig. 2.4 *– Evolution of GCMs components description. Models grew more sophisticated over time, incorporating clouds, land surface features, ice, and other elements descriptions.*

For such reasons dynamical downscaling is more effective and particularly important where the landscape changes shape frequently (e.g. on the coastal line and in the mountains) where local phenomena are pronounced and more relevant than global ones. The outputs of the GCM serve as boundary condition to run the RCM. The output yielded

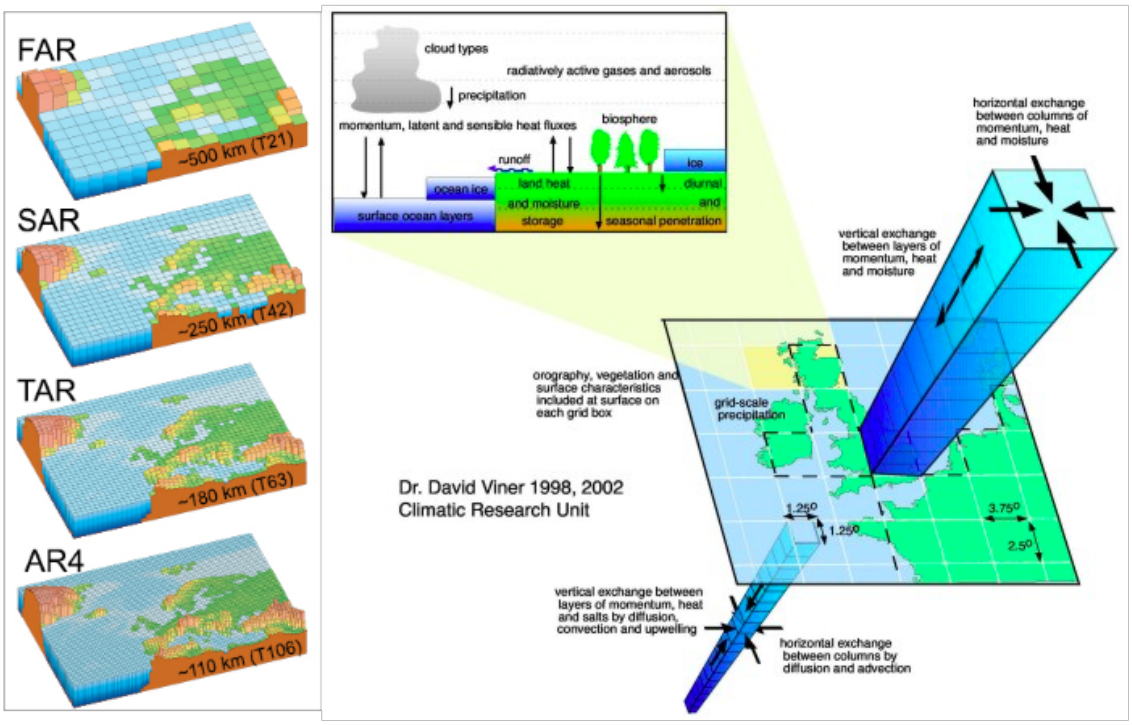

Fig. 2.5 *– On the left: approximated grid of a GCM; on the right GCM scheme – source: IPCC*

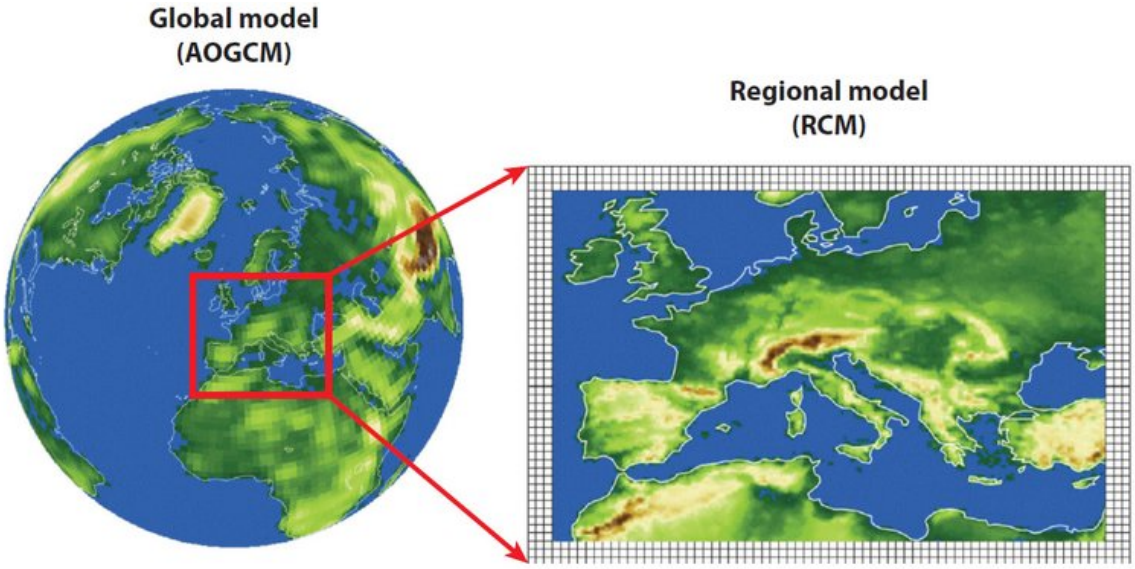

Fig. 2.6 *– Scheme of nesting RCM in GCM. RCM shows a finer grid than GCM and mountain regions and coastal shapes are well developed and characterized.*

by RCMs simulations are dynamically downscaled meteorological variables. RCMs typically employ a 25km resolution grid.

In this thesis we use EURO-CORDEX scenarios, which have been obtained as described. The flourishing on climate modeling in past decades was not followed by an equal number of studies on models reliability, limits and strengths. Coordinated Regional climate Downscaling Experiment (CORDEX) project was born to provide a unique and worldwide-recognized framework mainly focused on dynamical downscaling procedures and provides climate change scenarios for the 21st century [Giorgi et al., 2009]. The scenarios produced in European domain are grouped in the EURO-CORDEX project.

For our applications a further downscaling is required. Its scope is to achieve a further finer spatial resolution; moreover, EURO-CORDEX scenarios carry the biases both of the GCM and RCM model used in their computation, which more than other errors affect the result of the analysis [Chen C. et al., 2011; Chen J. et al., 2011]. Sharma et al. [2007] demonstrate a second statistical downscale can greatly enhance local scenarios quality. Statistical downscaling techniques are applied to dynamically downscaled scenarios provided by RCMs. They link the state of variables representing a large scale (GCM or RCM grid scale) predictors and the state of other variables at smaller scale, as for example the catchment scale (the predictands). A simple and effective statistical relation describes the nexus between predictors and predictands. Observation data are always required in order to estimate the statistical relation. Several types of statistical downscaling techniques have been proposed: delta change method [Hay et al., 2000], neural network [Olsson et al., 2001], analog method [Zorita and Von Storch, 1999], weather generator [Wilks and Wilby, 1999], and unbiasing method [Deque, 2007]. In the present study, we adopt Quantile Mapping [Boé et al., 2007], which will be described in detail in Chapter 4.

Statistical downscaling allows removing the biases originally present in GCMs output and gaining site-specific information. Predictors and predictands usually represent the same physical variable, but it is not strictly necessary, since the relation between them is merely mathematical. These techniques are also flexible and computationally inexpensive. The drawbacks are that the quality of the result is strongly dependent on the quality of the observation and the length of the available historical data [Boé et al., 2007]. Moreover, they rely on stationarity of the correction assumptions, which supposes that the estimated relation between predictor and predictands remains unchanged in time. This aspect will be further deepened in Chapter 4. The climatic scenarios we use in this thesis are presented in detail in Chapter 4 and analyzed in Chapter 6.

2.2 TOPKAPI-ETH

The impact of climate change on hydrological regime can be valued using a physically based model that accurately reproduces the hydrologic cycle. Topkapi-ETH is the hydrologic model adopted in the present work. Topkapi-ETH (Topographic Kinematic Approximation and Integration model) was originally developed by Todini and others [Liu and Todini, 2006; Ciarapica and Todini, 2002; Liu and Todini, 2002], then enhanced at the department of Hydrology and Water Resources Management, in the Institute of Environmental Engineering of the Federal Institute of Technology in Zurich.

This spatially distributed model presents a regular grid where the smallest computational element is the single grid cell. The main processes that are modeled in Topkapi-ETH are shown in figure 2.7. Each grid cell receives water from up to three upstream cells and provides water to a single downstream cell. The model vertical discretization of belowground consists of three layers. The deepest layer is implemented as a linear reservoir to reproduce the behavior of slow components such as fractured or porous rock aquifers, while the first two layers, implemented as non-linear reservoirs, represent deep and shallow soil. Topographic gradients connect the grid cells to the surface and to subsurface. The potential infiltration rate is calculated with an empirical formula and saturation excess or infiltration processes regulate the runoff.

The topographic effects on radiation (particularly significant in mountainous terrains) are regulated as described in Corripio [2003]. Priestly Taylor equation [Priestley and Taylor, 1972] regulates evapotranspiration and a monthly correction is applied to distinguish between different land uses. Snow and ice-melt are computed with an empirical temperature index model, which employs only shortwave radiation and air temperature [Pellicciotti et al., 2005; Carenzo et al., 2009]. Compared to other mechanistic hydrological models, Topkapi-ETH does not represent all the hydrological processes in a detailed and rigorous manner [Fatichi et al., 2013], but can reasonably be regarded as a compromise between hydrological process representation and computational time for large catchment. Moreover the latest upgrades of Hydrology and Water Resources Management department at ETH Zurich allow including some artificial infrastructures such as reservoirs, river diversions and water abstractions in the model setup. Topkapi-ETH must be fed with the values of air temperature, cloud cover transmissivity and precipitation for each grid cell at the temporal and spatial resolution selected for the model simulation. Further spatial inputs must be included in the model

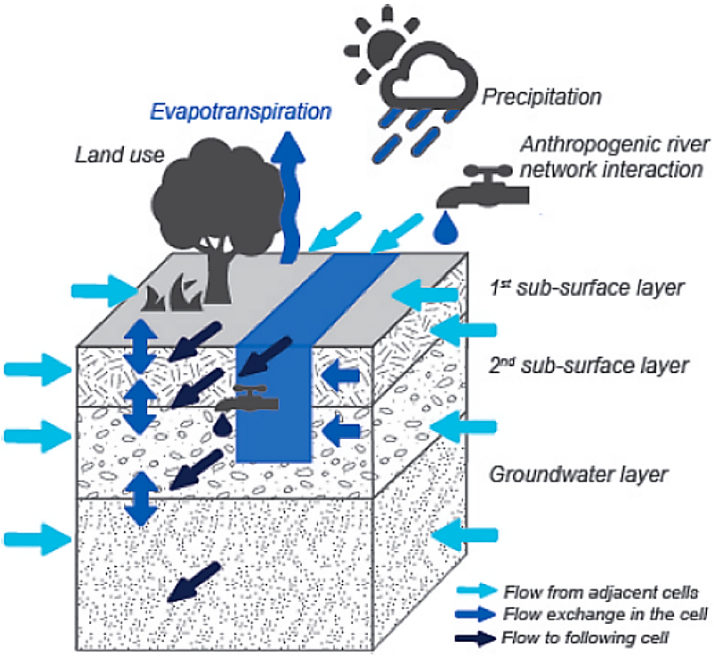

Fig. 2.7 - *Scheme of Topkapi-ETH structure at grid cell level.*

setup: a digital elevation map of the catchment, a soil map, a land use map, and a map of the glaciers. Several output time-series are available: water volume in upper subsurface layer, effective saturation in upper sub-surface layer, effective saturation in lower subsurface layer, effective saturation in groundwater aquifer, channel flow, flow in upper subsurface layer, flow in lower subsurface. Optional spatial outputs, such as precipitation, snow and ice cover, evapotranspiration and many others, are also available as average over the yearly period or in established time.

Topkapi-ETH purpose for this thesis is to compute the inflow scenario to the reservoir for 21st century when fed with the downscaled scenarios of meteorological variables. Moreover, thanks to its inner distributed nature, we can analyze in detail other key variable of the hydrological cycle and monitor the evolution of glaciers under climatic forcing. The results of TE simulations are shown and analyzed in Chapter 6.

2.3 RESERVOIR OPERATIONAL MODEL

The reservoir operational model we implement in this thesis is a normative model [Soncini-Sessa et al., 2007], which focuses on the decision-making problem as an optimization problem, renouncing to an accurate description of the physical system. : According to this category of models, the decision maker is represented as a rational agent

that wants to maximize one or more utility functions. Utility functions usually represent measurable criteria that the decision maker uses to rank different decisions/options.
The criteria we suppose the decision-maker follows are the maximization of the energy production and the maximization of the revenue by energy selling. Production is related to water availability only, while revenue is also linked to the price of energy. We thus suppose the only drivers that force decision-maker decision, are the energy price at the time of the decision and the inflow, which reflects the water availability. We thus set up a Multi-Objective optimization problem. We use Dynamic Programming (DP) algorithms [Soncini-Sessa et al., 2007] to solve the Multi-Objective problem.

Dynamic Programming can be used in a variety of problems with really broad conditions (step-cost and object separability, uncorrelation of the inflows), which are satisfied in our case, as explained in Chapter 5. Given the disturbances of the system as input (i.e. inflow and energy price), DP computes the optimal decision, the volume of water to release from the reservoir, at each time for the whole optimization horizon. The output of optimization is the reservoir optimal policy. The approach to uncertainty is a key feature in DP algorithms and will be exploited in the experiments of this thesis. Disturbances take place and vary continuously in time, but the model considers them to be discrete in time. Their value is settled at the end of the time-step they refer, while the decision has to be taken at the beginning of the time-step in order to manage the system. That's the intrinsic uncertainty associated to disturbances, from which this name comes from. In Deterministic Dynamic Programming (DDP) disturbances realization is supposed to be already known at the moment the decision is taken. We can optimize a DDP policy only knowing inflow time-series. This approach figures out an ideal experiment that is impossible to reproduce in reality, but establishes the best decision that could be taken using a fixed disturbances realization. In other words DDP constitute an upper limit to the performances of any other policy designed for that system and for this reason is used to design the Benchmark Policies (BP) we introduced at the beginning of the chapter. Stochastic Dynamic Programming (SDP) instead supposes that at the moment the decision is taken we only know a statistical representation of the disturbance, its probability density function. SDP policy can be most likely applied in reality, thus the operating policies (BAU and ADA) are computed with this algorithm. The policy designed with SDP algorithm is not designed for a specific disturbance realization, but for a specific statistical characterization of the inflow. SDP policies can thus absorb natural variability of the inflow and to a certain degree, even slight variations introduced by climate change. Further information about DP can be found in literature [Castelletti et al., 2010; Castelletti

et al., 2008; Soncini-Sessa et al., 2007; Nandalal and Bogardi, 2007]. The implementation of the hydropower system policies is explained in Chapter 5 while the results are commented in Chapter 6.

3
CASE STUDY

3.1 ADDA RIVER BASIN

Lake Como, also called by Latin Lario, is a natural lake with glacial origins located in the southern part of the Alps (figure 3.1). With a surface of 145 Km^2 and a volume of 23.4 km^3, it's the third largest Italian lake, following Lake Garda and Lake Maggiore, and

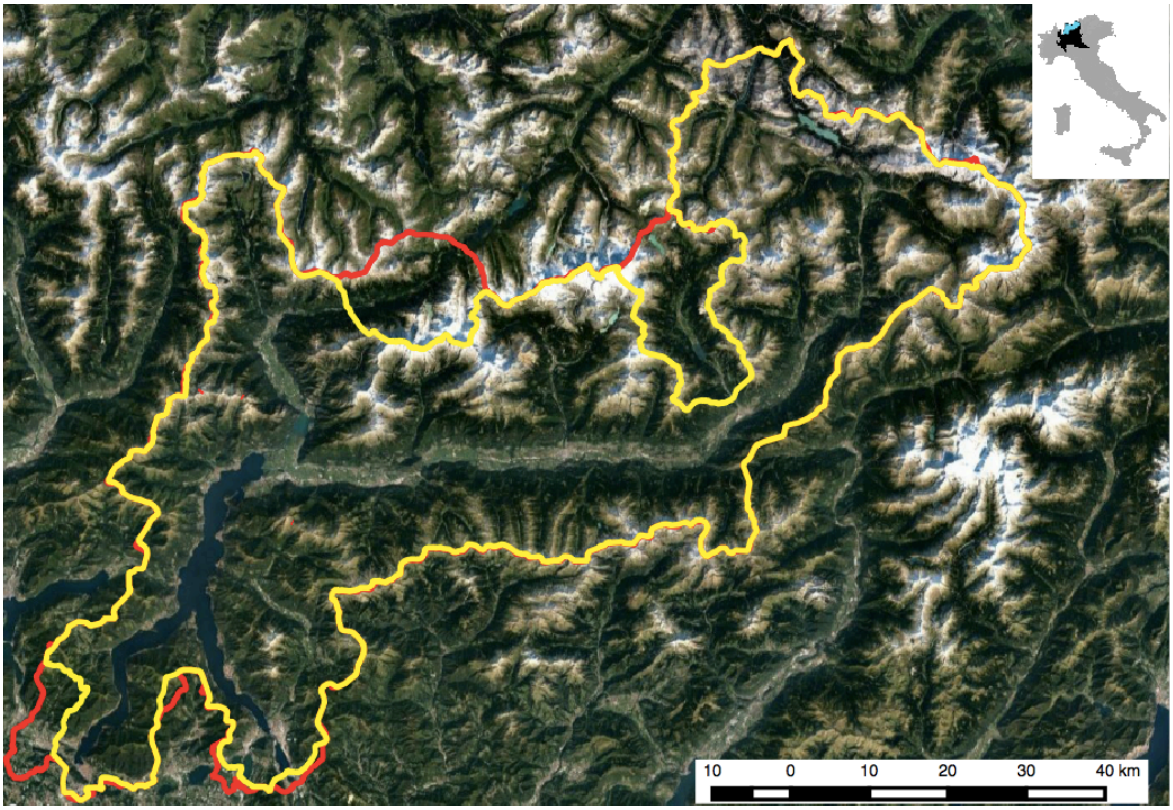

Fig. 3.1 *– Lake Como catchment. Italian territory is highlighted in yellow, Swiss territory in red.*

the first for perimeter length (about 185 Km). It's also the deepest Italian lake, with its 410m, and also one of the deepest in Europe. In the mountains upstream the lake, several torrential tributaries rise: Mera, Varrone, Pioverna and Adda are the main ones. Adda river in particular rises on Italian Alps at the border with Switzerland in the area of Bormio and flows trough Valtellina territory. It's major tributary of the lake, with an average discharge of 88 m^3/s at Fuentes, and its only emissary, which ultimately joins the Po River. Considering Olginate as closing section, the Lake Como catchment has an area of 4550 km^2, of which 2598 km^2 belong to upper Adda river basin closed at Fuentes. 90% of the catchment territory is Italian, while the remaining 10%, constituted by Val Bregaglia and Val Poschiavo, lays in Swiss territory.

Since the construction of the Olginate dam in 1946, Lake Como has been a regulated lake, with the main purpose of water supply for the numerous downstream agricultural districts and flood mitigation on the lakeshores.

The basin is characterized by a typical mixed snow-rain dominated typical, which shows two streamflow peaks in late spring and autumn due to snow-melting and precipitations respectively, and relatively low average streamflow in winter. Adda river basin is also highly glaciarized, with a cover of more than 88km^2 of ice sheets.

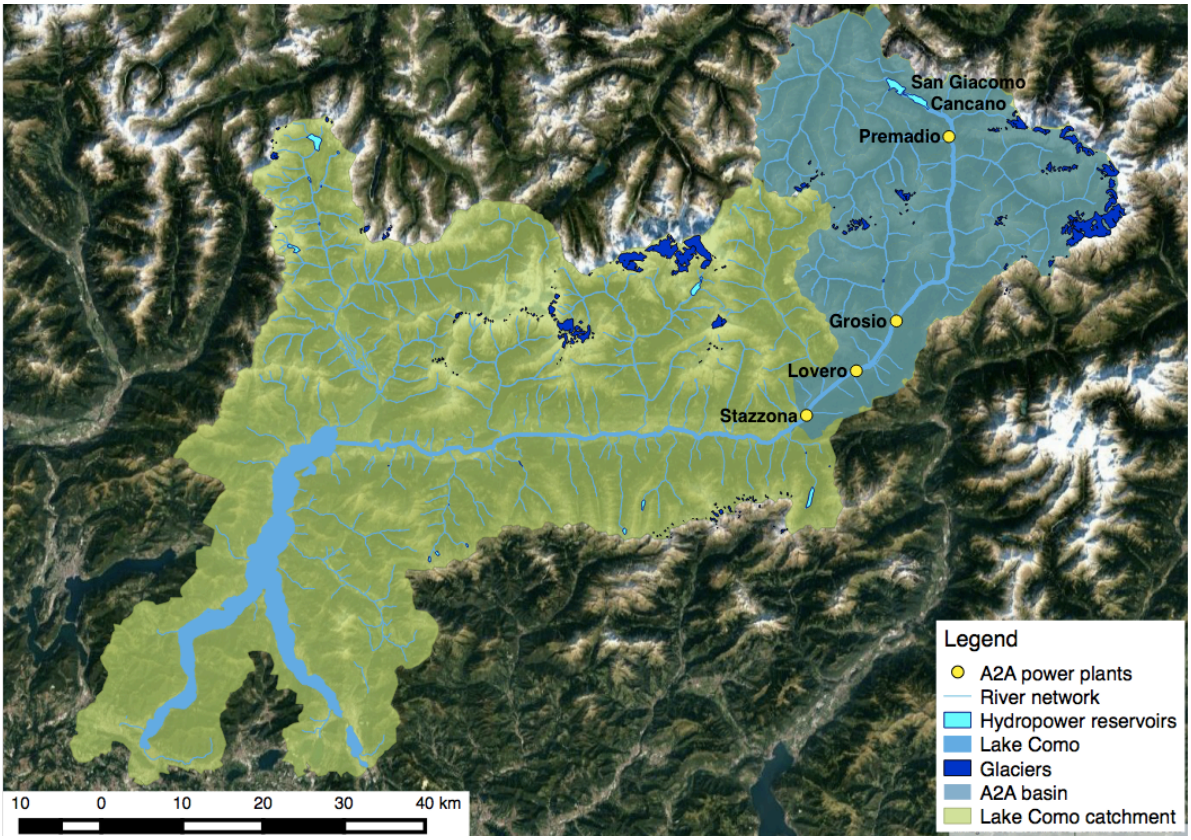

***Fig. 3.2** – Map of the main features of A2A system and Lake Como catchment.*

Since the 1920s, the upstream Adda river area has been exploited with the construction of many dams for hydropower production purposes (figure 3.2). Valtellina complex hydropower system counts 14 main reservoirs and 71 hydropower plants and is managed by four main energy companies: A2A, Enel, Edison and Edipower. The total storage capacity of the artificial reservoirs sums up to 545Mm^3, twice the operative volume of Lake Como (254Mm^3 [Denaro et al., 2017]). The presence of the reservoirs in Adda river basin largely affects the inflow regime: in spring, hydropower retains snowmelt water that would naturally flow to the lake and releases high water volume to produce energy in winter, when natural inflow to Lake Como would be naturally low.

3.2 A2A HYDROPOWER SYSTEM

A2A hydropower system is one of the most important in Valtellina, with an annual energy production of 1.7 TWh and 10 power plants. Its construction begun in the 40s to satisfy the electricity demand of Milano. The power network is fed by the two contiguous reservoirs, Cancano and San Giacomo (figure 3.3), located in Fraele valley, which collect the waters of several nearby basins through a massive diversion facility.

***Fig. 3.3** – Fraele valley with Cancano (on the back) and San Giacomo (in the front) reservoirs.*

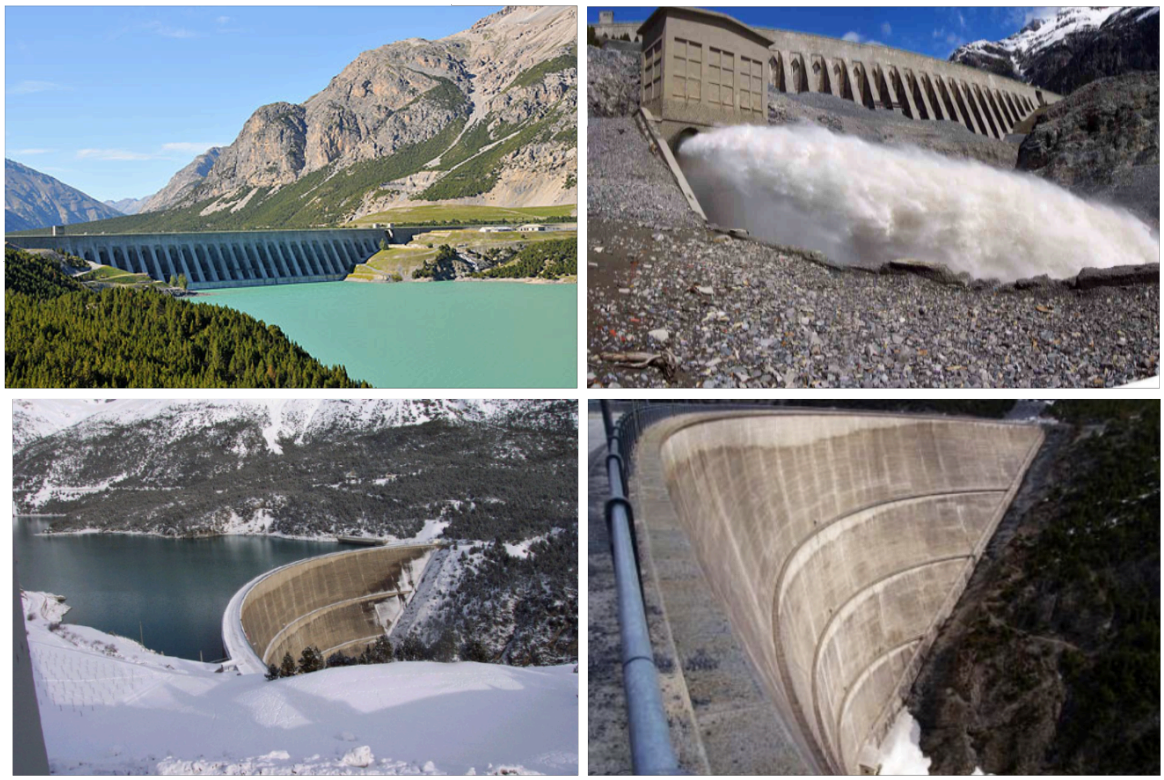

Fig. 3.4 – *San Giacomo dam (top) and Cancano dam (bottom)*

The higher reservoir, San Giacomo (top figure 3.4), was built in 1950 at 1951.5 m a.s.l. with a storage capacity of 64 Mm^3. It collects the waters diverted by the streams Gravia, Frodolfo, Alpe, Zebrù, Forcola, and Braulio, which rise in Forni glacier on the Cevedale-Ortis group, together with the first part of Adda river. From 1964, up to 90 Mm^3 per year are diverted into San Giacomo Lake from the River Spoel, which waters would naturally flow to Danube catchment.

Lake Cancano (figure 3.4 bottom) was built in 1956 below San Giacomo reservoir, at 1902 m a.s.l. with a maximum capacity of 123 Mm^3. It receives water directly from Lake San Giacomo and from the channel Viola. The catchment of the two reservoirs has an area of 36 Km^2, but considering the connected basins it goes up to 322.3 Km^2. The whole hydropower system covers an area of more than 1000 km^2, exploiting a 1800m hydraulic head and more than the 90% of the meteorological waters of upper Adda basin.

These two big artificial reservoir directly feed the power plant of Premadio, built in 1956, which has an installed capacity of 226 MW and a maximum penstock capacity of 41.06 m^3/s. Downstream of the power plant of Premadio, the run-of-the-river power plants of Grosio, Lovero and Stazzona are located in cascade (figure 3.5). The hydropower group constitutes the 90% of the installed capacity of A2A hydropower system. Grosio power

plant has an installed power capacity of 480 MW and is fed by the residual water of Premadio power plant, in addition to waters of Vallecetta, Massaniga, Vindrello, Eita and Sacco torrents. Lovero power plant has been in operations since 1948 with a maximum capacity of 49 MW and exploits mainly the residual waters of Grosio. Lastly, Stazzona power plant, the older, was put into operation in 1938, with an installed power of 30 MW.

Fig. 3.5 – *Scheme of A2A hydropower system in Alta Valtellina*

The waters from Lovero and from the Adda river feed the last plant. The power system is put into operation when prices are high and water availability can sustain production. Agenzia Regionale per la Protezione Ambientale (ARPA) Lombardia provides reservoirs cumulative storage and release historical data in 1975-2014 period. Net inflow time-series was derived by ARPA by inverting the mass balance of the reservoir, considering the storage as the sum of the reservoirs storages. The inflow data to the reservoir is considered to be the sum of all the diverted inflows to the single reservoirs.

Hourly energy price data referred to 2005-2014 period are provided by GME (Gestore del Mercato Energetico). As already mentioned, prices future variation are excluded from this thesis analysis in order to focus on the hydrological aspect of the assessment. For sake of completeness, an insight on energy price formation on the energy market and prices pattern is given in the next section.

3.2.1 Energy prices

Since 2004 the energy Italian market has been liberalized. The electricity prices are defined hourly at the energy exchange on the basis of operators' supply and demand. The market is managed by GME, the authority for electricity and gas spot trading in Italy. If there is no congestion related to maximum transmission limits of energy in the national grid the so-called PUN (Prezzo Unico Nazionale) represents the national energy price, otherwise the market is divided into zones where different prices are defined. The results of this market separation allow energy operators to compete in smaller areas.

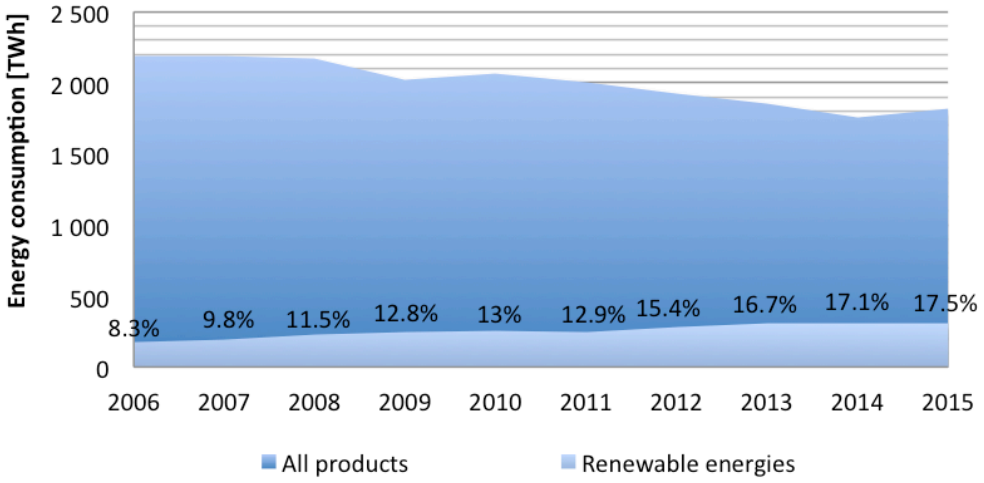

Fig. 3.6 *–Renewable resources growth in Italy in terms of gross inland consumption compared to all products energy consumption – source: European Commission*

Another important revolution in Italian market is due to renewable resources introduction. The adoption of the 20-20-20 EU Directive (Climate Action and Renewable Energy Package) in 2007 will ensure EU to meet its climate and energy target for the year 2020. The objectives of the plan are the reduction of the 20% of greenhouse gas emissions with respect to 1990 levels, 20% of total EU energy coming form renewable sources and the improvement of the power plants efficiency of the 20%. Renewable energy sources, mostly solar and wind power, have entered the market massively since 2009, as shown in fig 3.7. The rapid increase of renewable sources shares led Italy to meet and overcome its target of 17% of renewable sources production (fig. 3.6).

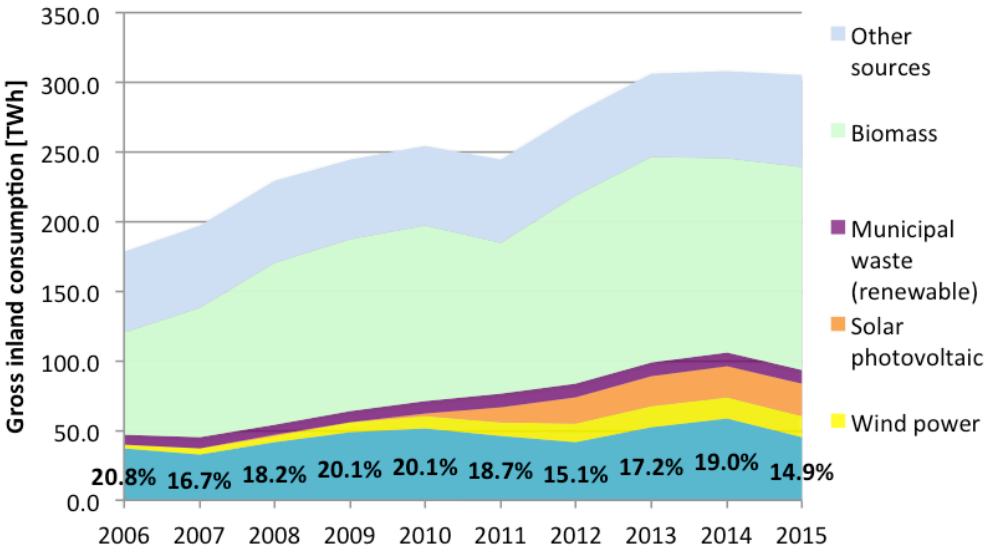

Fig. 3.7 *–Renewable source portfolio in term of consumption; in bold, the share of hydropower in percentage – source: European Commission*

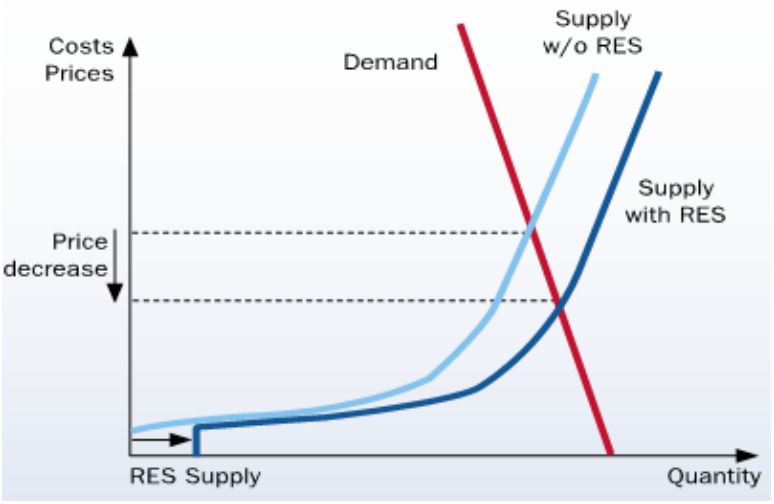

Fig. 3.8 *–Merit order effect diagram*

The mechanism of formation of the price is based on energy demand and supply. Supply curve is related to marginal production cost, which grows really slowly with the amount of energy produced for renewable energies. In fact, once the power plants are set, renewable energies have little marginal production cost. On the contrary, traditional energy technologies have a considerable marginal production cost, due to the cost of the fuel and the maintenance. Since supply curve on Italian market is organized according to marginal cost of the technologies, renewable sources, which have almost zeroed marginal costs of production, have a lower supply curve than traditional technologies. The total supply curve shifts down towards lower costs, thus meeting the demand curve at a lower market price. The overall effect of the massive renewable energy sources entry in the market is the reduction the energy price in the market: this phenomenon is known as merit order effect (figure 3.8) In order to better represent the merit order effect, prices used for policy design in the historical condition refer to 2009-2014 period, and thus inflow period is selected as well. This choice is also reasonable in future conditions because the contribution of renewable sources to the energy panel is likely to increase in future [Elleban et al., 2014]. Daily energy prices exhibit a great variability in several time intervals (figure 3.9 upper box). In the most productive periods for industries and services, energy demand increases and consequently the prices on the energy market. Three main periodical patterns can be found in the price series: a daily one, the alternation between weekdays and weekends and inter-annual variations. The bottom box in figure 3.9 shows prices weekly cycle: prices are generally higher during working days than in weekends and holidays, according to working schedule; in the same box the pattern on yearly basis shows high prices in winter and summer, which are respectively determined by working schedule and heating and by air conditioning, while prices lower significantly in spring. On daily basis the variation between daytime and nighttime is also marked, with peaks in energy demand at about 10 and 19 (figure 3.9, central box). All these trends will probably undergo to changes due to the variation of the energy mix, which will probably include increases in renewable sources shares, further lowering energy prices.

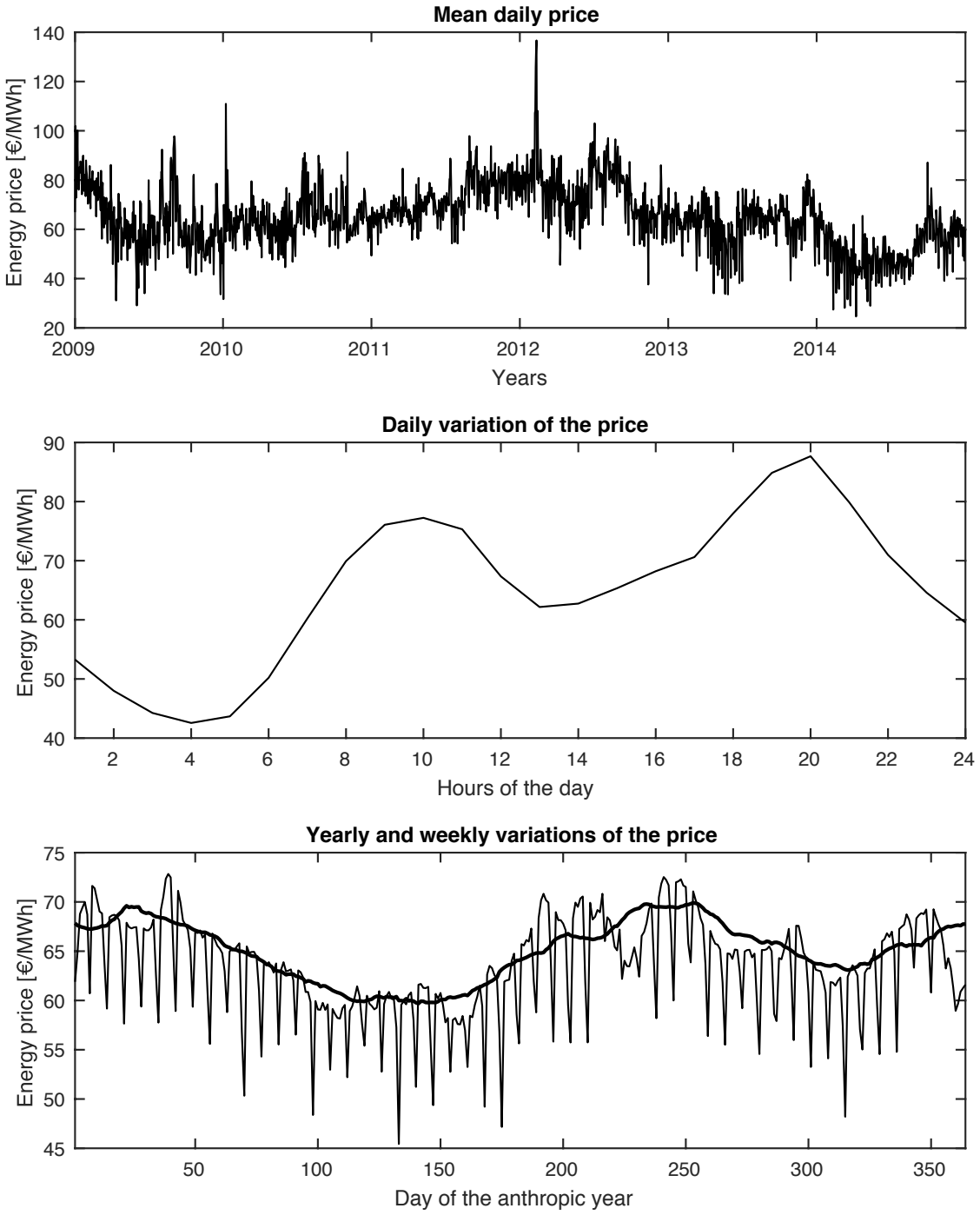

Fig. 3.9 – *Price time-series and periodical patterns. Mean daily price series in 2009-2014 is showed in the top panel. The central panels show the daily trend using an average on hourly basis, where price exhibit a day-night variation due to working time. Weekly and annual trends are shown in the third panel. Weekly cycle is well highlighted by the alternation of high prices during weekdays and low prices in the weekends, while in bold the annual trend, with winter and summer demand enhances, is displayed*

4

CLIMATE CHANGE SCENARIOS

Climate change information at local scale is necessary to estimate how climate change could impact on hydropower system and to develop suitable adaptation and mitigation strategies for the future. Future climate is expected to be warmer and with scarcer precipitation regimes. Higher temperatures are accelerating glacier melting and penalizing snow accumulation. Such changes will alter the hydrological regime as well, reducing water availability for the reservoir. Moreover, higher temperature will anticipate the timing of snow-melting, anticipating the peak of the hydrograph.

Temperature and precipitation daily projections provided by climatic models allow us simulating future water availability. Local temperature and precipitation projections adopted in the following work are derived by EURO-CORDEX scenarios. As already mentioned, CORDEX constitutes a worldwide recognized framework mainly focused on dynamical downscaling procedures, providing climate change scenarios for the 21st century. According to CORDEX framework, GCM are forced with RCPs and initial condition to evaluate global scenario for climate change in terms of interesting atmospheric variables. A nested RCM is used to downscale the projection to a finer scale, adapting it to regional specific conditions. The scenarios produced in European domain are grouped in the EURO-CORDEX project.

Within the EURO-CORDEX scenarios ensembles, only RCPs 4.5 and 8.5 driven were considered in the analysis. RCP4.5 was developed in the United States by the Joint Global Change Research Institute. In RCP 4.5, also referred to as “stabilization scenario”, radiative forcing is stabilized shortly after 2100 without reaching the peak during the 21st century [Van Vuuren, 2011; Thomson et al., 2011; Clarke et al., 2007] and the green

house gases emissions projections associated are diminishing after a peak in 2040. Emission mitigation policies may be imposed to meet scenario requirements. Scientific community believes this scenario will be the most likely to occur in future thus it's commonly adopted in literature to investigate the long-term response to stabilizing the radiative forcing. RCP8.5 was developed in Austria at the International Institute for Applied System Analysis. RCP 8.5 corresponds to a high greenhouse gas emissions pathway excluding any mitigation strategy adoption [Riahi et al., 2007]. Radiative forcing reaches 8.5 W/m^2 and its stabilization is expected after the end of the century, about at 12 W/m^2. RCP 8.5 is considered an upper bound for RCPs taken into account by IPCC and it's included in the analysis as the worst-case scenario. The projections are affected by "model configuration" uncertainties, which are associated to RCMs and GCMs imperfect descriptions of atmospheric phenomena. In order to filter uncertainty, three ensemble projections computed by different institutions are considered: Danish Meteorological Institute (DMI), Koninklijk Nederland Meteorologish Instituut (KNMI), Swedish Meteorological and Hydrological Institute (SMHI). In the table 4.1 the GCM-RCM combinations, considered in this thesis, are presented.

Tab. 4.1 *– GCM-RCM combination for the production of the scenarios used in the thesis*

Institute	Global Circulation Model	Regional Circulation Model
DMI	EC-EARTH	HIRHAM5
KNMI	HadGEM2-ES	ESRACMO22E
SMHI	CERFACS-CM5	RCA4

These scenarios are provided at a high spatial resolution of 12.5 Km (0.11 degree). The scenarios were chosen between the 22 considered in Culley et al. [2016], who analyzed the maximum operational adaptive capacity of Lake Como systems with respect to future hydro meteorological states. These scenarios have proven to provide good and robust adaptation scope for Lake Como performances both in close and middle term. They also exhibit different statistics that allow us to capture variability between the scenarios. The original European domain is cut over the region of interest, the Lake Como catchment. Each EURO-CORDEX scenario consists of a control period, a retrospective historical simulation fed with the meteorological variables in the period 1951-2005, and the proper projection in 2006-2100, both performed on daily basis.

Overall, our analysis considers six scenarios for each climatic variable, which will be named by variable, the institution and RCP used for the simulation (e.g. DMI4.5). The spatial resolution is still too coarse for the analysis of the impacts. Moreover, we need to remove GCM and RCM biases to enhance the quality of the local projections. We thus statistically downscale RCM scenarios to provide local projections for daily air temperature, precipitation and cloud cover transmissivity.

4.1 STATISTICAL DOWNSCALING

Murphy [1999] highlights that though dynamical and statistical downscaling approaches generate similar reproductions of current climate, they can differ significantly in their projections of future climate. Bias correction of the climate model output by statistical downscaling is needed to assure meaningful results in subsequent applications. Statistical downscaling (SD) techniques are based on the evidence that local climate is

conditioned both by large-scale circulation, described by GCM-RCM, and small scale characteristics, mainly represented by topography, land-use or land-sea contrast.

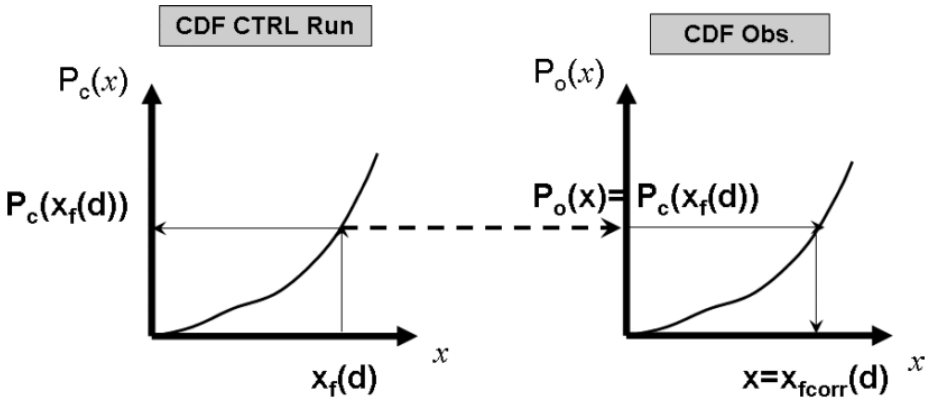

Fig. 4.1 - *Scheme of bias correction using QM. Cdf stands for empirical Cumulative Distribution Function. The subscript o, f, c stand for the historical observation, the climate scenario model output and the control simulation respectively. For the value $x_f(d)$ of the variable x in the day d in the climate scenario, the corresponding seasonal cumulative frequency $Pc(x_f(d))$ where $P(x) = P_r(X \leq x)$ is searched in the calculated cdf of the climate control simulation. After that, the value of x such as $P_o(x) = P_c(x_f(d))$ is searched on the cdf of the historical observations. This final value ($x_{fcorr}(d)$), is used as the corrected value of $x_f(d)$ - [Boé et al., 2007]*

The latter is not adequately described by RCMs, despite high resolutions. SD techniques establish some empirical relationship linking large-scale information (predictor) and local small-scale variables (predictand) in historical climate. The relation is then applied to the scenarios to derive the local climate projections. In order to perform SD we thus need three elements: the scenario, control period time-series and the observations of the local time-series.

The predictor is usually the same variable of the predictand, but in principle could be any variable physically linked to the predictand: we use the same variable scenarios provided by EURO-CORDEX.

Several types of statistical downscaling techniques have been proposed in literature: delta change method [Hay et al., 2000], neural network [Olsson et al., 2001], analog method [Zorita, 1999], weather generator [Wilks and Wilby, 1999], unbiasing method [Deque, 2007]. In this thesis, we applied quantile mapping (QM) technique. First introduced by Wood et al. [2004], QM technique uses a statistical transformation to find a correction function f between predictands and predictors. The method consists of two distinct phases:

- Calibration: a function f between observed data cumulative density function (cdf) (O) and control scenario cdf (C) is calibrated.

$$O = f'(C) \quad [4.1]$$

- Projection: the calibrated correction function f is applied to the scenario data (F). A linear interpolation is applied between two percentiles. We thus obtain the downscaled projection (F').

$$F' = f'(F) \quad [4.2]$$

QM was chosen as a computationally inexpensive, easy to implement and flexible method [Gudmundsson et al., 2012; Boé et al., 2007; Deque, 2007]. It allows removing the biases ordinarily present in GCMs output and gaining site-specific information. This method could also be applied both to annual and monthly period to better capture variability of the bias during the year. Since uncertainty linked to the periodicity is proven to be marginal compared to other sources (e.g. GCM uncertainty), in this thesis QM is applied only to the annual periodicity [Chen C. et al., 2011; Haerter et al., 2011].

The drawbacks of this method are that, as all the functional approaches, QM could undergo over fitting problems. Moreover, the quality of the result is strongly dependent on the quality of the observation and the length of the available historical data [Boé et al.,

2007]. If a forecast value exceeds the quantiles computed a constant correction equal to the 99th or 1st quantile is applied.

This might happen in climate change and could result in a not accurate description of extreme events. Gudmundsson et al. [2012] shows also that orographic effect rather limits the quality of the results in the downscaling. At last, QM as all the other SD techniques, relies on the assumption of stationarity of the correction, which means that the correction function estimated on the control period remains unchanged in future. This hypothesis is necessary in order to apply the correction also to distant periods in time. Frias et al. [2006] demonstrate the hypothesis can be partially verified, while the extensive adoption of the method in literature tested the method's robustness [see e.g. Piani et al., 2010a; Hanssen-Bauer and Førland, 2001; Nieto et al., 2004].

Observations time-series are provided by ARPA Lombardia meteorological network, which collects daily precipitation, temperature and cloud cover transmissivity data. In this thesis we consider data series recorded in 9 stations for precipitation, 4 for temperature and 1 for cloud cover transmissivity. We choose the stations considering the longer time-series, the higher completeness of the data and the best spread positions on catchment territory. The maps in figures 4.2 and 4.3 show the position of precipitation and temperature stations respectively, while cloud cover transmissivity time-series was measured in Sondrio.

Tab. 4.2 *– List of meteorological variables stations*

Precipitation [mm]	**Temperature [°C]**	**Cloud cover transmissivity**
Le Prese	Bormio	Sondrio
Cancano	Tirano	
Santa Caterina Valfurva	Colico	
Alpe Entova	Lecco	
Samolaco		
Bormio		
Oga San Colombano		
Aprica		
Colico		

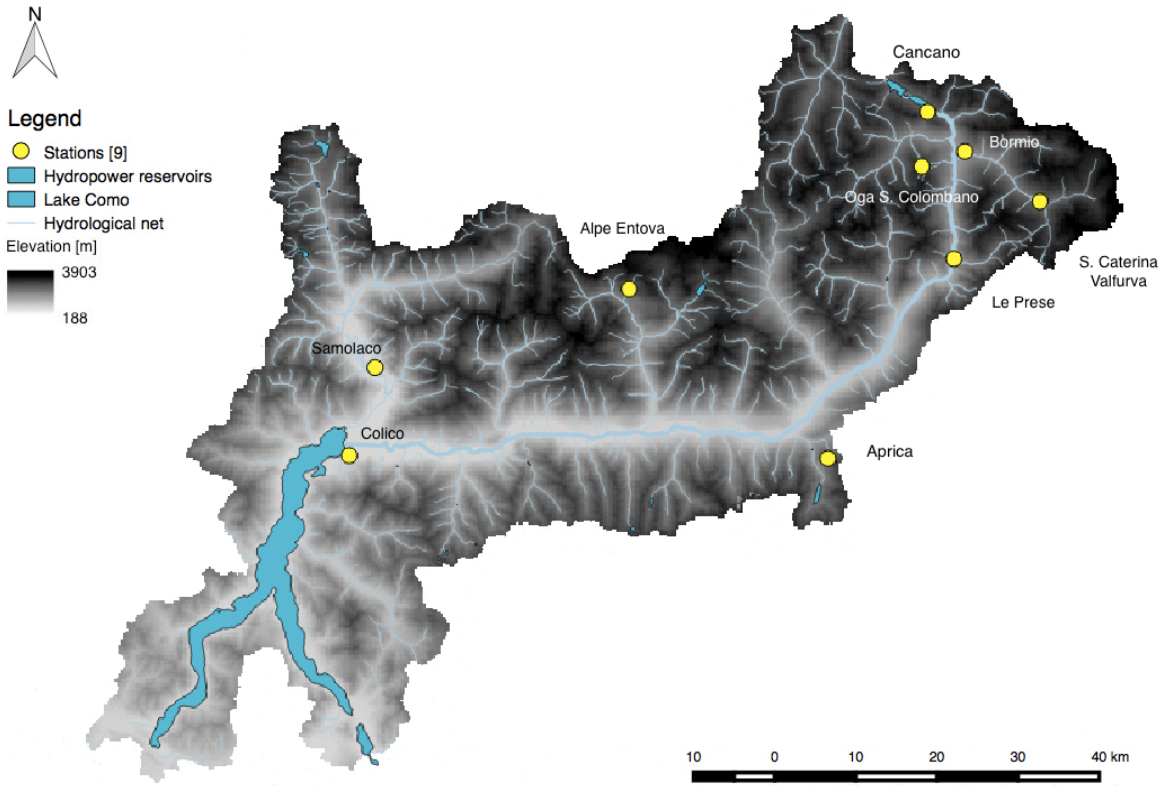

***Fig. 4.2** – Precipitation stations considered in upper Adda river basin*

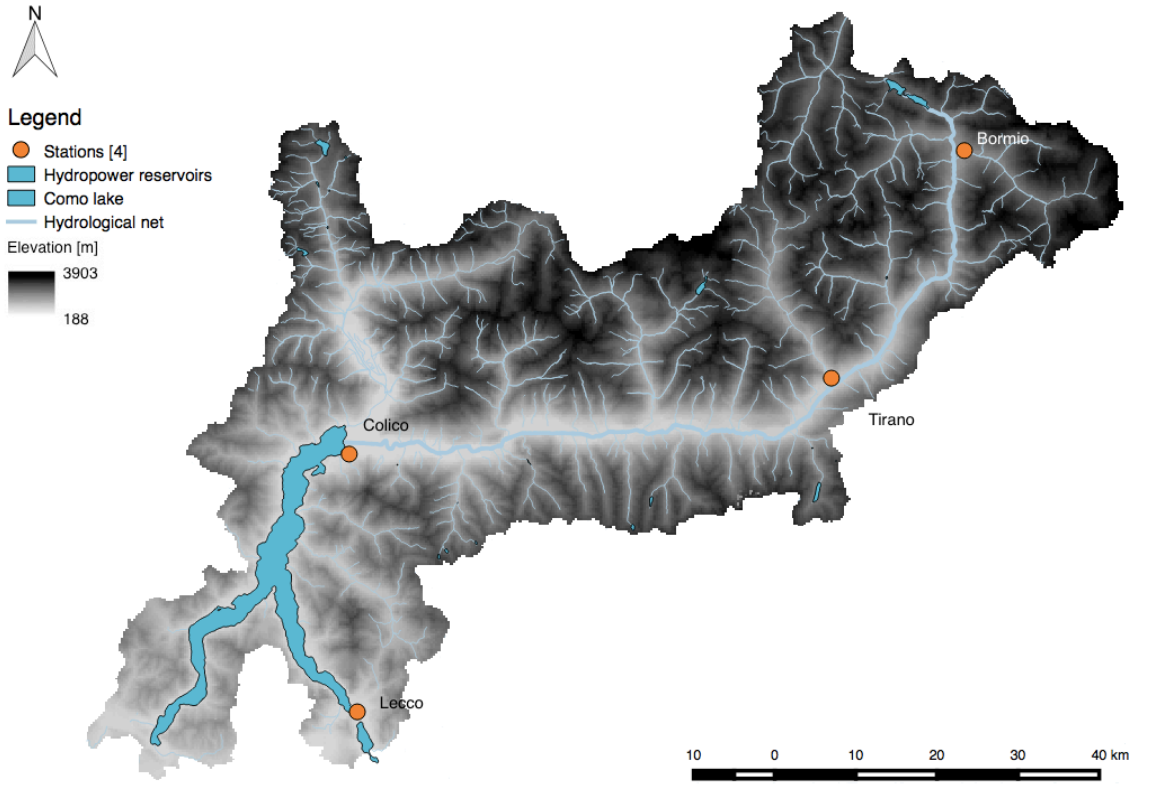

***Fig. 4.3** – Temperature stations considered in upper Adda river basin*

Control data must consistently overlap observations to derive their quantile-quantile function, which is not our case. Observation data are complete in period 2004-2013 and the series is too shot to accurately estimate the correction function, for which at least 30 years observations are advised [Anghileri et al., 2011; Wilby and Dessay 2010, Boé et al., 2007]. The flexibility of the method opens to a variety of QM variations which were explored in literature, testing short series or a cascade of downscale on different temporal scales [Haerter et al., 2011; Piani et al., 2010a; Piani et al., 2010b]. Its robustness allows us to implement it calibrating the function between control period and scenarios and applying it the correction to the observation period (figure 4.4).

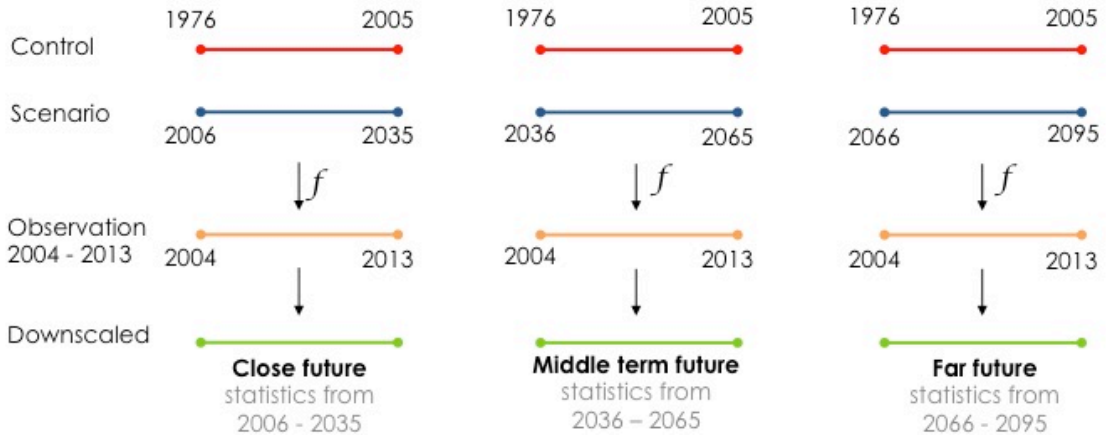

Fig. 4.4 *– Scheme of the implementation of QM used in this study. In the calibration phase, the correction function is derived by comparing the quantiles of the scenario and the control. The scenario is split into three 30-years-long periods in order to analyze close term (2006-2035), middle term (2036-2065) and long term (2066-2095) climate change effect. The considered control period 1976-2005 is 30-years-long as well. Each correction in short, middle and long term is applied to the same 10-years-long observation time-series, producing three periods for each scenario (close future, middle term future, far future), each carrying the statistics of the scenario it was calibrated with.*

For each variable, calibration phase is performed on 30-years-period: control period (1976-2005) is considered while the scenario is split in time periods (figure 4.4). This division allows to better analyze the impact of close term, middle term and long term climatic changes. We estimate the correction for each couple control period – scenario in the three periods, then we apply the corrections to the same 10-years-long observation to obtain the downscaled projections (green bar in figure 4.4). In other words, in our analysis 10-years-long projections represents the statistics of a 30-years-long future period. In this way, the calibration reproduces global climate change trends in long and short run that are superimposed to the local circulation effect given by the observation.

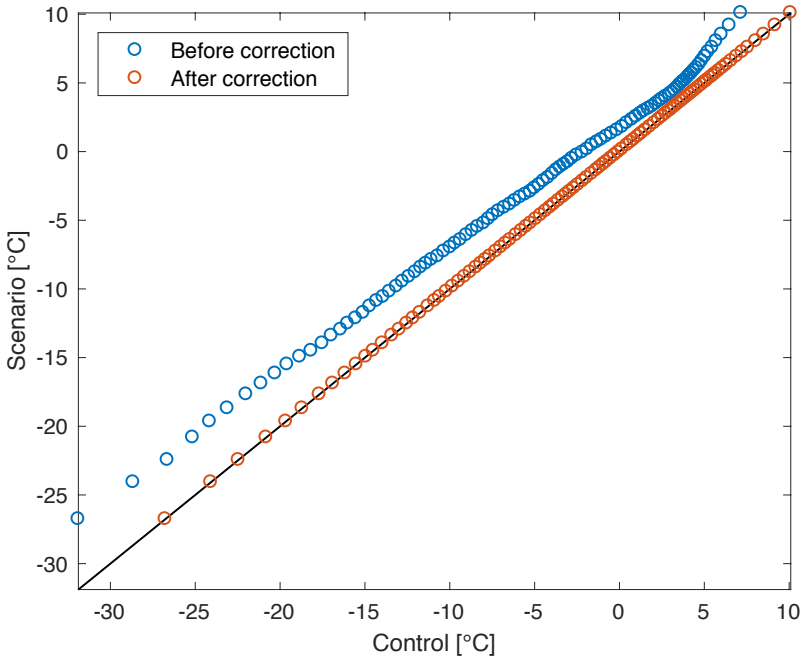

Fig. 4.5 – *Example of the calibration function (blue) for Bormio temperature. SMHI RCP8.5 at middle term (2036-2065) control and scenario are used for calibration. In red, we test the accuracy of the downscale: the downscaled control quantiles and the observations quantiles must be equal and line up on the bisector*

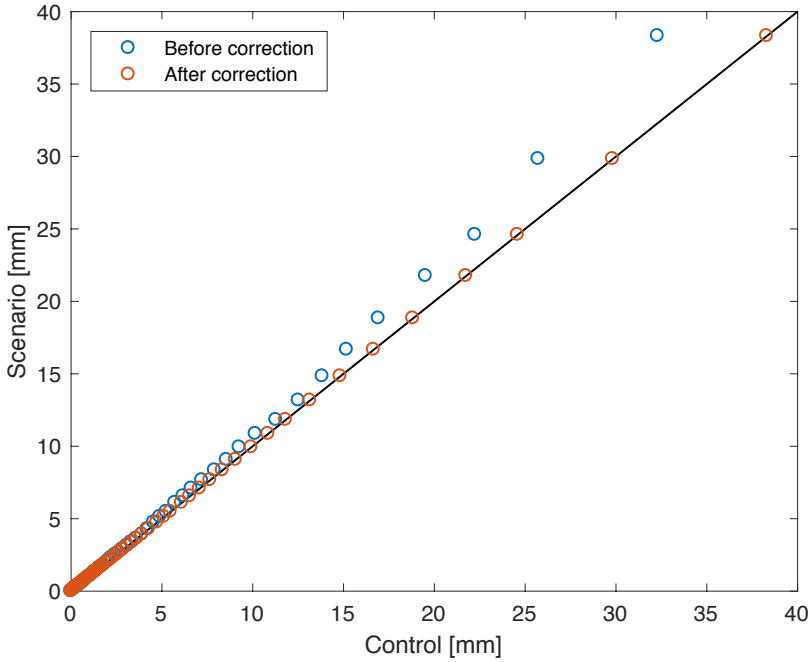

Fig. 4.6 – *Example of the calibration function (blue) for Bormio precipitation. SMHI RCP8.5 at middle term (2036-2065) control and scenario are used for calibration. In red, we test the accuracy of the downscale: the downscaled control quantiles and the observations quantile must be equal and line up on the bisector.*

QM calibration describes the functional relation between the statistics of future climatic variables and historical climatic variables. This implementation supposes the statistics of the control period are the same as the observations ones. We can thus apply the calibrated function to generate future local scale projections. In other words, we can imagine performing a downscale in time, applying future statistics on present climatic series.

In figures 4.5 and 4.6 the correction functions (blue) for Bormio temperature and precipitation in the middle-term future are given as example. Projections derived from SMHI8.5 for all the climatic variables are shown in figure 4.7 as example. Temperature and precipitation refer to Bormio station, cloud cover transmissivity to Sondrio. The growing trend in temperature, cloud cover transmissivity and precipitation introduced by climate change is evident in the series: the further periods exhibits greater corrections than the previous ones.

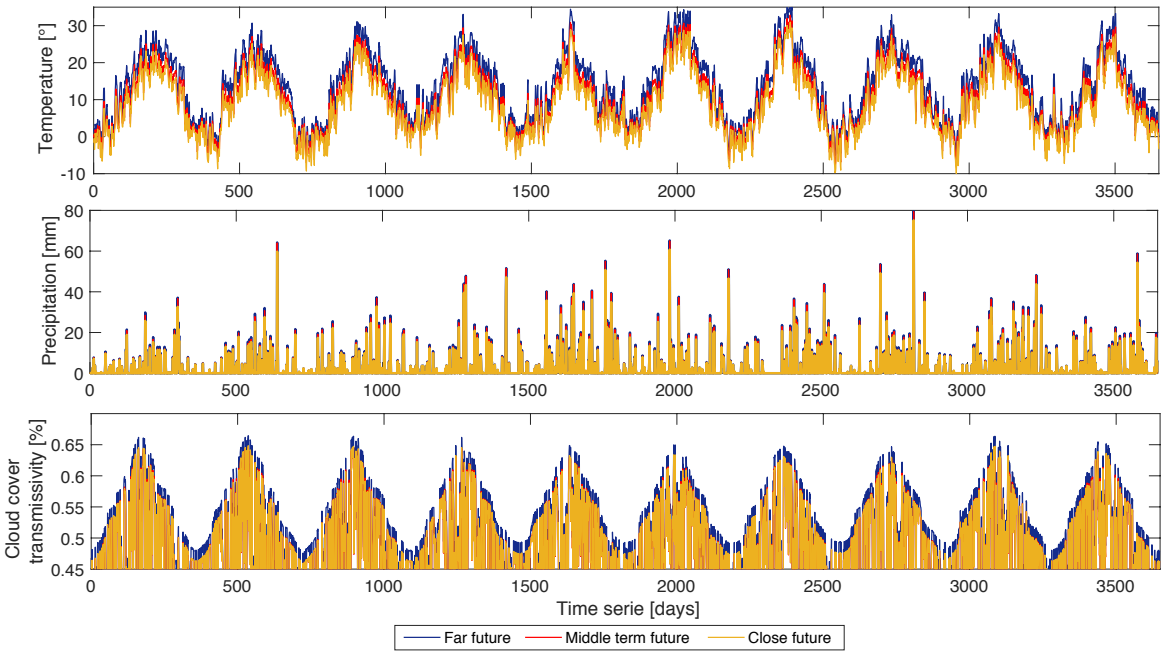

***Fig. 4.7** – Influences of QM on the meteorological variables in different time periods. On top and in the middle, downscaled SMHI RCP8.5 scenarios of temperature and precipitation for Bormio and on the bottom cloud cover transmissivity SMHI RCP8.5 scenario for Sondrio station are shown. The time periods of the scenario are indicated in color: close future (statistics 2006-2035) in yellow, middle term future (statistics 2036-2065) in red, far future (statistics 2066-2095) in blue.*

QM daily values of the variables are simply scaled by a magnitude factor. For this reason statistical downscaling better performs with continuous variables as temperature

Tab. 4.3 *– Average of the yearly minimum and maximum temperature and precipitation in every station and average over the whole time-series. Data are divided in the three time periods to better understand the trend in the data set.*

Observed temperature 2004-2013[°C]		
Minimum	**Maximum**	**Average**
-4.58	27.78	11.79

Observed precipitation 2004-2013 [mm]		
Minimum	**Maximum**	**Average**
0	59.42	2.56

	DMI RCP 4.5 temperature[°C]			**KNMI RCP 4.5 temperature[°C]**			**SMHI RCP 4.5 temperature[°C]**		
	Close future	**Middle term**	**Far future**	**Close future**	**Middle term**	**Far future**	**Close future**	**Middle term**	**Far future**
Min	-4.03	-3.05	-2.86	-3.55	-2.42	-1.88	-3.15	-2.11	-1.52
Max	28.67	29.42	29.94	28.49	31.25	31.11	28.86	30.23	30.36
Avg	12.45	13.22	13.56	12.60	14.40	14.40	12.79	13.74	13.74

	DMI RCP 8.5 temperature[°C]			**KNMI RCP 8.5 temperature[°C]**			**SMHI RCP 8.5 temperature[°C]**		
	Close future	**Middle term**	**Far future**	**Close future**	**Middle term**	**Far future**	**Close future**	**Middle term**	**Far future**
Min	-3.90	-2.61	-1.44	-3.12	-2.00	-1.03	-3.57	-1.46	0.41
Max	29.36	29.60	31.44	29.63	31.06	34.25	28.76	29.65	32.82
Avg	12.77	13.46	13.46	13.28	14.83	14.83	12.55	13.79	13.79

	DMI RCP 4.5 precipitation[mm]			**KNMI RCP 4.5 precipitation[mm]**			**SMHI RCP 4.5 precipitation[mm]**		
	Close future	**Middle term**	**Far future**	**Close future**	**Middle term**	**Far future**	**Close future**	**Middle term**	**Far future**
Max	61.20	61.77	64.88	63.04	58.49	61.94	62.74	62.27	64.29
Avg	2.57	2.57	2.57	3.08	2.74	2.74	2.66	2.61	2.61

	DMI RCP 8.5 precipitation[mm]			**KNMI RCP 8.5 precipitation[mm]**			**SMHI RCP 8.5 precipitation[mm]**		
	Close future	**Middle term**	**Far future**	**Close future**	**Middle term**	**Far future**	**Close future**	**Middle term**	**Far future**
Max	59.89	63.94	64.49	60.84	61.64	63.78	61.90	64.44	65.34
Avg	2.45	2.83	2.83	2.93	2.86	2.86	2.62	2.81	2.81

and cloud cover transmissivity. The correction of precipitation is a delicate problem [Haerter et al., 2011]: it's more difficult to draw conclusions for changes in total

precipitation due to phenomenon intermittency and noise, because statistical downscaling only concerns precipitation intensity, not affecting frequency of the events of the series (figure 4.7). The scaling factor for precipitation grows with precipitation intensity: in table 4.3 we can see mean precipitation is more or less constant in the three periods. This result is in agreement with Frei et al. [2006], who confirmed an intensification of extreme events in climate change context and a not appreciable variation of average total precipitation [see also Gao et al., 2006]. Main differences in precipitation downscaled series are due to GCM/RCM models, which differ for the response in the basic intensity and occurrence of precipitation events.

General results we obtain are consistent with literature ones. Several studies [e.g. Beniston et al., 2011; Beniston, 2003] agree the climate change will increase the temperatures on the Alps. Our analysis shows mean temperature rises in the three time periods will be respectively +0.82°C, +2.00°C and 2.11°C for RCP.45 and +1.08°C, +2.24°C, +2.24°C for RCP8.5. This result reflects Beniston [2003] findings of a 2°C temperature rise in some locations of the Alps. Temperature increase leads also to higher water to snow precipitation ratio. Consequently, an accelerated and conspicuous ice melting phenomenon will take place as well, which in its turn will lead to ice volume shrinkage first, then fragmentation and the premature disappearance of the glaciers [Diolaiuti et al., 2012; Huss et al., 2010; Haeberli and Beniston, 1998].

4.2 HYDROLOGICAL RESPONSE SIMULATIONS

In order to transform meteorological variables in catchment runoff we need a hydrological model that reproduces the physical processes that occur in Alpine hydrological cycle. This model is Topkapi-ETH (TE now on), introduced in section 2.2, which more specifically describes Adda river basin. Its spatially distributed inner structure of the model allows to assess the hydrological response to future climate in any interesting closing section of the basin and to perform spatial analyses on river network, glaciers, and hydropower reservoirs. We implement the model with 250 m^2 spatial grid and a daily temporal resolution.

For each cell, TE requires as inputs daily precipitation, air temperature and cloud cover transmissivity observations, as well as maps describing various spatial features of the basin. Since the calibration of the model goes beyond the purposes of the thesis, we're

not dwell on details on the description of the mentioned maps. We advise the reading of Giudici [2016] for further information about calibration.

We conducted six simulations, given by the combination of RCPs and GCM/RCM, in which the three scenarios of air temperature, precipitation and cloud cover transmissivity were given as input. In order to provide a proper initial condition to any future simulation, we can reasonably assume continuity between the three periods statistics. Meteorological variables series were thus constructed joining 2004-2013 observations and the three 10-years-long projections reproducing 2006-2035, 2036-2065 and 2066-2095 statistics.

We then performed a 40-years horizon simulation with daily time-step. TE allows to record different hydrological variables as output, both in form of point specific time-series and spatially distributed layers. We mainly focus on daily inflow to A2A reservoirs time-series, which provide the input to our reservoir operational models, and glacier volume maps for each year of the horizon. Since ice sheet component is really sensitive and exhibit a very rapid reaction time to changes in climate, glaciers play a key role in understanding the impact of climate change on the catchment hydrological behavior and the influences on Cancano reservoir inflow series. Moreover, their permanent character makes them a pillar of Alpine hydrology and the main long-term source of water for hydropower, thus constituting an important information for A2A decision-maker.

Considering the combination of GCM/RCM, the RCP they processed and the three time periods, we obtain an ensemble of 18 10-year-long inflow series. The results of the simulation are discussed in section 6.1.

4.3 VALIDATION

We first validate our QM implementation by checking the accuracy of the DS: if the technique is properly performed, the quantiles of the downscaled control should equal the quantiles of the observation. This is our case as shown in figures 4.5 and 4.6 (red points). We can thus reasonably assume this implementation of QM produces reliable time series.

We then validate TE results by comparing TE inflow simulation, forced with meteorological variables observations on 2004-2013, with observations inflow time-series on the same period. The comparison is showed in figure 4.8. The hydrograph is mainly

dominated by snow-melting, which starts in April and lasts for the whole spring, and autumnal precipitations, concentrated in November, while during the rest of the year the inflows are small. The hydrological model well reproduces the current average pattern of the inflows while it mostly fails in peak overestimation, in capturing the second peak and in smoothing the low inflow signal.

Table 4.4 highlights once more that TE simulation overestimate the yearly inflow, and thus is likely overestimating also inflow future projections. Anyway, this effect might be compensated in our analysis by the fact the inflow time-series we consider in historical policy design (2008-2014) is characterized by abundant inflow, thus placing the scenarios and present inflow in a common wet condition.

The quality of TE simulation can be considered satisfying for this thesis purposes.

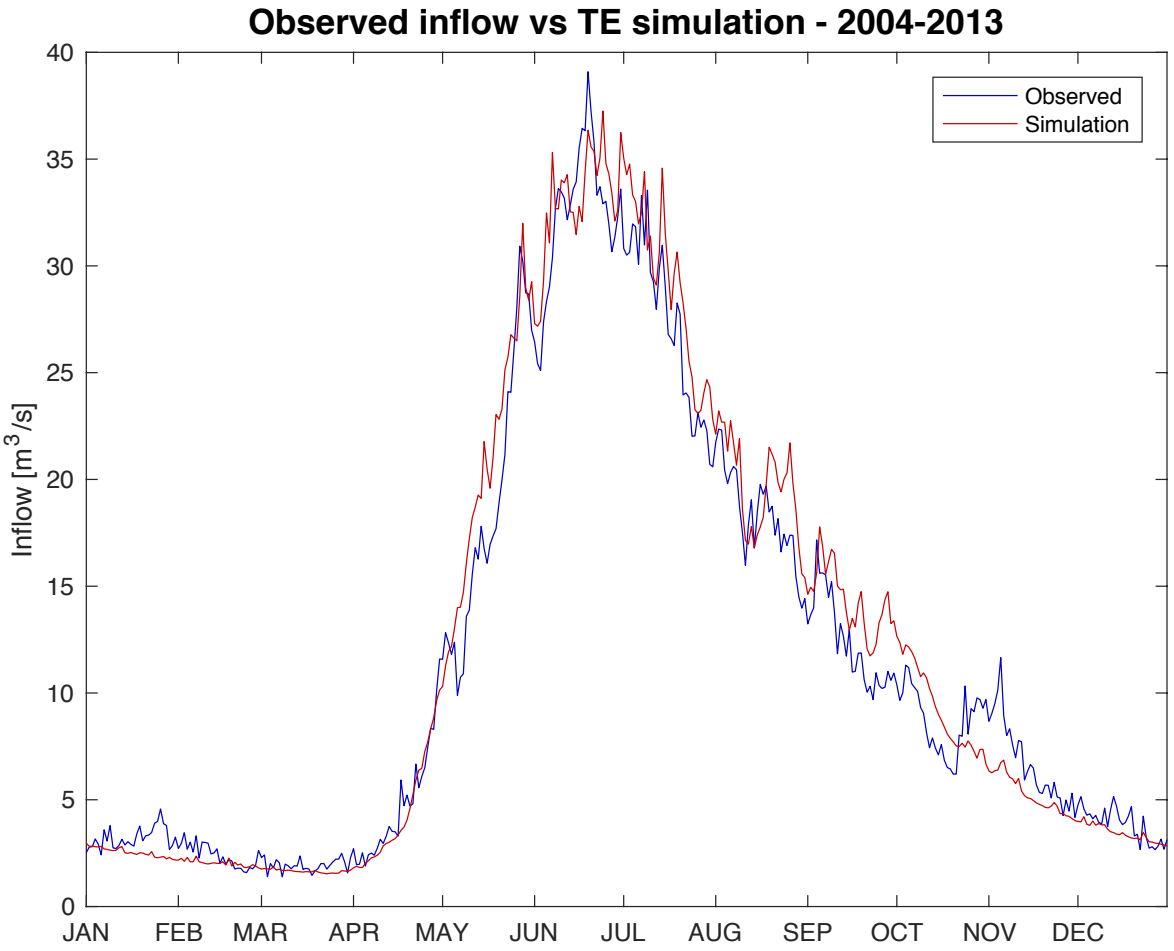

Fig.4.8 *– A2A power system inflow: cyclostationary mean of the observation (blue) compared with the same average of TE inflow simulation (red), forced with meteorological variables observations on 2004-2013.*

Tab. 4.4 *–Comparison of yearly inflow water volume [Mm^3] in the historical period. TE inflow simulation, inflow observation in 2004-2013, inflow observation on 2008-2014. The latter observation will be used for subsequent policy design For each time interval the average cyclostationary water volume [Mm^3] is calculated from daily inflow time-series. The comparison between observation and TE simulation in 2004-2013 confirms that the simulation overestimate the overall volume of inflow. On the other hand, comparing the observation of 2004-2013 period and 2008-2014, which is the period we are considering for policy design in present conditions, we can see 2008-2014 inflow are particularly high, compensating the overestimation effect introduced by TE.*

	Topkapi-ETH simulation 2004-2013	**Observation 2004-2013**	**Observation 2008-2014**
Mean yearly water volume [Mm^3]	387.91	371.00	418.87

5
HYDROPOWER OPERATIONAL MODEL

In order to quantify the impact of climate change on the hydropower system, we need a model of the hydropower reservoir operation.

In first place, the complex A2A hydropower system is simplified to reduce computational effort. The two reservoirs are treated as an equivalent reservoir of 180Mm^3 of storage capacity, which is the sum of the physical reservoirs storage. The inflow to the reservoir is the sum of all the diverted inflows to the single reservoirs while we indicate as release the Premadio turbined flow time-series. As regards the downstream power plants hydraulic scheme, we refer to an equivalent power plant as well. Its maximum capacity is Premadio plant (41.06 m^3/s), since is the only plant directly connected to reservoir, while the others exploit also other water sources. All the other technical features and net head of each power plant are summarized in a energy conversion coefficient, provided by A2A, which allows to compute the energy produced in each power plant for a unit of turbined flow. The equivalent energy conversion coefficient is computed as the sum of the coefficients of the single power plants (3.365 KWh/m^3) [Amodeo and Anghileri, 2007].

Tab. 5.1 *– Main technical features of A2A power plants*

Power plant	**Installed capacity [MWh]**	**Maximum capacity of the turbine [m^3/s]**	**Energy conversion coefficient [KWh/m^3]**
Premadio	226	41.06	1.522
Grosio	480	83.33	1.4
Lovero	49	59.10	0.235
Stazzona	30	40.06	0.208

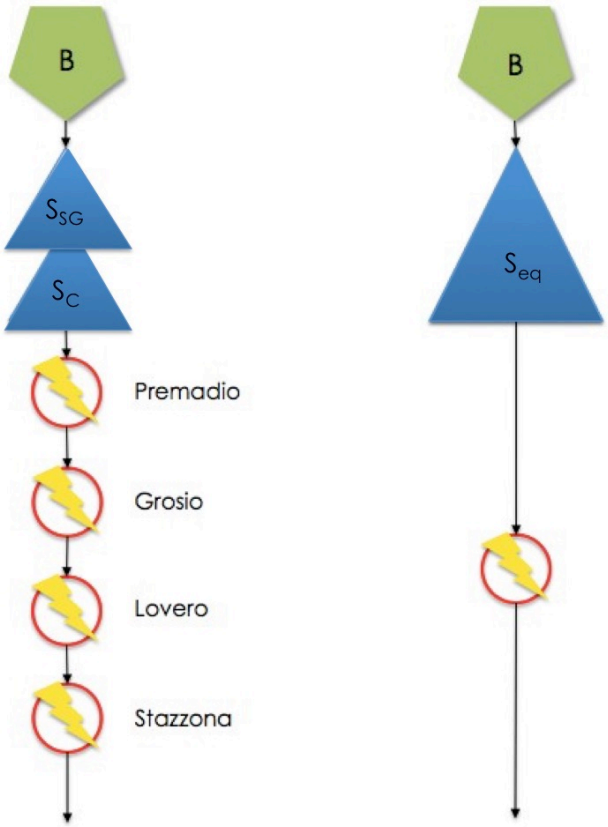

Fig. 5.1 *– Conceptual A2A system structure and its reduction.*

In this thesis, we model the A2A reservoir operation using a normative approach, which describes the decision making process as an optimization problem. The decision maker is considered a rational agent who maximizes a given utility function. Utility functions represent measurable criteria that the decision maker uses to rank different decisions/options. The decision maker objectives we consider in our case study are revenue and production, to be maximized on the year on daily basis. We suppose a rational agent would release water at maximum turbine flow capacity only in the most profitable hours of the day, when prices are high. The choice of releasing or keeping water volumes in an hour or another generates the conflict between the two objectives. The release decision is univocally related to the number of operating hours per day and the decision can be interpreted how many hours per day the decision maker should release at maximum flow

$$u_t = \frac{Q_{max}^T \cdot h_t}{24} \qquad [5.1]$$

where u_t is the decision, $Q_{max}^T = 41.06\, m^3/s$ is the maximum turbine capacity, h_t is the

number of turbine operating hours. It's important to highlight that the hourly release is fixed at 41.06m^3/s, while the volume of water released in h_t hours from the reservoir is averaged over the daily time-step. Reservoir release is defined on according to two main disturbances: inflow and energy prices.

The production is calculated on daily base by multiplying the hourly production, supposed to be constant, by the number of functioning hours of the turbine

$$E_h = \psi \, Q^T_{max} \cdot 3600 \qquad [5.2]$$

$$g^P_{t+1} = E_h \cdot h_t \qquad [5.3]$$

where E_h is the energy produced in one hour of turbine functioning, $\psi = 3.365$ $[kWh/m^3]$ is the energy conversion coefficient of the turbine and h_t are the number of operating hours of that day. g^P_{t+1} $[MWh]$ is the daily production in the time interval [t,t+1).

Since water is released on the most profitable hours of the day, the decision also depends on the prices. Energy price is a disturbance of the system and, since we're dealing with a problem with yearly periodicity, we need to define the drivers in a cyclostationary way. Using hourly data provided by GME in the period 2009-2015 we generate the cyclostationary matrix of the prices by averaging (figure 5.2).

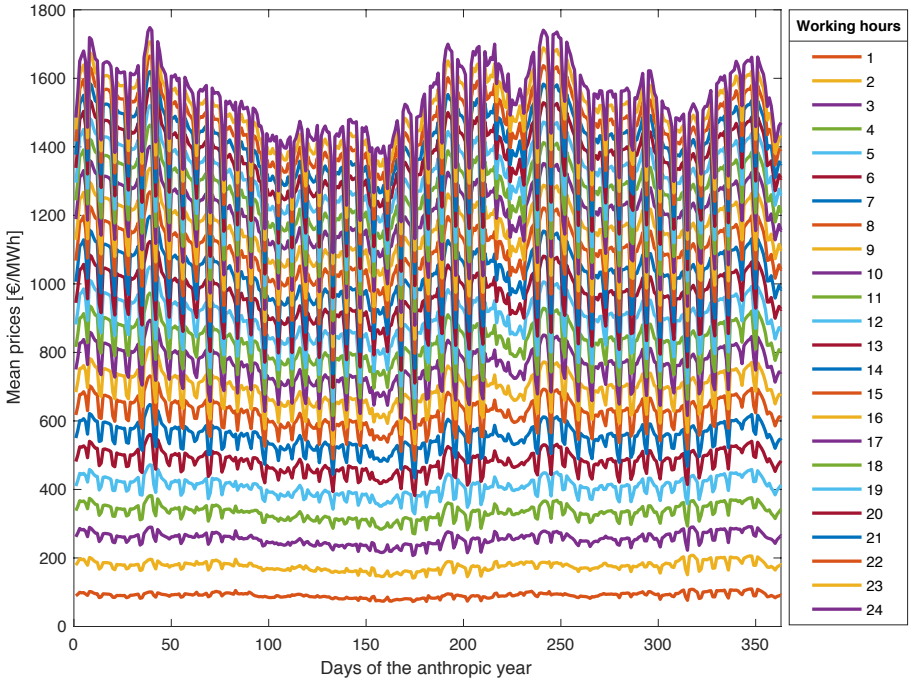

Fig. 5.2 *– Cyclostationary matrix of the prices. Mean energy prices on the period 2009 – 2015 are averaged and cumulated from the lowest to the highest profitable hours*

Each cell *i* contains the cumulate price of the most profitable *i* hours of the day of the anthropic year, a non-leap year of 364 days starting on Monday. The anthropic time allows keeping distinct weekdays from weekends to mark the weekly pattern. The matrix is derived by averaging weekdays in a moving average with 5 days windows amplitude, while no window is used weekends. Everyday prices are then ordered form the highest to the lowest and cumulated. Higher cumulated prices are associated to longer intervals of production, but the longer the turbine works, the lower is the marginal price associated to the last working hour.

The revenue is then obtained multiplying the production by the cumulate price of energy for the respective operating hours.

$$g_{t+1}^{R} = E_h \cdot p_{t,h_t} \quad [5.4]$$

in which g_{t+1}^{R} is the daily revenue [€] and p_{t,h_t} the cumulate price of the *t*-th day of the anthropic year for a number h_t of operating hours of the turbine.

We thus set up a Multi-Objective decision problem. As mentioned in section 2.3, we solve the optimization problem adopting Dynamic Programming (DP). DP founds on the solution of Bellman equation

$$H_t^{*}(s_t) = \max_{u_t} \mathop{\mathrm{E}}_{e_{t+1}} [\, G_t(s_t, u_t, e_{t+1}) + H_{t+1}^{*}(s_{t+1})] \quad [5.5]$$

in which $H_t^{*}(s_t)$ is the optimal cost-to-go at stage t, only depending on the value of the state, the storage, at the same time-step, $G_t(s_t, u_t, e_{t+1})$ is the step-cost of the *t*-th stage, and $\mathop{\mathrm{E}}_{e_{t+1}}$ is the expected value over the disturbances. Bellman equation exploits the multi-stage conformation of the problem to compute its solution in a recursive way, by proceeding backwards from the final stage to the initial one. The result of the DP optimization is provided as a look up table containing the optimal cost-to-go associated to s_t. The optimal cost-to-go is the sum of the step-costs associated to the optimal decision taken in each stage from s_t to the final stage.

DP application is based on the main assumption of the separability of the objective, which in its turn derives from step-cost separability. The step-cost expresses the cost produced in the transition from s_t to s_{t+1} by a given decision. In order to be separable a step-cost must be a function of variables related to [t, t + 1) time interval only and the same must hold for the objective. At each stage, the step-cost $G_t(s_t, u_t, e_{t+1})$ depends on the state of the system, the release decision and the inflow. For convention, e_{t+1}referst to

the inflow occurring in the interval [t, t+1), after the moment in which the decision is taken.

$G_t(s_t, u_t, e_{t+1})$ is a linear combination of the step-costs showed in 5.3 and 5.4., which makes it separable.

In order to apply DP algorithm, the system must be an automation, i.e. the sets in which the state, control and disturbances assume their values, are finite for every t. It is therefore necessary to implement their discretization.

Storage grid considers 59 states spacing from 0 to 200Mm^3. An irregular discretization, thinner to the extremes of the active volume (which is the volume in which the regulator can freely establish the release decision) of the reservoir, is adopted to better describe water scarcity and water spillage conditions. As previously explained, control discretization is strictly linked to turbine functioning description. It ranges from 0 to 41.06m^3/s, which is the turbine maximum flow capacity, within 24 steps. The discretization is reported in table 5.1.

Tab. 5.2 *– Discretization of the feasible decision set*

Working hours per day h_t [h/d]	**Release decision u_t [m^3/s]**	**Working hours per day h_t [h/d]**	**Release decision u_t [m^3/s]**	**Working hours per day h_t[h/d]**	**Release decision u_t [m^3/s]**
0	0.00	9	15.40	18	30.80
1	1.71	10	17.11	19	32.51
2	3.42	11	18.82	20	34.22
3	5.13	12	20.53	21	35.93
4	6.84	13	22.24	22	37.64
5	8.55	14	23.95	23	39.35
6	10.27	15	25.66	24	41.06
7	11.98	16	27.37		
8	13.69	17	29.08		

Inflow discretization ranges from 0 to 120 m^3/s, which is the maximum inflow occurring in historical observations or inflow projections, with a step of 1 m^3/s. As already mentioned in chapter 2, we implement DP in two forms, deterministic (DDP) and stochastic (SDP), which mainly differ for the approach to the disturbances. DDP requires a perfect knowledge of the inflow, i.e. the inflow is know before the decision is taken, and is thus implemented using a time-series of the inflow. It provides an optimal control for each day of the design horizon of the policy. This policy represents an ideal experiment that

allows evaluating the upper boundary to DP policies performances. For this reason, we will refer to DDP policies as Benchmark Policies (BP).

SDP implementation requires a statistical description of the disturbances, which is given as the probability distribution of the inflow to the reservoir. We suppose the inflow probability has the functional form of a lognormal. Using inflow time-series, the parameters of the lognormal (mean and standard deviation) are computed with a moving window of 40 days on cyclostationary basis on the anthropic year (364 days) Given this inflow representation, the solution of the SDP problem provides a cyclostationary policy. Unlike DDP, SDP is not designed for a specific inflow realization, but for a specific statistical characterization of the inflow. SDP can thus absorb natural inflow variability and reproduces realistically the decision-maker partial knowledge at the moment in which the decision is taken. For this reason, SDP policy better reproduces the operating policy of the hydropower system.

In order to solve the Multi-Objective problem, we must reduce the problem to a Single-Objective one, adopting an aggregation method. The step-costs [5.3] and [5.4] are aggregated by the weighting method, which consists of a weighted sum of the individual step-costs according to arbitrary weights

$$G_t(s_t, u_t, e_{t+1}) = \sum_i \lambda_i \cdot g^i \qquad [5.6]$$

$$\sum_i \lambda_i = 1 \qquad [5.7]$$

which sum up to 1. The two extremes are optimized according to a single objective problem, giving complete priority to revenue or production, while the other combinations of weights give 8 intermediate ranking of the two objectives. Each weights combination represent an alternative to the decision maker.

Tab. 5.3 *–Weights associated to the different alternatives*

Weights of the revenue	1	0.9	0.5	0.4	0.3	0.1	0.05	0.01	0.001	0
Weights of the production	0	0.1	0.5	0.6	0.7	0.9	0.95	0.99	0.999	1

The problem is solved applying Bellman equation [5.5] recursively, getting the policy of the hydropower system.

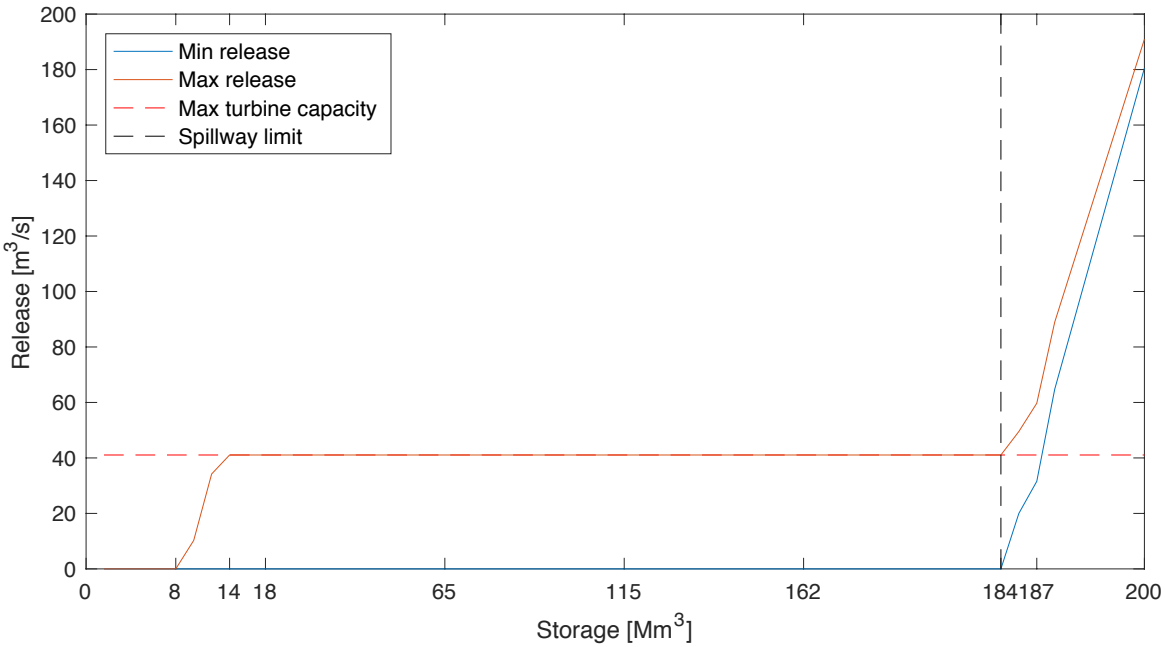

Fig. 5.3 *– Minimum and maximum instantaneous release curves for the Cancano-San Giacomo equivalent reservoir*

Each policy must be simulated in order to obtain hydropower system performances and the reservoir dynamics (release and storage trajectories). The model of the reservoir is based on mass balance equation at daily time step

$$s_{t+1} = s_t + e_{t+1} - r_{t+1} \quad [5.8]$$

$$r_{t+1} = \min\left(\max(Q_{min}, u_t), Q_{max}\right) \quad [5.9]$$

where s_t, e_{t+1} and r_{t+1} are respectively storage [m^3], daily net inflow [m^3/s] and daily release [m^3/s] at the same time-step.

Release is bounded by the curves of minimum and maximum instantaneous release (fig 5.3). For each storage s_t, they express the maximum and minimum release in the time-step on the basis of the instantaneous inflow. Since the inflow $e_{t+1}$is know only in discrete time-steps, the instantaneous release curves must be integrated over the time-step to obtain the minimum and maximum release curves. The curves describe storage-release relation, implicitly describing the operative features of the reservoir. For each couple (s_t, e_{t+1}) we can thus define the maximum and minimum release Q_{max} and Q_{min}.

The performances of the system, mean daily revenue and mean daily production, are defined by the objectives values, computed as

$$J^P = \frac{1}{H}\sum_{t=1}^{H} g_t^P \quad [5.10]$$

$$J^R = \frac{1}{H}\sum_{t=1}^{H} g_t^R \quad [5.11]$$

where g_t^P and g_t^R are the step-cost defined in [5.3] and [5.4] and H is the simulation horizon.

The objectives define a bi-dimensional space, called objective space. For every decision u the two objectives are the components of a vector

$$J = \left(J^P(u), J^R(u)\right) \quad [5.11]$$

which individuate a point in the objective space. Each point is associated with a specific objectives ranking and constitutes an alternative. In its turn, each alternative is associated to an optimal policy. The ensemble of the optimal policies points in objective space constitutes a sampling of the Pareto front, which constitute a simple and effective visual way to value and compare the overall performance of the hydropower system for different alternatives.

5.1 VALIDATION OF THE HISTORICAL OPERATIONS

In order to validate the model, deterministic (DDP) and stochastic (SDP) policies are optimized and simulated in the historical period, i.e. 2008-2014. The perfect knowledge of the inflow in DDP context allows us to conduct an ideal experiment, from which we can gain the maximum optimal performance for each alternative. The stochastic approach used in SDP optimization produces an operating policy, which could be adopted to regulate the reservoir. The Pareto fronts of the two policies, as well as the historical performance of the system, are shown in figure 5.4. Best alternatives tend to place in top right corner. In first place, SDP frontier has overall worst performances than DDP, due to deterministic approach to the disturbances of the latter. The distance in the objective space between the two frontiers is thus the improvement space defined in Chapter 2. SDP operations can be enhanced towards DDP performances including other information in policy design (e.g. forecasts, snow cover, glaciers state, temperature forecasts and so on).

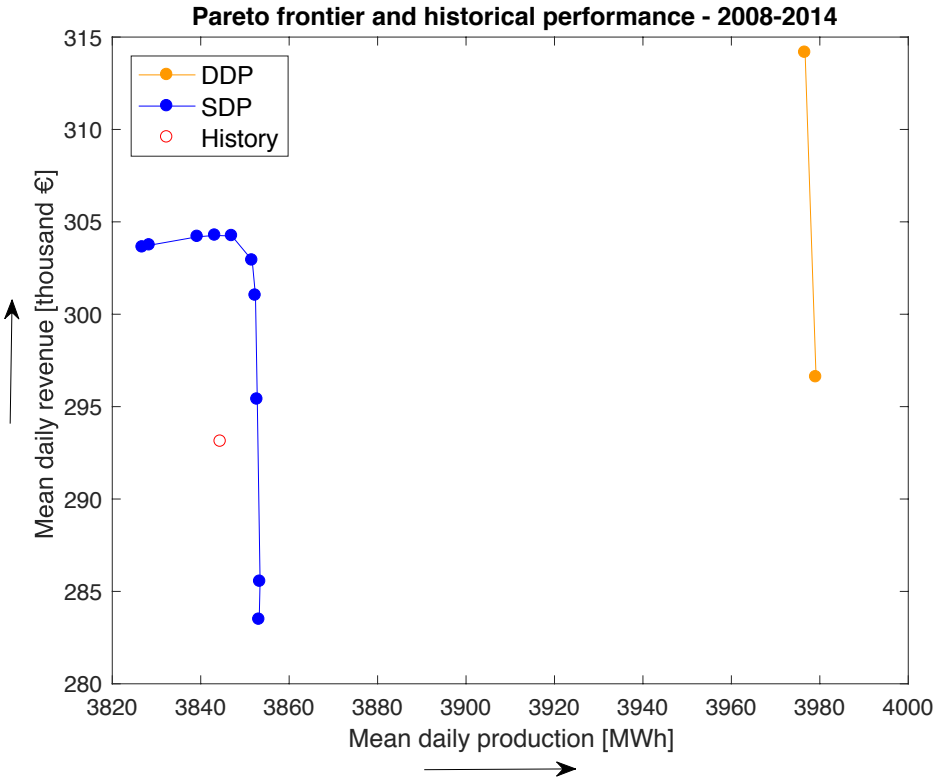

Fig.5.4 *– Pareto front for the Multi-Objective stochastic (SDP - blue) and deterministic (DDP -orange) policies. The arrows indicate the improvement direction of the objectives. In red, the performances of the decision maker obtained using the recorded release series.*

Further analyses on this result are shown in chapter 6. Referring to the frontier extremes, we can measure the distances in percentages, which are reported in table 5.4. The numbers suggest the performances of SDP are already pretty good and the improvement space is small. SDP front shows distinctly the trade-off between the objectives introduced by mean of the weights. Raising the importance of production compared to revenue, the points of the front move to better productions lowering the revenue. The alternatives with weights on the revenue between 1-0.3 show a contextual enhance both in revenue and production performances. The shape of this part of the Pareto front is probably linked to the fact that

Tab. 5.4 *– Improvement space for SDP policy in historical simulation: the distance in terms revenue and production between the extremes on the SDP frontier and their corresponding extremes on DDP is measured in percentages.*

Objective improvement	**Revenue extreme**	**Production extreme**
Revenue [%]	3.49	4.62
Production[%]	3.92	3.27

2008-2014 period is a wet one compared to average conditions, because of abundant precipitation. Following our assumption, the conflict between the objectives stands out in water scarcity conditions, because the alternative use of water becomes more important, while in condition of abundant inflow, the more we produce the more the revenue. The conflict on SDP is very clear when the weight given to revenue is lower than 0.3, which is when we put our attention on mostly production. The push on energy production leads to longer turbine operating time intervals: water is thus allocated in the hours of the day in which the marginal hourly price is low, with limited profits. In the last part of the frontier the production doesn't increase with consistent loss on the revenue objective: the points of the frontier with this characteristic are called semi-dominated.

DDP shape is much different from what expected: only the extremes are clearly distinguishable and the shape is almost vertical. All the points representing the compromise alternatives collapse in the revenue extreme and the production extreme is semi-dominated by the revenue extreme: all the alternatives yield the same production objective's value. This means that even optimizing the policy according to production objective only, the production doesn't improve, while the revenue decreases. In other words, the optimization of revenue objective provides also the maximum production objective value possible, because there's no conflict between the objectives (table 5.5).

Tab. 5.5 – *Conflict between the objectives for SDP and DDP policies in historical simulation: the distance in terms of revenue and production between the extremes on the SDP frontier and on DDP is measured in percentages. The spread between the extremes points of the frontier indicates the magnitude of the conflict in action: greater distances are index of consistent conflicts between the objectives. Focusing on production, the conflict with revenue is already meager in SDP experiment and in DDP the conflict on production is fatherly reduced.*

Objective improvement	SDP	DDP
Revenue [%]	8.17	4.38
Production[%]	0.63	0.15

Because of the lack of conflict in deterministic experiment, we reduce the Multi-objective problem to a Single Objective one. Since the production objective is already optimized when revenue maximization is optimum, we focus on revenue maximization.

In figure 5.5 the dynamics of the Single Objective policies for the hydropower system are compared.

Keeping in mind the yearly trend of prices, the reservoir is used to store water during spring to release it during summer and winter, when the prices are high. Storage

DDP and SDP trajectories diverges mainly in the first part of the year, when the inflow is low and the reservoir is emptying. The release trajectories in the same period are comparable until the point in which the reservoir is empty in SDP while in DDP has still residual water to exploit: this phase is the one that marks the major difference in the DDP-SDP performances. During the filling phase, the trajectories show that both the policies well intercept the spring peak of the inflow, as well as the historical records. However, it's important to see how in May SDP release trajectory slightly start rising previously and before the DDP ones. This is due to DDP complete information about peak timing, which can vary from year to year and is not known to SDP. SDP can rely only on the statistical probability distribution of the inflow, which describes the average time peak over the period of calibration of the distribution. Overall, SDP dynamics tend to equal DDP ones both in release and in storage.

We lastly compare SDP trajectories (red in figure 5.5) and the historical operating rule dynamics (blue in figure 5.5) and their performances in terms of objective's values. As regards performances, SDP yields much better revenue than historical operating rule (figure 5.4). SDP well follows the weekly pattern presented by historical operating rule release during the whole year. Moreover, historical release exhibits two main variations from DP trajectories, both in storage and release, in September and November, which are not due to low prices or water availability. We presume these deviations in trajectories reflect secondary objectives of the decision maker that are not modeled in our problem. Because of the exploitation of water reserve during these periods, the historical operating rules can sustain lower release from February to April.

The comparison between the recorded trajectories and SDP ones shows that revenue objective is sufficient to describe decision maker behavior and once more supports the reduction to a Single- objective problem. Since SDP patterns well follow the operative rule of the reservoir, we will refer to SDP policy in historical period as Business as Usual (BAU) policy.

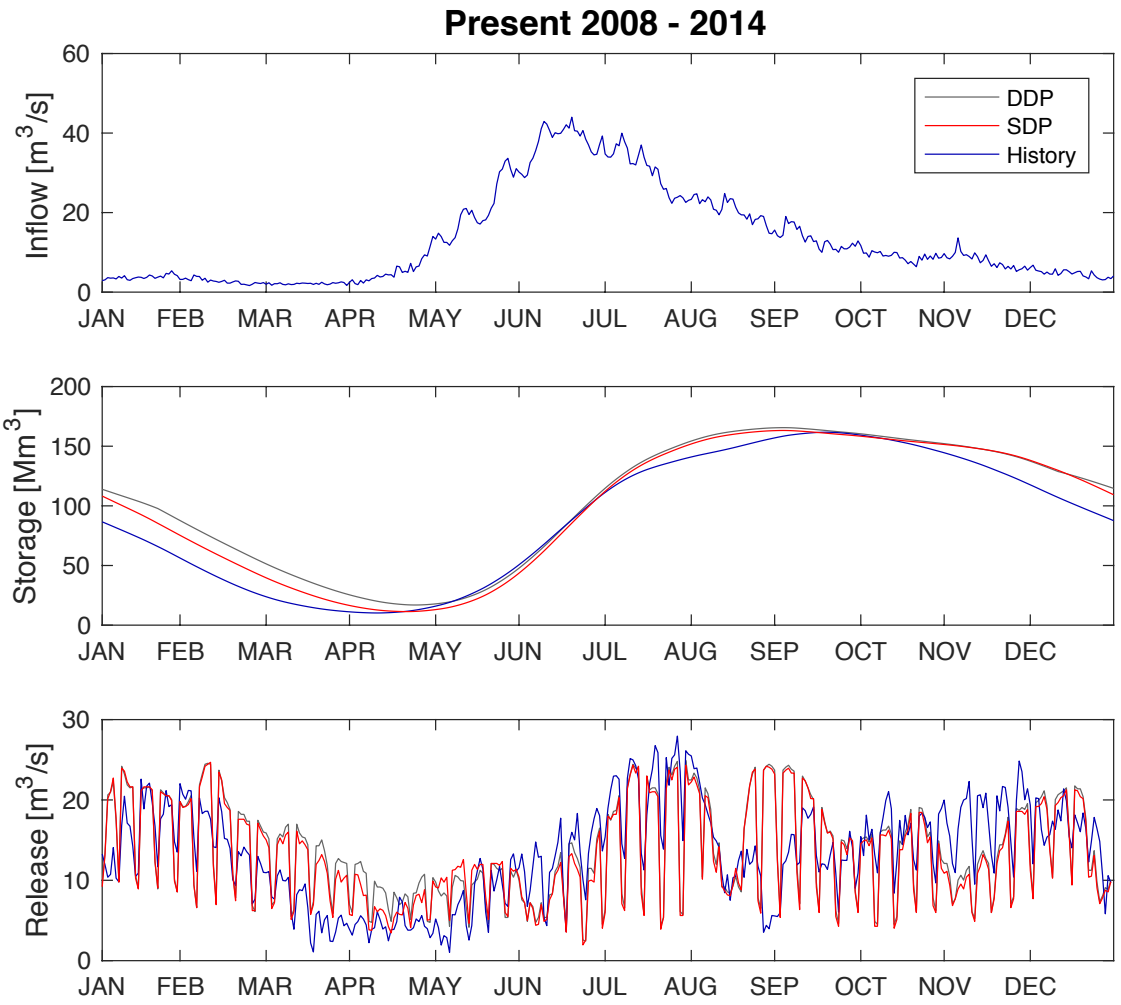

Fig.5.5 *– Dynamics of the reservoir operated under Single-Objective SDP and DDP, compared to observed trajectories. Cyclostationary mean inflow with moving average of 20 days window on the top, mean cyclostationary storage with moving 20 days window in the middle, mean cyclostationary release in the bottom square. DDP and SDP trajectories refer to the ones optimized and simulated with the inflows, while "History"(blue) refers to the recorded trajectories of the operative rule of the reservoir.*

6
RESULTS AND DISCUSSION

6.1 CLIMATE CHANGE ON THE ALPS

Future climate is going to alter consistently the hydrology of the Alpine environment. In Chapter 4 we have described how climate change scenarios are downscaled to reproduce Adda river basin climatic conditions. Then the hydrological model Topkapi-ETH was used to simulate the inflow to the reservoir under changing climate and the impacts of climate change on the hydrological cycle. We remind that the projection is split in three periods, named close future, middle term future and far future, which represent scenarios statistics respectively for the periods 2006-2035, 2036-2065, and 2066-2095. In this paragraph we discuss the peculiarities and trends of the inflow projections as well as glaciers evolution monitoring.

In figure 6.1 and 6.2 the inflow projections to A2A reservoir are showed for all the scenarios. Close future patterns are similar to historical ones, both in timing and water volumes: this means we don't expect any significant change in hydrology until 2035. Moving towards the end of the century, we can observe a general anticipation of the snowmelt peak and a diminishing of the associated water volume, particularly evident in DMI and SMHI scenarios, followed by increasingly dry summers, highlighted in KNMI scenarios. On average, snowmelt peak in close future anticipate the current ones by only a few days, while in middle term future and far future, peak anticipation can reach even over 30 days, shifting from late June to early May. Moreover, the snow-melting season seems to last longer in the far future than at present. These results have been confirmed in several

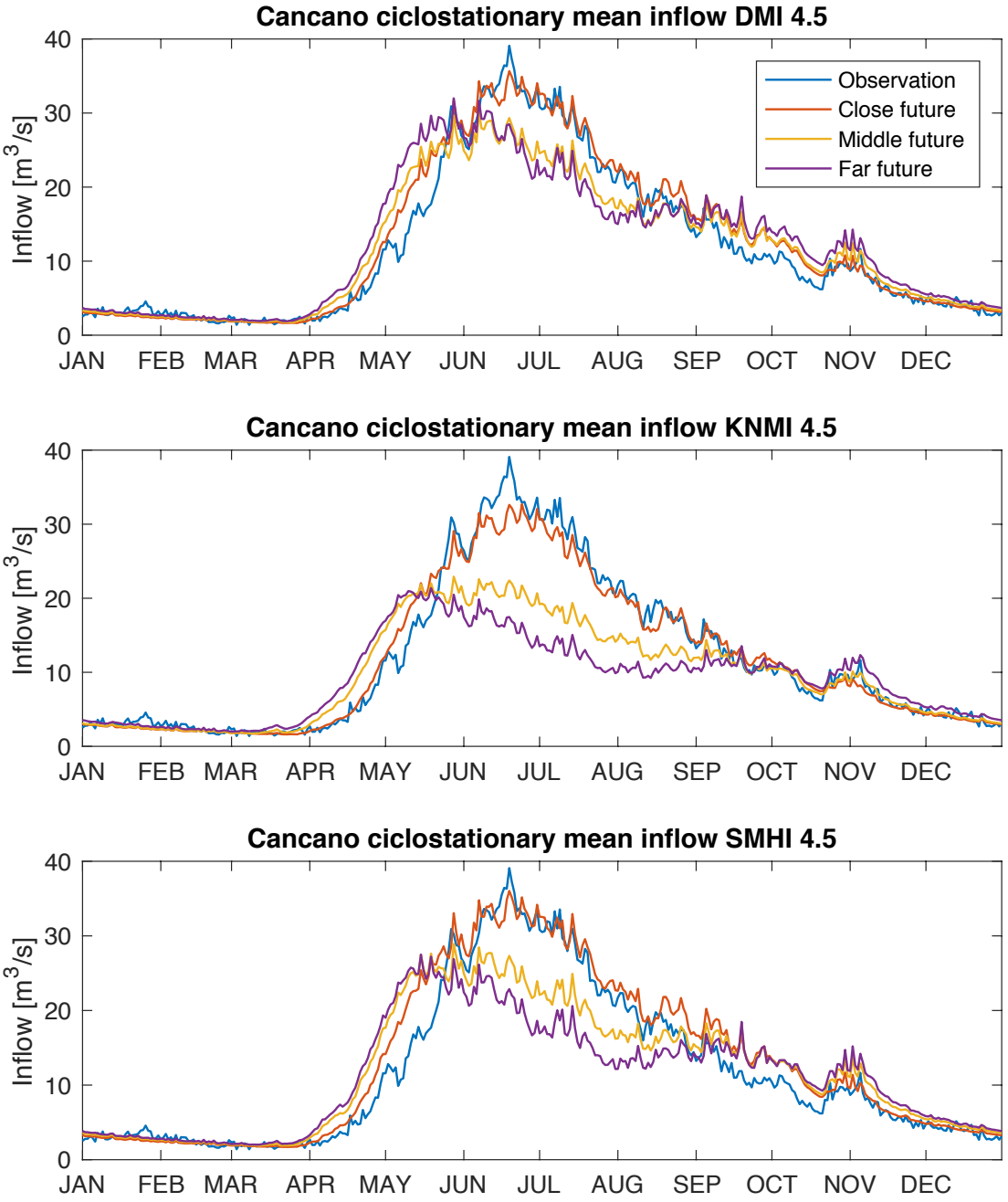

Fig.6.1 *– A2A power plant inflow for the scenarios RCP 4.5. All time series are averaged with a moving window of 10 days amplitude. Close future (2006-2035), middle term future (2036-2065) and far future (2066-2095) characteristics are represented respectively in red, yellow and purple lines. For a quick comparison, TE simulation of current inflow (2004-2013) is reported as well (blue line). Close future pattern doesn't differ significantly from historical inflow. All the scenarios exhibit an anticipation of the peak due ice melting and a sensible reduction in the yearly volume. The latter is particularly marked in KNMI scenarios, the former in DMI. All the scenarios agree in a growth of the inflow in November.*

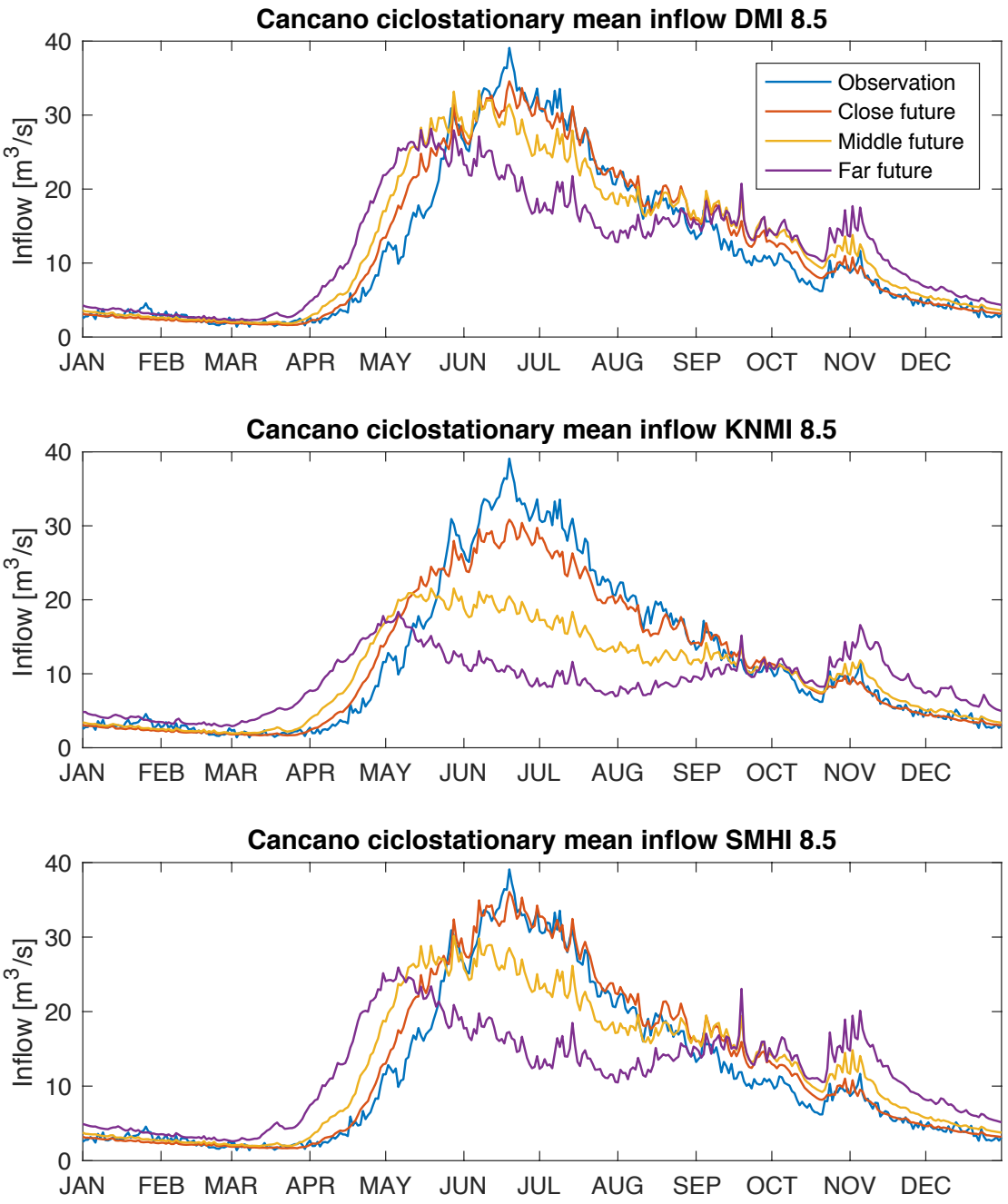

Fig.6.2 *– A2A power plant inflow for the scenarios RCP 8.5. All time series are averaged with a moving window of 10 days amplitude. Close future (2006-2035), middle term future (2036-2065) and far future (2066-2095) characteristics are represented respectively in red, yellow and purple lines. TE simulation of current inflow (2004-2013) is reported as well (blue line). Close future pattern doesn't differ significantly from historical inflow. Compared to RCP 4.5 scenarios, inflow exhibits the same changes, but water volumes and peak values are further diminished, while November inflow gains importance in the yearly balance*

Tab. 6.1 *– Peak anticipation in the different scenarios. The day of the year of the peak of the mean hydrograph of each scenario per period is reported, as well as the average over the scenarios per period.*

		RCP 4.5			RCP 8.5		
Periods	**Present**	**Close future**	**Middle term future**	**Far future**	**Close future**	**Middle term future**	**Far future**
DMI	175	170	148	148	170	148	135
KNMI	175	175	148	139	170	139	126
SMHI	175	170	148	135	170	148	126
Average	175	172	148	140	170	145	129

Tab. 6.2 *–Yearly water volume [Mm^3] per period in each scenario. For each period the average cyclostationary water volume [Mm^3] is calculated as in table 6.3. Yearly water volume derived from observation in 2004-2013 is reported as comparison. The yearly water volume projections are likely overestimated by TE, but show an evident diminution moving towards far future.*

	DMI		KNMI		SMHI	
Periods	**RCP 4.5**	**RCP 8.5**	**RCP 4.5**	**RCP 8.5**	**RCP 4.5**	**RCP 8.5**
Present	371.00	371.00	371.00	371.00	371.00	371.00
Close future	394.14	389.64	361.88	358.46	410.50	400.53
Middle term future	366.51	401.21	307.80	308.87	371.94	392.94
Far future	384.27	383.08	289.24	278.68	350.85	369.97

Tab. 6.3 *– Variations in yearly water volume [Mm^3] between periods in percentage for each scenario. The comparison of all the scenarios highlight the reduction of inflow water volumes moving towards far future, but not in a uniform way. The decrease is more conspicuous and monotonous in KNMI scenarios, while DMI and SMHI show an increased water volume in close future (within 20135) to decrease in the subsequent period. All RCP 4.5 scenarios show the most consistent diminution takes place in middle term future (2036-2065), while in RCP8.5 the most consistent decrease is shifted in far future period (2066-2095).*

	DMI		KNMI		SMHI	
Periods	**RCP 4.5**	**RCP 8.5**	**RCP 4.5**	**RCP 8.5**	**RCP 4.5**	**RCP 8.5**
Close future vs Present	1.60	0.45	-6.71	-7.59	5.82	3.25
Middle term future vs Close future	-7.01	2.97	-14.94	-13.83	-9.39	-1.90
Far future vs Middle term future	4.84	-4.52	-6.03	-9.78	-5.67	-5.85

studies on Alpine catchments of comparable dimensions and characteristics [Clarvis et al., 2014; Anghileri , 2014; Beniston et al., 2011]. Another interesting feature of future patterns is the inflow increase in November, also confirmed in literature [e.g. Anghileri, 2014], which is due to autumnal precipitation. Comparing the two peaks, we can see the second one will assume an increasing importance at the end of the century. In RCP 8.5, which represents extreme condition projections, the changes in the hydrograph highlighted hitherto are further stressed.

As regards inflow volumes, the main properties of inflow projections are highlighted in tables 6.1, 6.2 and 6.3, which compare the changes in yearly water volume of the inflow in the different time intervals of the scenarios.

All the scenarios agree the volume of available inflow is going to decrease in the 21st century. KNMI exhibits the strongest inflow reductions (table 6.3), more consistently moving towards far future, without showing appreciable differences between RCP 4.5 and 8.5. In DMI and SMHI the volume decrease is not monotonous, both in RCP 4.5 and 8.5: in close future the water volume is increasing to diminish in next periods. In all the RCP 4.5 scenarios, the decrease is concentrated in the middle term period, while in RCP 8.5 scenarios the most important reduction moves to far future.

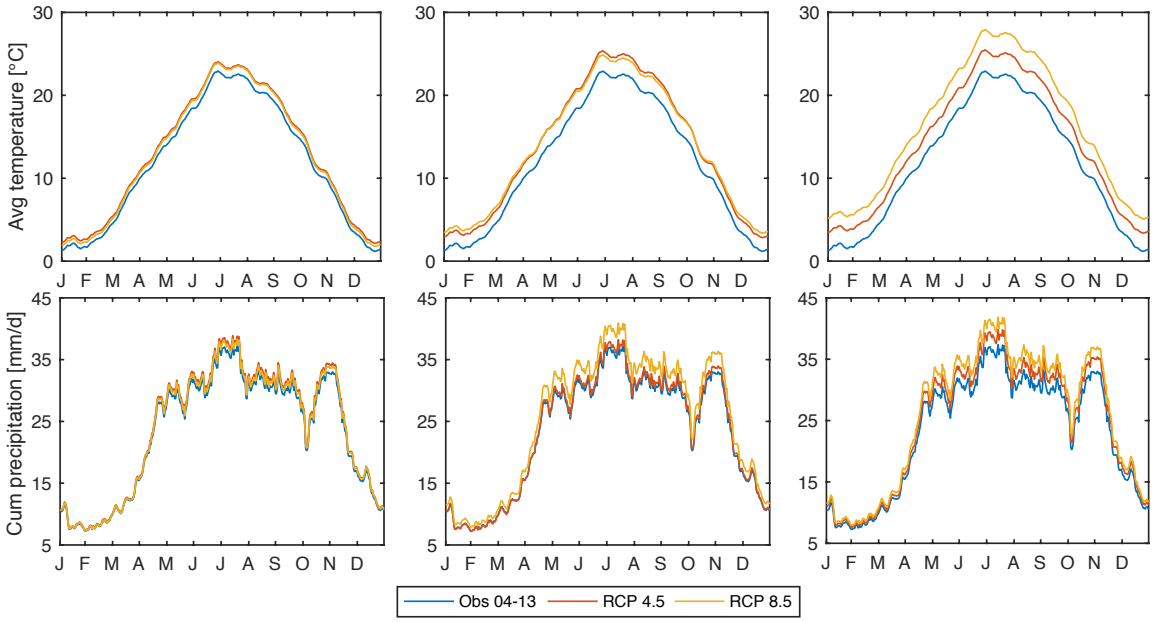

Fig.6.3 *– Cyclostationary mean temperature (first row) and cumulative precipitation (second row) for SMHI RCP4.5 (red) SMHI RCP 8.5 (yellow) and observations in 2004-2013 (blue) on the upper Adda river basin, computed with 20 days moving window. The three periods are highlighted from left to right. Moving towards far future, both temperature and precipitation are rising and the difference between RCPs becomes more marked.*

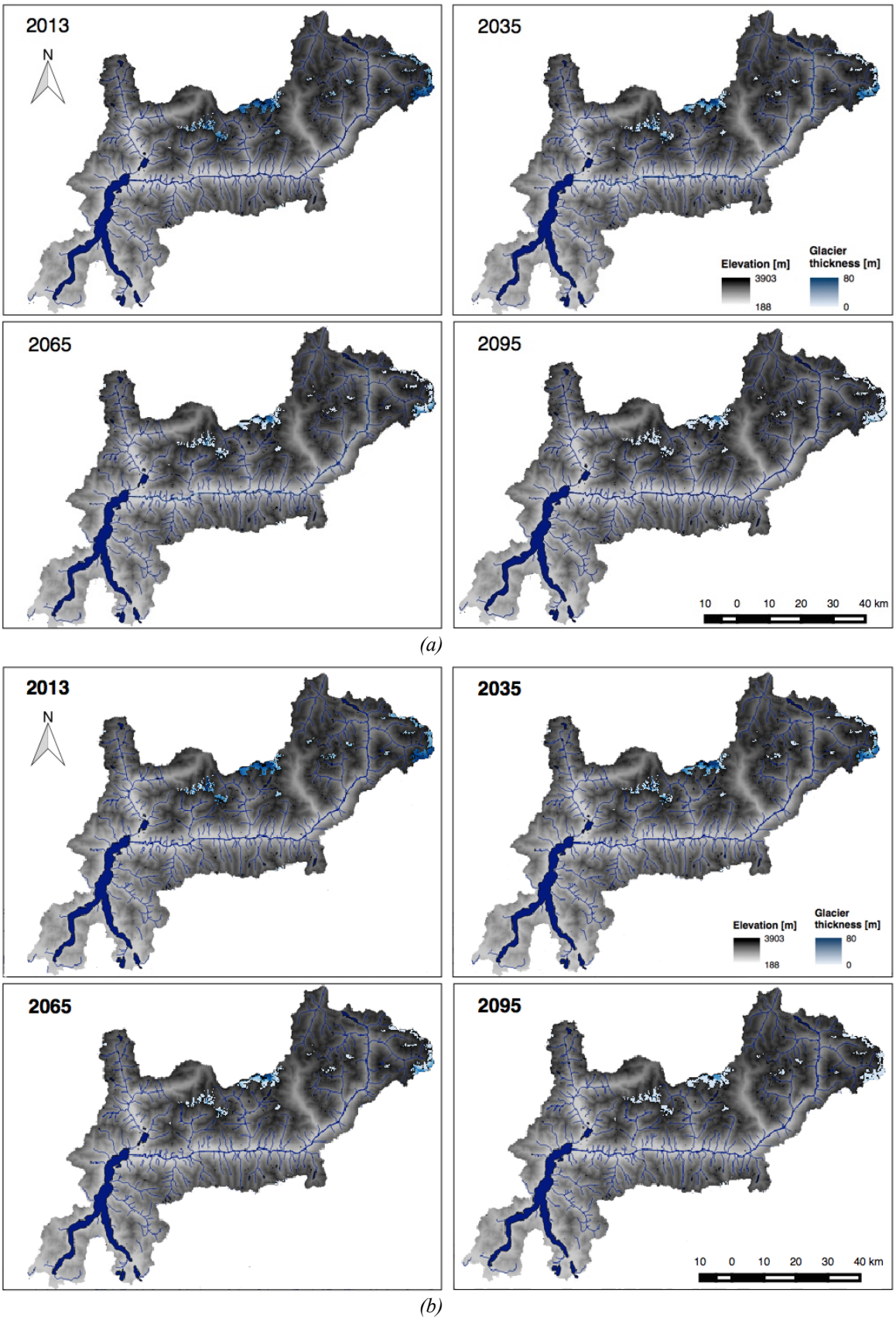

Fig.6.4 *– Maps of glacier thickness the end of the four periods. The maps have been produced simulating SMHI RCP 4.5 (a) and SMHI RCP 8.5 (b) scenarios with Topkapi-ETH model. Glacier shrinking is evident in Bernina (in the middle on the north side) and Ortis-Cevedale (north-east side of the basin) groups.*

Further analyses are conducted on SMHI scenarios, which well represent both peak anticipation and summer volume decrease. To explain these variations, we exploit TE potential as a spatially distributed physically based model. The model can provide multiple output, both distributed maps and point specific time series, concerning different hydrology aspects. Here we focus our attention on glacier pack. Glaciers are an important permanent storage that strongly affect the runoff regime. They recharge in winter accumulating snow that melts in the summer months providing a considerable runoff. Temperature rise causes an anticipated melting of the snow cover, which explains peak anticipation. The warmer climate melts the snow cover much rapidly than in past, causing a more consistent melting of the ice pack, which is left uncovered during the summer. Ice pack contribution to runoff is thus more appreciable at the end of the summer. When permanent ice pack is lost, we observe a consistent reduction in inflow volumes in summer time. Moreover, although precipitation is slightly rising too, higher temperature will favor liquid precipitation instead of snow falling: the winter snow pack will be smaller, thus affecting also ice pack accretion. Beniston [2003] showed the snow-line is likely to move up 150m per each degree of temperature rise. Overall, warmer temperatures and scarce snow accumulation conditions favor glacier-shrinking phenomenon, which has been widely treated in literature [Diolaiuti et al., 2012; Beniston, 2012; Huss 2011; Huss et al., 2010; Horton et al., 2006; Beniston, 2003; Haeberli and Beniston, 1998]. According to Diolaiuti et al. [2012], in 1991-2003 main Lombardy glaciers have already lost 25km^2 of cover. In close future, the most part of runoff contribution will come from small glaciers (<5km^2), which are common in Valtellina territory and are more sensitive to temperature changes. In the middle period, big glaciers will be affected by climate change, experiencing fragmentation first and retreat after (figure 6.5). RCP 4.5 shows the glacier shrinkage peak will take place within 2065, while in RCP 8.5 the peak will be reached within 2095. In both cases, the glaciers are likely to disappear by the end of the 21st century. These results are in line with other studies findings [Marzeion et al., 2012; Beniston , 2012].

Tab. 6.4 *– Analysis of glacier data in Adda river basin. Each statistics is calculated at the end of each period i.e. 2013, 2035, 2065, 2095 and derived from the maps in figure 6.5. Cover area is computed for each period, then the percentage of remaining ice cover and volume compared to 2013 and the variation between consequent periods and are computed.*

		SMHI RCP 4.5			SMHI RCP 8.5		
Periods	**Present**	**Close future**	**Middle term future**	**Far future**	**Close future**	**Middle term future**	**Far future**
Area [km^2]	80.5	61.75	33.9375	18	62.875	36.5625	9.5
Comparison to present [%]		76.71	42.16	22.36	78.11	45.42	11.80
Variations between periods [%]		-23.29	-45.04	-46.96	-21.89	-41.85	-74.02

Tab. 6.5 *– Analysis of glacier data in Adda river basin. Each statistics is calculated at the end of each period i.e. 2013, 2035, 2065, 2095 and derived from the maps in figure 6.5. Mean volume is computed for each period, then the percentages of remaining ice volume compared to 2013 and the variation between consequent periods and are computed.*

		SMHI RCP 4.5			SMHI RCP 8.5		
Periods	**Present**	**Close future**	**Middle term future**	**Far future**	**Close future**	**Middle term future**	**Far future**
Avg Volume [Mm^3]	3676.10	1676.51	396.48	89.94	1768.81	485.76	31.10
Comparison to present [%]		45.61	10.79	2.45	48.12	13.21	0.85
Variations between periods [%]		-54.39	-76.35	-77.32	-51.88	-72.54	-93.60

Tab. 6.6 *– Analysis of Forni glacier group data. Each statistics is calculated at the end of each period i.e. 2013, 2035, 2065, 2095 and derived from the maps in figure 6.6. Cover area and mean volume are computed for each period, then the percentage of remaining ice cover and volume compared to 2013 and the variation between consequent periods and are computed.*

		SMHI RCP 4.5			SMHI RCP 8.5		
Periods	**Present**	**Close future**	**Middle term future**	**Far future**	**Close future**	**Middle term future**	**Far future**
Area [km^2]	14.625	14.5625	11.6875	4.75	14.5625	11.6875	1.9375
Comparison to present [%]		99.57	79.91	32.48	99.57	79.91	13.25
Variations between periods [%]		-0.43	-19.74	-59.36	-0.43	-19.74	-83.42
Avg Volume [Mm^3]	40.10	27.85	10.87	3.10	28.59	11.16	0.80
Comparison to present [%]		69.44	27.12	7.72	71.30	27.82	2.00
Variations between periods [%]		-30.56	-60.95	-71.53	-28.70	-60.98	-92.82

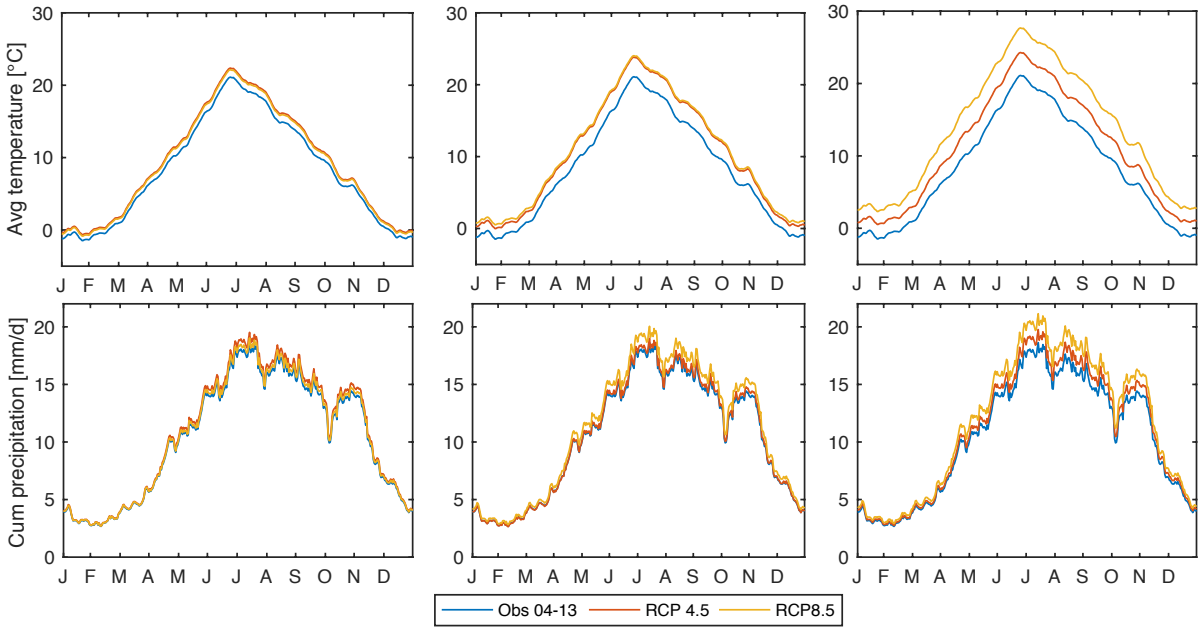

Fig.6.5 *– Cyclostationary mean temperature (first row) and cumulative precipitation (second row) for SMHI RCP4.5 (red) SMHI RCP 8.5 (yellow) and observations in 2004-2013 (blue) in Cancano-San Giacomo drainage basin, computed with 20 days moving window. Moving towards far future, both temperature and precipitation are rising and the difference between RCPs becomes more marked.*

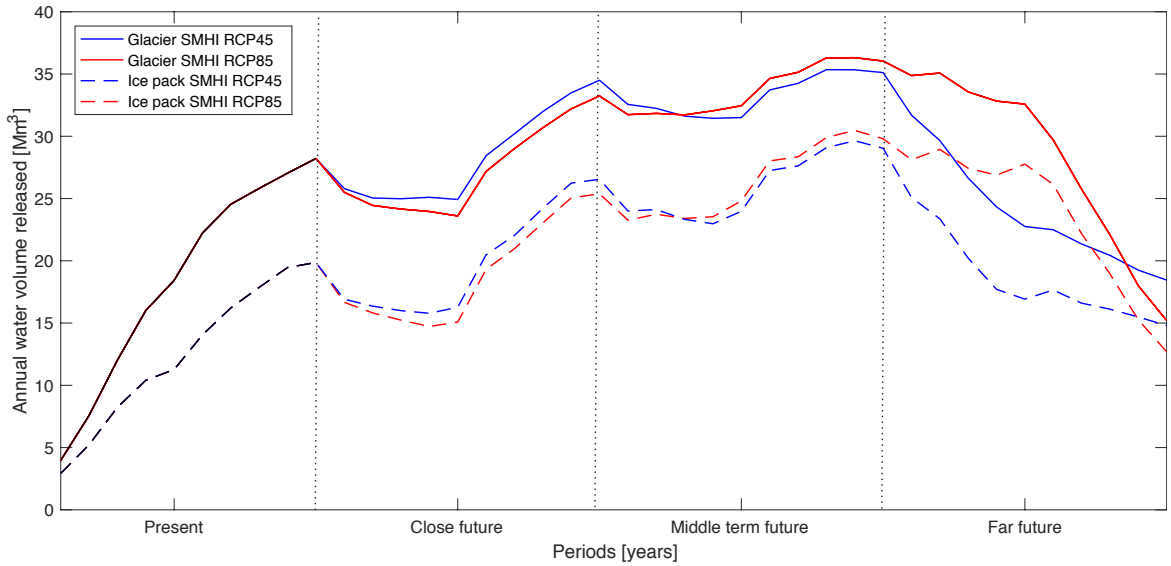

Fig.6.6 *– Mean yearly runoff volume released from Forni glacier, computed with 5 years moving window. Solid lines represent the total volume released by snow pack ice pack, dashed lines represent the release by ice sheet only. The series have been produced simulating SMHI RCP 4.5 (blue lines) and SMHI RCP 8.5 (red lines) scenarios with Topkapi-ETH model. Simulation of the observed drivers is reported in black.*

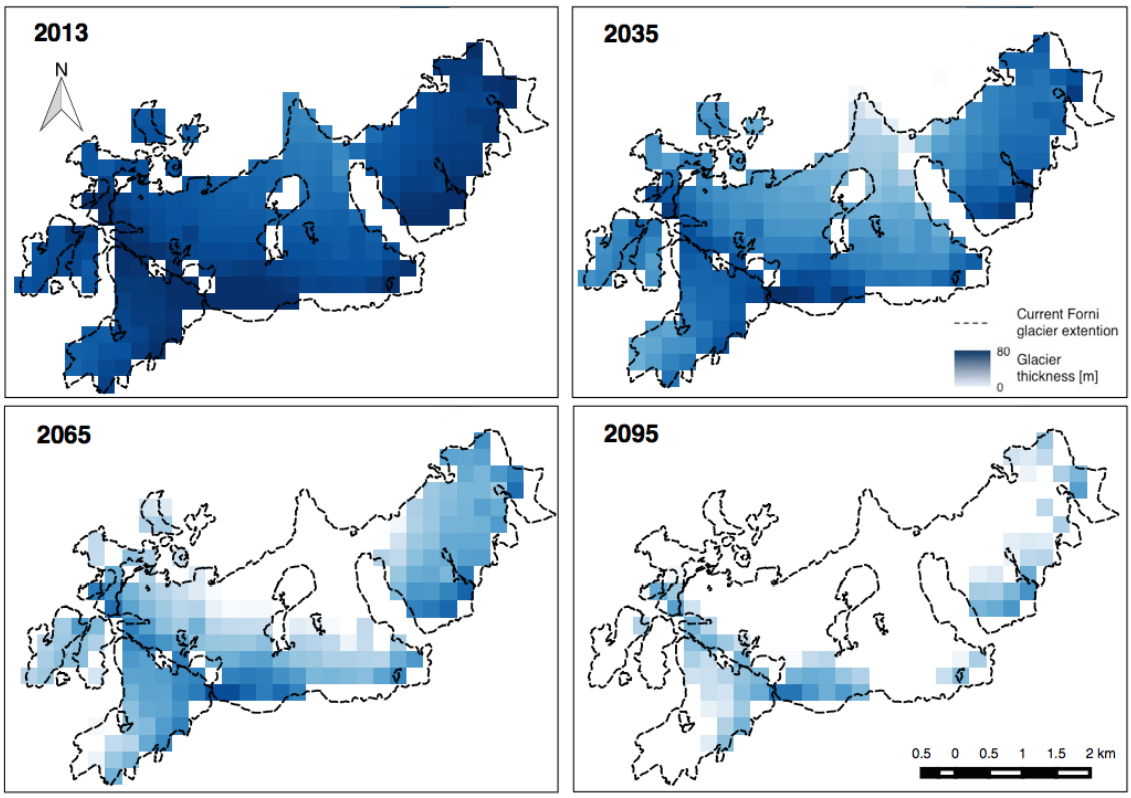

(a)

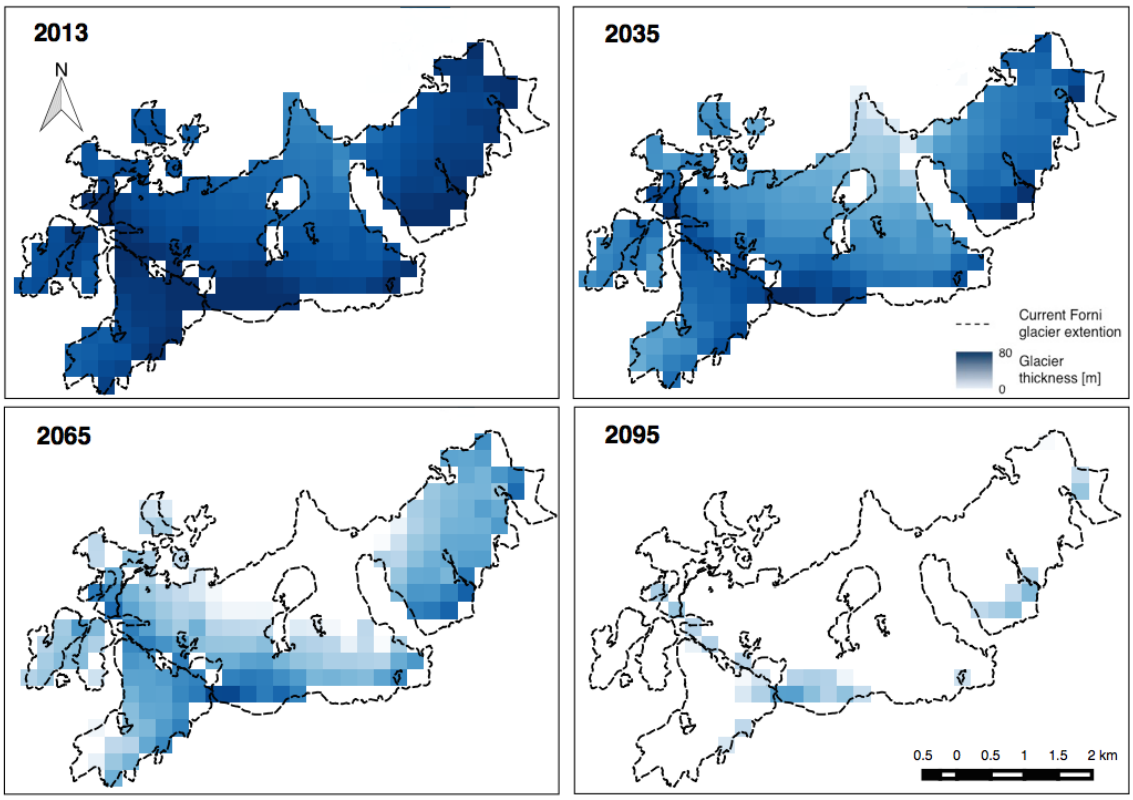

(b)

Fig.6.7 *– Maps of glacier thickness at present and the end of the three periods – focus on Forni glacier. The maps have been produced simulating SMHI RCP 4.5 (a) and SMHI RCP 8.5 (b) scenarios with Topkapi-ETH model. The dashed line represents Forni extension at the end of 2013.*

Since 90% of A2A reservoir inflow is diverted from streams that originate from glacier's runoff, it's worth to focus on the impacts of climate change on the main glacier in Cancano-San Giacomo basin, Forni glacier group. Located between 2541-3544m a.s.l. in the east end of Alta Valtellina, with its 12km^2 it's one of the biggest Italian glaciers [Diolaiuti and Smiraglia, 2010] and its runoff constitutes a significant inflow volume for A2A reservoirs system.

In figure 6.5 climatic conditions that force Forni glacier's dynamic are shown, while Forni glacier's evolution is shown in figure 6.7. As confirmed in other studies' results, the glacier will loose most of its volume and surface around 2040-2050. The trend in the runoff series (figure 6.8) grows until end of the middle term period (2040-2050) to decline in far future. Shrinkage accelerating phenomenon is responsible for the initial increase in runoff regime: as long as the permanent ice pack stores water, high temperature will favor its release from the glacier. When eventually the glacier is completely depleted, its contribution to runoff becomes negligible for the inflow. This explains the severe lack of water during summer months. Moreover, the runoff series confirms the snow pack is reducing from 2040-2050 as well, because high temperature will create unfavorable conditions for snowing even at high altitudes, and the reduction is more stressed in RCP 8.5 than in RCP 4.5.

6.2 IMPACT OF CLIMATE CHANGE ON A2A HYDROPOWER SYSTEM

Climate change will affect the hydrological system of upper Adda river territory and Cancano-San Giacomo reservoir inflow. As explained in chapter 5, the currently operating policy (BAU) has been design using historical inflow statistics (2008-2014). Since future climatic conditions will be consistently different from historical ones, BAU policy might not be able to guarantee the same hydropower system performances as in history. In this section we explore the impacts of the new hydrological regimes on energy production. For this purpose, we simulate the hydropower system using BAU policy under future inflow projections. The performances of the system in terms of revenue are expressed in table 6.7. Changes in the inflow conditions cause a decrease in the hydropower performance for all the scenarios considered. In particular the decrease in hydropower revenue is due to the reduced water availability. In fact the worsening is more severe in middle term future and

far future, when the yearly volume of inflow is conspicuously reduced. The extreme conditions represented by RCP 8.5 scenario experience further volume reduction than RCP 4.5 average condition. The impact in close future is smaller than in middle term and far future, because close future inflow distribution is quite similar to historical one. It's interesting to note that, although the water availability rises in DMI and SMHI close future (see table 6.2), BAU yields worst performances than in historical period. This is mainly the effect of snow-melting timing, which is anticipated by 5 days on average (table 6.1). On the contrary, KNMI scenarios, which experience -7% in yearly water volume in the first period but not an evident peak anticipation, perform much worse than DMI and SMHI. This consideration once more confirms performances degradation is mainly due to inflow volume reduction. For sake of brevity, now on we show the results on SMHI RCP4.5 and SMHI RCP8.5 scenarios only, which better reflect literature findings about change in the inflow regime and well summarize both the characteristics of DMI and KNMI scenarios.

Tab. 6.7 *– BAU performances in terms of mean daily revenue [thousands €] in present and future. The operating policy has been optimized on 2008-2014 inflow series and the cyclostationary matrix of the prices, then has been simulated on present inflow series (first row) and on the future periods inflow series (following rows).*

	DMI RCP 4.5	**DMI RCP 8.5**	**KNMI RCP 4.5**	**KNMI RCP 8.5**	**SMHI RCP 4.5**	**SMHI RCP 8.5**
Present (2008-2014)	304.82	304.82	304.82	304.82	304.82	304.82
Close future	288.48	285.75	267.61	265.59	299.12	292.70
Middle term future	268.47	291.19	230.82	231.25	271.92	285.54
Far future	281.29	279.52	218.87	210.73	258.81	269.82

Tab. 6.8 *– Variation between the referring period and present performances of the BAU policy [%].*

	DMI RCP 4.5	**DMI RCP 8.5**	**KNMI RCP 4.5**	**KNMI RCP 8.5**	**SMHI RCP 4.5**	**SMHI RCP 8.5**
Close future	-5.36	-6.26	-12.21	-12.87	-1.87	-3.98
Middle term future	-11.93	-4.47	-24.28	-24.14	-10.79	-6.33
Far future	-7.72	-8.30	-28.20	-30.87	-15.10	-11.48

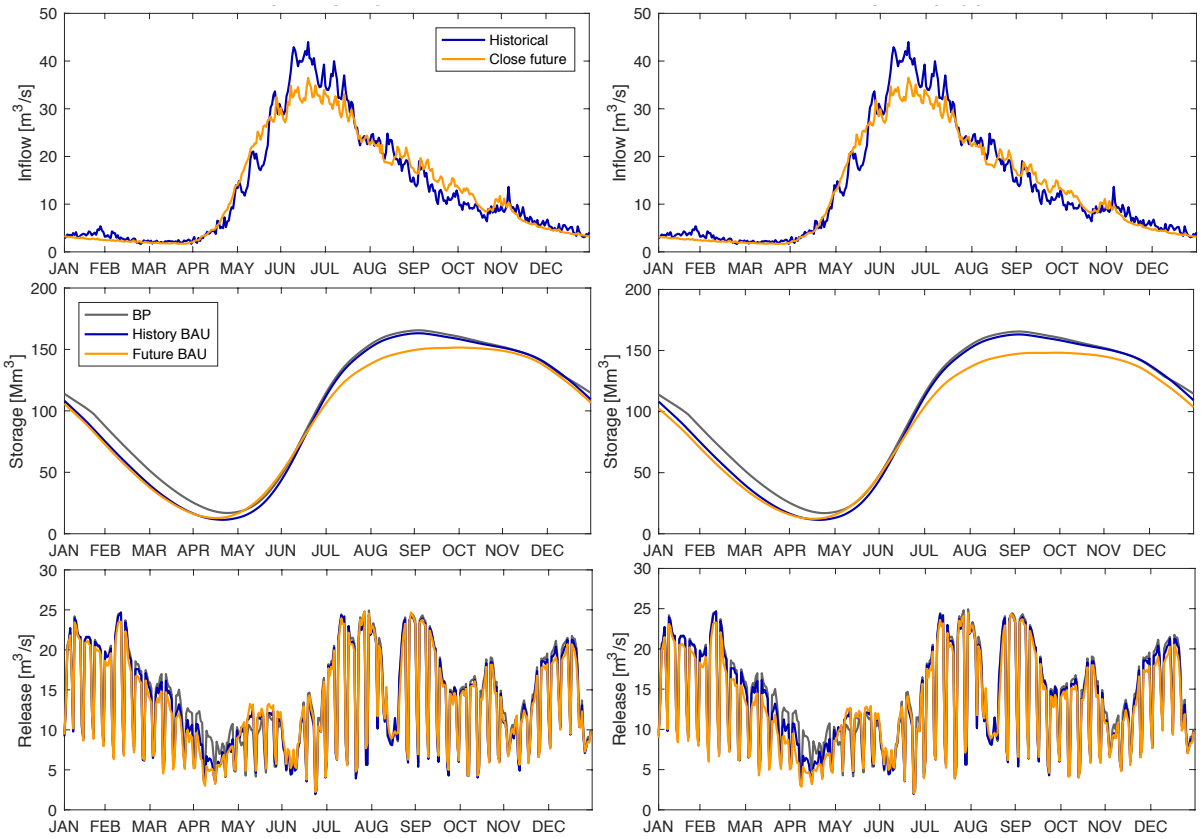
Historical
Close future
Inflow [m3/s]
BP
History BAU
Future BAU
Storage [Mm3]
Release [m3/s]
JAN FEB MAR APR MAY JUN JUL AUG SEP OCT NOV DEC

(a)

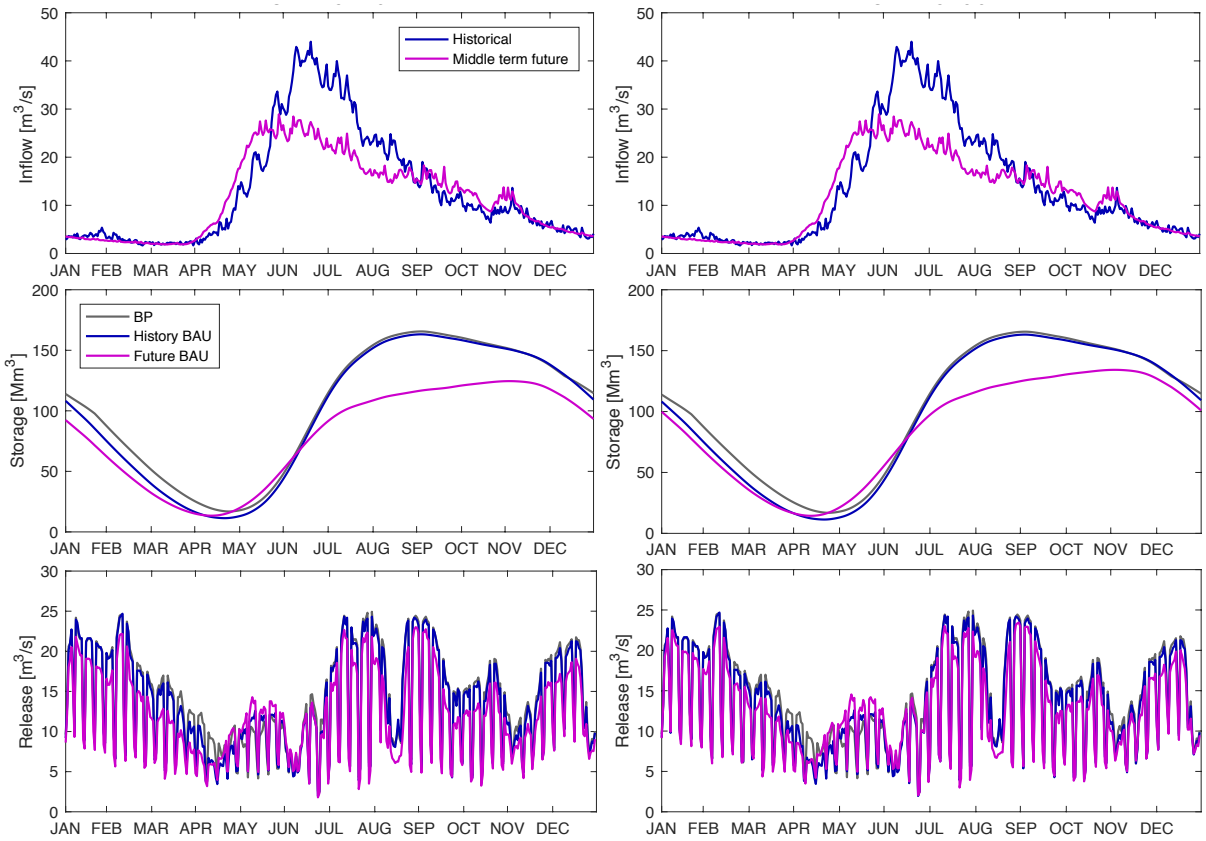
Historical
Middle term future
Inflow [m3/s]
BP
History BAU
Future BAU
Storage [Mm3]
Release [m3/s]
JAN FEB MAR APR MAY JUN JUL AUG SEP OCT NOV DEC

(b)

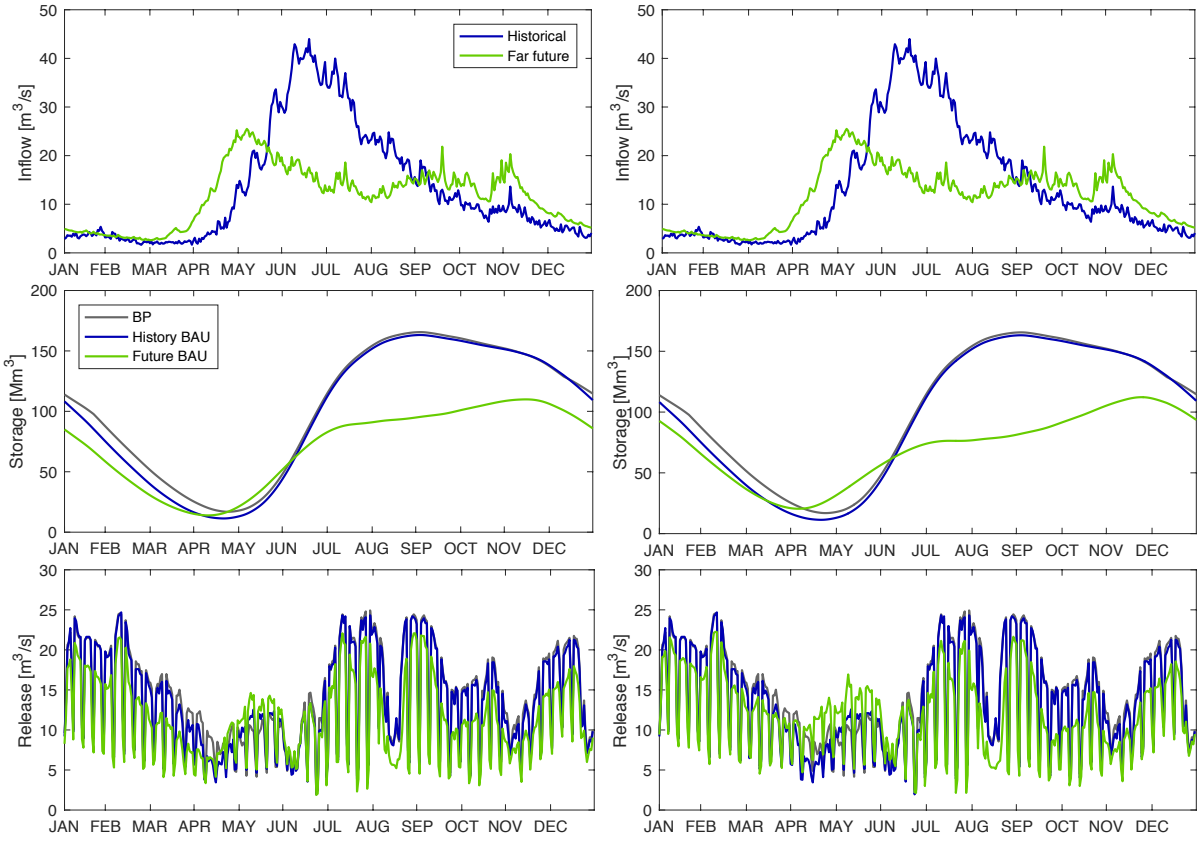

(c)

Fig.6.8 *– Reservoir dynamics with BAU policy in history and future. Inflow storage and release from the reservoir relative to close future (a), middle term future (b) and far future (c) are displayed, for SMHI RCP 4.5 (left) and SMHI RCP 8.5 (right). In all the figures, cyclostationary average inflow in future period (in color) and in historical (blue) are compared in the upper boxes; cyclostationary average storage dynamics computed with moving average of 20 days window is displayed in the middle boxes while cyclostationary release dynamics is shown in the bottom boxes. In storage and release trajectories boxes, blue lines indicate BAU policy simulated in historical conditions, colored lines indicate BAU policy simulated with future conditions, gray lines the BP in historical conditions.*

In order to better understand BAU policy vulnerability to climate changes we compare BAU policy reservoir dynamics under historical and future inflow (fig 6.8).

Water availability in future decreases conspicuously and future BAU releases (color in figure 6.8) is increasingly reduced moving towards far future. It's worth highlighting BAU policy behavior in the period of the spring snow-melting peak (half April - June): in this period future release are always higher than historical ones. BAU policy in fact is designed to intercept the peak of historical inflow, which is higher and more consistent than future ones, beyond occurring later in the year. When the small peak of the new

inflow arrives, the policy tends to release water immediately, expecting further inflows in the following days. Because of this mechanism BAU policy will not be able to intercept future inflow, with evident consequences on the storage trajectories.

BAU policy is optimal for the inflow condition it was designed for. The statistical description of the inflow guarantees a slight flexibility to the policy, which we can notice in DMI and more in SMHI scenarios. However, when the hydrological regime changes, the performances might not be optimal anymore. We thus observed an overall performance reduction.

6.3 ADAPTIVE CAPACITY

BAU policy has been designed to operate in 2008-2014 inflow regime, with good water availability, also stored in the ice pack, and an abundant peak from April to July. We've explained in chapter 2 that the decision maker could greatly benefit of forecasts information that might enhance design reservoir operating policy and thus the performances of the hydropower system. Since these conditions are mutating during the century, a straightforward strategy to improve future performance of A2A power system is adapting the operating policy to climate change by using inflow projections. In particular, inflow scenarios were used to compute a new probability density fucntion of the inflow to re-optimize the policy: we will refer to this policy as adapted (ADA) policy. We can thus test how A2A power system will behave in future conditions if the decision-maker chooses to adopt the ADA policy.

In figure 6.9 reservoir dynamics are compared for ADA policies and BAU policy simulated in future conditions, as well as future BP policy. We remind the benchmark policy is the optimized via DDP considering a perfect knowledge of the inflow. It provides the best performance for the A2A hydropower system in the DP family of policies.

As regards release dynamics, we can notice an overall diminishing of release volumes moving from close future to far future, which is naturally linked to inflow scarcity. The ADA policy pattern follows very well the BP one, failing mostly in April-May, at the end of the production period and before the occurring of inflow peak. In this period, in fact the storage is almost empty, but thanks to the perfect description of inflow, BP policy has still stored water to continue producing, thus showing higher release than ADA and BAU policies.

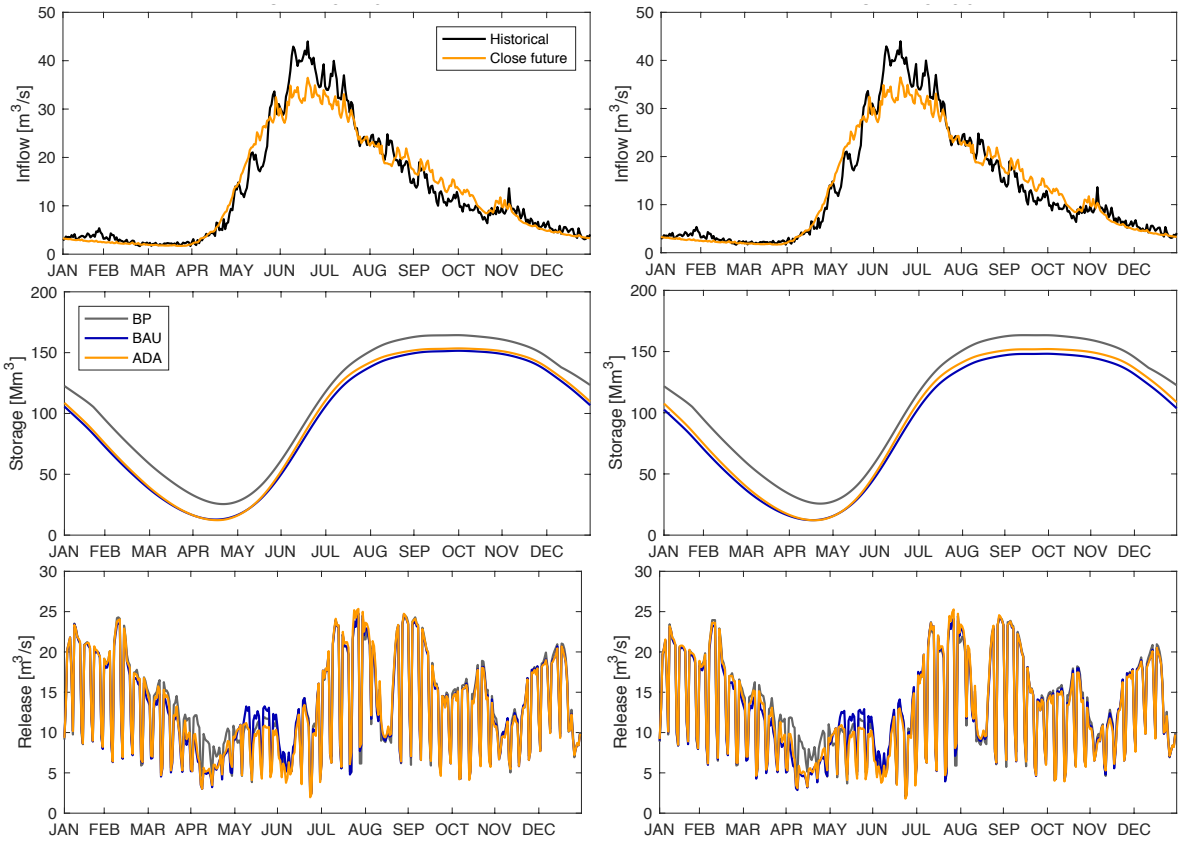
Historical
Close future
Inflow [m3/s]
BP
BAU
ADA
Storage [Mm3]
Release [m3/s]
JAN FEB MAR APR MAY JUN JUL AUG SEP OCT NOV DEC

(a)

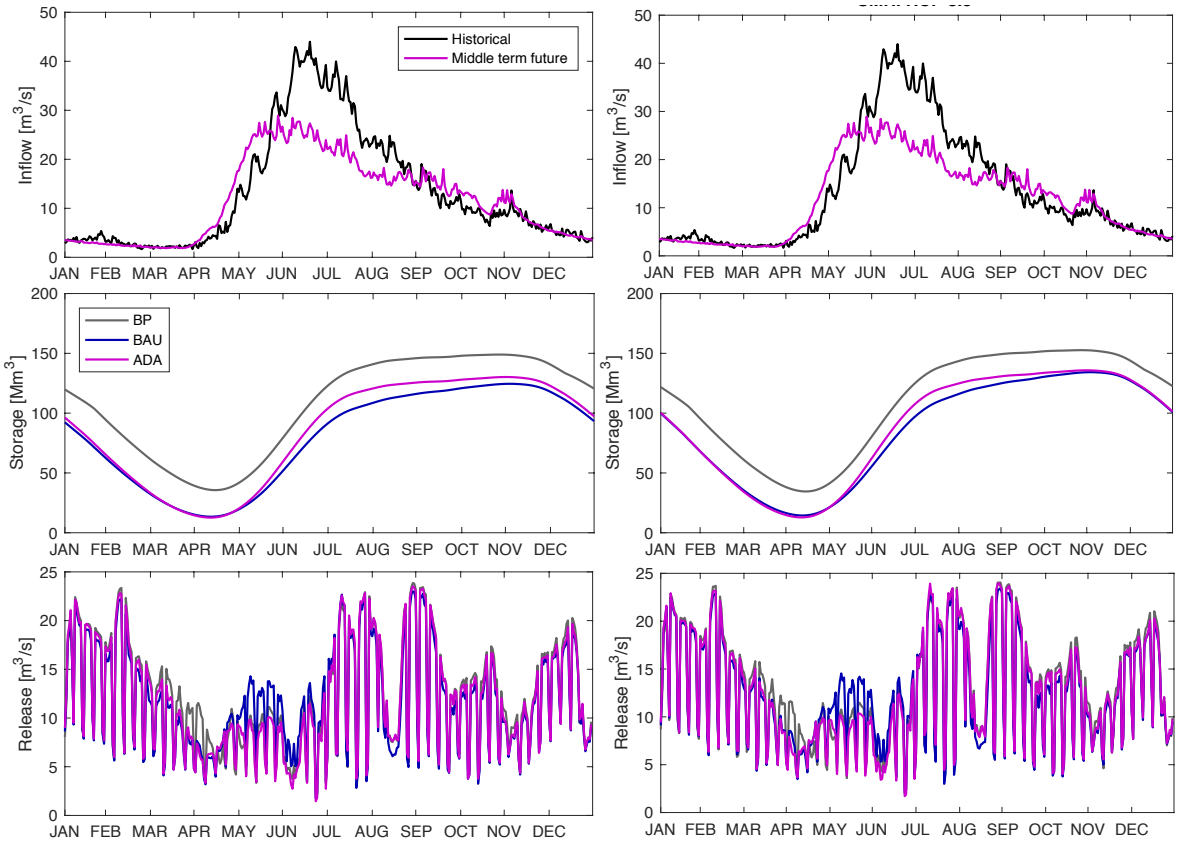
Historical
Middle term future
Inflow [m3/s]
BP
BAU
ADA
Storage [Mm3]
Release [m3/s]
JAN FEB MAR APR MAY JUN JUL AUG SEP OCT NOV DEC

(b)

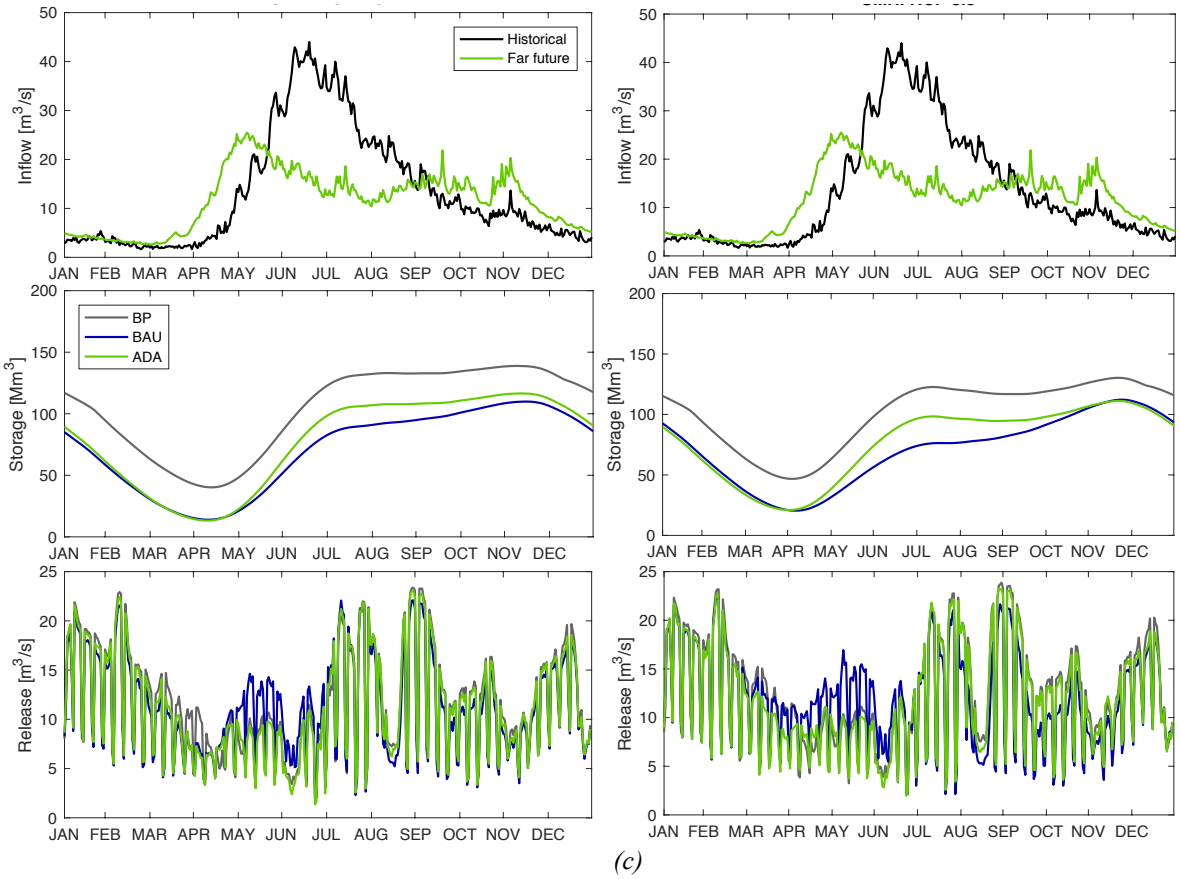

(c)

Fig.6.9 *Reservoir dynamics with ADA policies in future. Inflow storage and release from the reservoir relative to close future (a), middle term future (b) and far future (c) are displayed, for SMHI RCP 4.5 (left) and SMHI RCP 8.5 (right). In all the figures, cyclostationary average inflow in future period (in color) and in historical (black) are compared in the upper boxes; cyclostationary average storage dynamics computed with moving average of 20 days window is displayed in the middle boxes while cyclostationary release dynamics is shown in the bottom boxes. In storage and release trajectories boxes, blue lines indicate BAU policy simulated under future inflow scenarios, colored lines indicate ADA policy optimized and simulated with future inflow scenarios, gray lines the BP in future conditions.*

Comparing the reservoir dynamics of the ADA policy and of BAU policy, the former outperforms the latter mostly in snow-melting period: BAU is designed for a later snow-melting inflow to the reservoir and fails in capturing and saving the entire melting peak from its beginning. This behavior leads to reduced water availability in summer, which affects the release from August to October. Comparing the three period, we can appreciate how the most evident change will occur in middle term future, from 2040s. In this period releases generally decrease, which is accentuated also in far future period. Although the tendency to store water in spring to release it in winter is still visible, storage

pattern is deeply altered. Inflow volume reduction reflects again in reduced storages for all the policies: considering that in the first period the maximum storage can reach 180Mm^3, we observe a reduction of more than 30Mm^3 in middle term and far future. Historical storage pattern is characterized by two well distinct phase of accumulation and storage from May to November and the emptying phase during winter, when prices are high. While in present and close future, accumulation phase starts in May to end in August and can sustain the whole year production (fig. 6.9a central), it will take place respectively about 15 days and a month earlier in middle term and far future conditions (fig. 6.9b and 6.9c central). In middle term future, when inflows are still enough to sustain both production and accumulation, the two phases yearly pattern is maintained, while in severe water scarcity of the third period water reserves are used also to support summer production (note the deflection in storage pattern in ADA line fig. 6.9c central). November precipitations will constitute a source of water of increasing importance both for accumulation for winter and immediate energy production, while in present conditions they're immediately allocated to energy production. BAU policy shows extreme difficulties in following BP pattern. Moreover, BP trajectories in consistent periods are almost insensitive to RCP 8.5 and RCP 4.5 scenarios differences, while the greater uncertainty associated to RCP 8.5 affect both BAU policy and ADA policies.

Analyzing revenue performances, BP and BAU policy simulated under inflow projections in consistent periods constitute an upper and lower boundary to ADA policies. Both BAU and ADA are operative policies optimized via SDP algorithm: ADA policies are an evolution of BAU policy and are designed considering inflow projections. The importance of taking into account the new inflow conditions in the design of the operating policy can be measured by comparing the improvement of the ADA polices performances respect to the BAU policy in future conditions ones: we refer to this difference as "adaptive capacity" (AC) of the BAU policy

$$AC_T = \frac{ADA_T - BAU_T}{ADA_T} \cdot 100 \qquad [6.1]$$

where the subscript T indicates the period which the simulation refers to, with *T* equal to close future, middle term future or far future. The difference in performances between the BAU policy simulated under changing conditions and future BP policy allows evaluating the complete improvement space (IS).

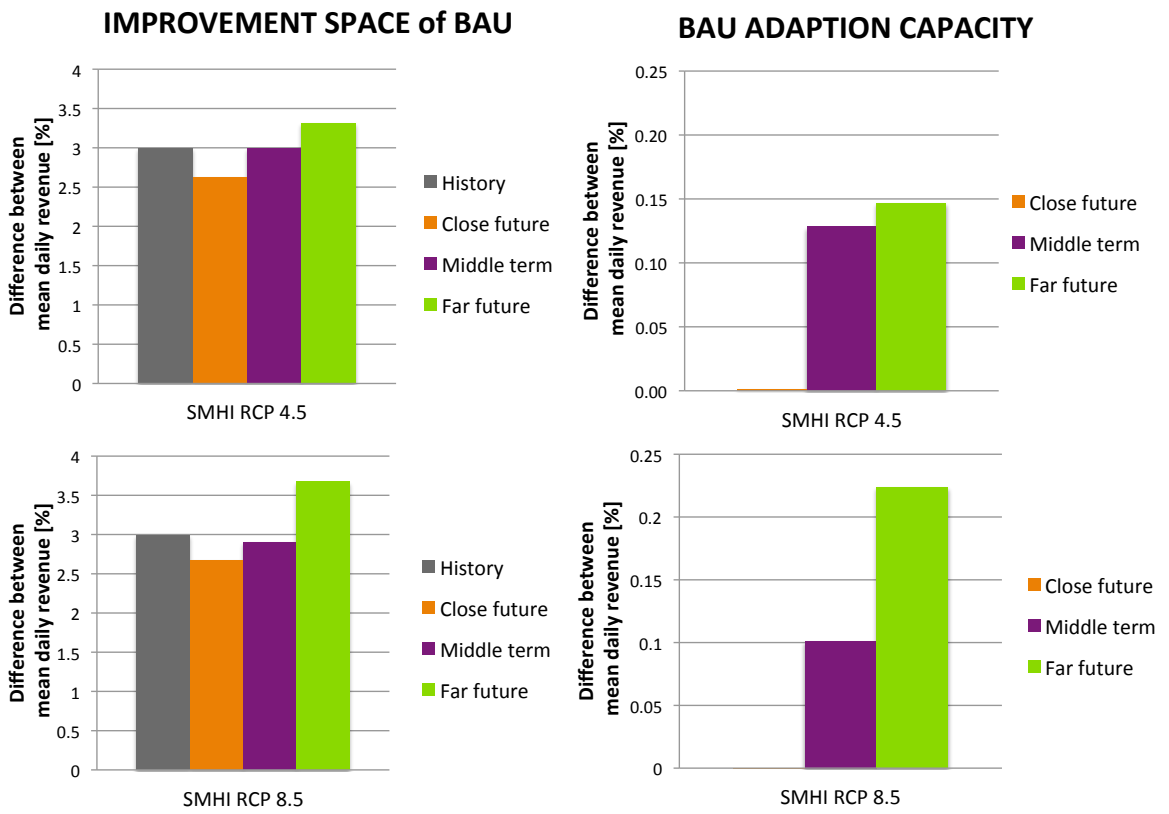

Fig.6.10 *– Improvement space (left) and adaptive capacity (right) of BAU policy for SMHI RCP4.5 and SMHI RCP8.5 in the different periods: gray refers to history, orange to close future, purple to middle term future, green to far future.*

$$IS_T = \frac{BP_T - BAU_T}{BP_T} \cdot 100 \qquad [6.2]$$

The improvement space can be filled by policy designed considering other information (inflow forecast, snow cover thickness, glacier state and son on), e.g. the ADA policies.

Figure 6.10 shows the BAU improvement space and adaptive capacity. More precisely, historical IS (gray) has been computed comparing the historical operating rule (i.e. the simulation of observed release trajectory) to BP optimized and simulated in historical period. Future IS is evaluated comparing BAU policy simulations under future inflow and future BP. Historical IS is quite consistent: the currently operating rule could gain 20835€/day adopting a perfect description of the inflow. On the other hand, it's important to underline that the historical operating rule is optimized also considering other drivers that were not included in our analysis (e.g. energy price or the secondary interest we mentioned in chapter 5). IS in future it's generally smaller: in absolute terms, the

added revenue is on average +7840€/day, +8222€/day and +8437 €/day in the three periods respectively. This means that, although the remarkable differences in reservoir storage and release trajectories, in terms of daily revenue BAU and BP are quite close. Reduction in water availability strongly affect future BP performances, with an average loss of 25600€/day from historical to future conditions: little improvement space tells there's no way to contrast future losses due to water availability reduction using only forecast inflow information. This result is confirmed also by adaptive capacity (right in figure 6.10).

Overall AC is practically negligible (+0€/day, +320€/day, +500€/day respectively in absolute numbers). Strong inflow reduction in future deeply affects both BP and ADA policies, flattening the performances. As expected, we can see the more yearly inflow pattern changes the higher the AC is. In close future, AC is zero, meaning that ADA policy doesn't offer any advantage respect BAU policy. In another perspective, BAU policy will be competitive with adaptive ones until about 2040s, which is the period the glacier will undertake a considerable shrinking. AC is higher for far futures, and in particular under RCP 8.5 scenario. Although little, the AC of BAU policy in middle term future and far future is more marked. As we've explained in section 6.2, in these periods the hydrological regime changes considerably and the snow-melting peak timing will be anticipated of more than 30 days on average because of warmer temperatures. ADA policies mainly adapt to this aspect of the new inflow description, better intercepting the waters deriving from snow cover and glaciers runoff.

6.4 ENERGY PRICES PROJECTIONS POTENTIAL

Hydropower operations are mainly driven by water availability and energy prices. A central assumption in this thesis assessment is neglecting energy prices future changes to focus on hydrological condition alterations. However, prices have a considerable influence on hydropower reservoir operations, maybe even more than inflow. In this section an insight of energy prices information is given. In out thesis, energy prices are included in the reservoir operations design considering a cyclostationary average, the matrix of the prices, derived by averaging from 2009-2015 hourly price series. The matrix reproduces in a simple manner the main trends in observed prices series and can thus be interpreted as the simplest descriptive model of the prices. We can reasonably suppose

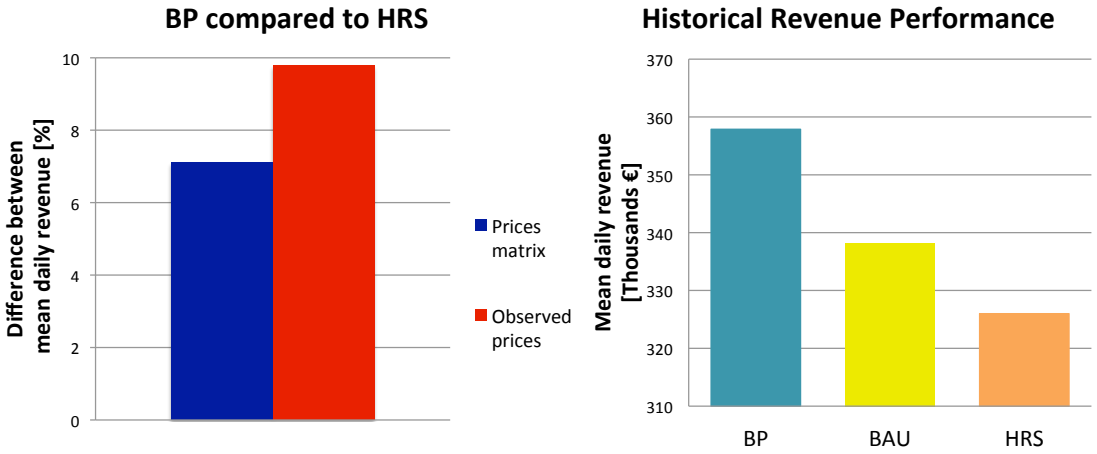

Fig.6.11 *– Prices modeling room for improvement. On the left, BP optimized with cyclostationary matrix of the prices (blue) and with observed prices (red) are normalized respect to historical release series simulated with observed prices (HRS). On the right, BP is compared to BAU policy simulated with observed prices and historical revenue series simulated with the observed prices.*

better information regarding socio-economic drivers could enhance hydropower system performances, as well as hydrological information.

We thus use energy prices time series to obtain a preliminary estimation of the value of price information in the historical period. We first focus on the total value of perfect information. We design a BP policy that considers both socio-economic drivers perfect knowledge and inflow perfect information in policy design. This BP is compared to BP designed respect to inflow information only. The performances of the two policies are normalized to the historical simulation of observed release series performances, then compared. The result is shown in figure 6.11 (left). The decision maker can gain up to 10% including also prices in policy design. The difference between the columns (+2,67%) highlights the gain in revenue yielded by price information only. In absolute terms, perfect price information can generate 31886 € per day. The room for improvement offered by price modeling seems to be quite consistent.

On the right in figure 6.11, revenue in historical condition is computed for BP, BAU and observed release series. BAU policy is optimized with the cyclostationary matrix of the prices and simulated under historical price series. The comparison between BAU and BP performances allows understanding the space of improvement of BAU. In absolute values BAU policy could improve its performances of 19697€ per day. In order to improve BAU performances, price future projection could be included in policy design, using the same approach applied to find mitigation measures to climate change.

Gaudard et al. [2013] demonstrate that a comprehensive approach that integrates hydrological and socio-economic aspect might be able to mitigate hydropower losses.

Energy prices are mainly influenced by energy demand and supply and by the energy generation portfolio used in the market. The transmission network configuration plays an important role too, causing congestion in energy transmission in intensive production areas that can separate energy market in isolated sub-markets with different energy prices. The increasing adoption of renewable sources and the need of reduction of fossil fuel technologies will probably lead to lower energy prices. Distribution networks are likely to be improved, moving towards faster and more efficient energy transmission. Forecasting prices scenarios in not an easy task: models have to consider several different aspect in prices formation and each market follows its own rules. Price scenarios can be simulated using model of the energy market reproducing the main drivers and technological implementations above described [Schlecht and Weigt, 2014a; Schlecht and Weigt, 2014b]. However, prices scenarios are still an open research question: the number of available and reliable detail energy market models is very limited.

7
CONCLUSIONS

In this work we assess the impact of climate change on the Alpine hydrological regime and hydropower. We carry out the assessment on a real case study, A2A hydropower system, located in the upper Adda river basin. More specifically, we first evaluate the how climate change is going to affect the hydrological regime of the upper Adda river basin in order to understand future water availability for the power system, paying particular attention to glaciers evolution in the 21st century. We then focus our attention on the impacts of climate change on hydropower, first establishing the operating rule for the power system reservoir in historical period. We test the vulnerability of the historical operating rule impact of future hydrological regime and search for mitigation measures to future hydrological conditions. We improve power system operations including in policy design forecasted information concerning future inflows in order to adapt the system to future hydrological conditions. Eventually we estimate the value of forecast to the A2A power system decision maker.

In first place, we need to model future climate. Starting from high-resolution data from EURO-CORDEX scenarios, we downscale temperature, precipitation and cloud cover transmissivity series to local scale via quantile-mapping technique, obtaining meteorological variables scenarios for the period 2006-2095. In literature, climate change has been proven to make remarkable changes in future Alpine environment. The trends described in literature are confirmed by our projections: temperature rising, reduced snowing and increasing of precipitation extreme events. The hydrological model of the Adda river basin fed with meteorological variables projections in several locations provides the inflow projections to A2A reservoir. Future inflow trends exhibit changes both in timing of the snow-melting period, which is anticipated (from few days in the

close future to a month in far future on average), and in yearly water volume availability, which is significantly reduced (+4%, -3.44%, -7.63% respectively in the three periods). The initial increase in water availability in close future is due to a consistent loss in permanent glacier. An analysis conducted on the whole glacial system in Adda river basin and focused on Forni glacier confirms literature forecasts: climate change is threatening glacier system, because high temperature is causing reduction in snow covers and consistent ice pack melting. Small glaciers are going to disappear within 2030s, while from 2040s climate change will severely affect major glaciers as Forni. Beyond these results, this work allowed us to establish a framework to analyze in detail future climate scenarios and produce a wide range of hydrological variables forecast that could be highly informative and useful to hydroelectric companies to adapt their operating rules (e.g. glacier long-term state).

In order to understand how climate change will influence A2A power system, we first set a model of the hydropower reservoir operation using a normative approach, which describes the decision making process as an optimization problem. We consider a Multi-Objective optimization problem, maximizing the energy production and revenue.

The Multi-Objective problem is solved using Dynamic Programming. Respect to inflow uncertainty, we solve Dynamic Programming in its Stochastic form (SDP) and in the Deterministic one (DDP), providing optimal management policies that reflect the behavior of a rational hydropower agent in deterministic and stochastic situations. SDP supposes a statistical description of the inflow is known at the moment the optimal release decision is taken, while DDP supposes a perfect knowledge of the inflow at the moment of taking the decision. SDP policy thus reproduces the operating policy (BAU and ADA) while DDP (BP) represents an ideal experiment to be used ad upper benchmark to compare SDP performances.

SDP and DDP policies are optimized and simulated on historical inflow (2008-2014). The performances are measured in terms of daily revenue and energy production and reservoir dynamics (storage and release) are compared as well. In first place, the conflict between the objectives was found to be really small in SDP policy and completely absent in the deterministic context. We thus reduced the Multi-Objective problem to a Single-Objective one focusing on revenue only.

The simulation of recorded release and SDP operating policy yield comparable revenue performances and the patterns of reservoir dynamics are quite similar. SDP model can thus well reproduce the main dynamics describing the behavior of the decision-maker.

We then answered the question of how current operating policy will behave in future hydrological conditions. Historical SDP policy optimized on 2008-2014 inflow series, which we refer to as BAU, is simulated under future inflow projections. The results show historical policy will maintain still acceptable performances in close future period (2006-2035) to worsen its performance in middle term (2036-2065) and far future (2066-2095). Revenue will decrease from 2-13% in close future, 4-24% in middle term future and 8-31% in far future, depending on the scenario. BAU policy fails in capturing melting-peak, experiencing water scarcity during the summer and autumn. These results are due to SDP sensitiveness to inflow pattern description. SDP is designed according to the historical inflow conditions: when this condition slightly change, the policy can still adapt to different inflow regime without consistent degradation in performances thanks to its statistical description of the inflow. When inflow conditions strongly differ from the conditions the policy was designed for, the policy is not able to adapt to new inflow conditions, degrading its performances. Moreover, BAU policy is really vulnerable to inflow availability decrease, which will be increasingly severe due to permanent glacier melting.

In climate change the inflow pattern changes considerably moving towards future. A straightforward idea suggests updating inflow information to enhance SDP performances. We thus solved the problem forcing both SDP and DDP with future inflows scenarios, producing adaptive operating policies (ADA) and their respective future benchmark (BP). ADA policies better capture inflow peak timing, storing all the available inflow volume, while November rains will become an important source of water especially in far future conditions.

We analyze the adaptive capacity of the BAU policy, defined as the variation in percentage between BAU policy performances simulated under future inflows and ADA policies ones. Adaptive capacity gives an estimation of forecast inflow information value, more specifically it quantifies the enhancement in policy operations due to the introduction of the forecasts. Adaptive capacity is really reduced (on average 0%, +0.1%, +0.2% in the three periods): newly introduced information allows mitigating snow-melting anticipation, better capturing the spring inflow peak, but could not mitigate in any case the consistent reduction in water volumes.

We also compared BP policies performances to BAU policy ones in future conditions, in percentage as well: this is the total space of improvement of BAU policy. Improvement space quantifies the enhancement in policy operations due to perfect knowledge of inflow, which is the most accurate description of inflow possible. Adaptive

policies (e.g. ADA) optimized considering other information in policy design, could fill the gap between BAU policy and BP, enhancing the performances of BAU policy. Our ADA simple policy only considers inflow projections. Total improvement space is really reduced, both in historical and future conditions (3%, 2.67%, 2.95%, 3.49%). The decrease in water availability affects both BP and BAU policies: this leads to BP revenue decreasing to BAU revenue levels. Although the value of inflow forecast increases in future periods, because of conspicuous hydrological changes, the value of inflow forecast information to hydropower decision-maker seems to be rather small. In order to obtain further improvement in performances of the ADA policies, a more accurate description of inflow could be provided, by introducing a parameter to model melting-season starting date or by a more accurate modeling of inflow variability. Other information, such as glaciers state or snow-pack thickness, could be directly included in policy design to adapt it to future conditions.

Moreover, hydropower could benefit of socio-economic forecasted information. Water availability and energy prices are the main drivers leading the reservoir operations. In this thesis, we focused on hydrological impact neglecting prices change in future. Future prices pattern are likely to change in future.

We estimate the value of price complete information in historical period comparing BPs optimized and simulated with inflow and prices time series or inflow only. Preliminary results show that the value of price information only is comparable to inflow information one. Energy prices, modeled in this thesis by a simple cyclostationary average, could be modeled in more sophisticated ways and used in policy design to enhance hydropower system performances. Future prices are likely to significantly differ both in magnitude and pattern to historical one. The increasing importance of renewable changes on the market and more efficient transmission network are likely to produce lower future prices. Prices scenarios can be produced using transmission network models that describe the main drivers influencing price formation, but this is not a simple task, and reliable and accessible prices scenarios are difficult to obtain.

However, socio-economic driver influence on A2A hydropower system is an interesting aspect that shall find room in a more comprehensive analysis.

BIBLIOGRAPHY

Alfieri, L., Perona, P., & Burlando, P. (2006). Optimal water allocation for an Alpine hydropower system under changing scenarios. *Water resources management*, *20*(5), 761-778.

Allen, C. D., Macalady, A. K., Chenchouni, H., Bachelet, D., McDowell, N., Vennetier, M., ... & Gonzalez, P. (2010). A global overview of drought and heat-induced tree mortality reveals emerging climate change risks for forests. *Forest ecology and management*, *259*(4), 660-684.

Amodeo, E., Anghileri, D., Sessa, R. S., & Weber, E. (2007). Conflitto tra uso irriguo e idroelettrico delle acque del Lario. *Rapporto interno*, *51*, 7.

Anghileri, D., Pianosi, F., & Soncini-Sessa, R. (2011). A framework for the quantitative assessment of climate change impacts on water-related activities at the basin scale. *Hydrology and Earth System Sciences*, *15*(6), 2025.

Anghileri, D. (2014). Management of multi-purpose reservoirs under climate change: impact assessment and adaptation strategies.

Barontini, S., Grossi, G., Kouwen, N., Maran, S., Scaroni, P., & Ranzi, R. (2009). Impacts of climate change scenarios on runoff regimes in the southern Alps. *Hydrology and Earth System Sciences Discussions*, *6*(2), 3089-3141.

Beniston, M. (2003). Climatic change in mountain regions: a review of possible impacts. *Climatic change*, *59*(1), 5-31.

Beniston, M., Stoffel, M., & Hill, M. (2011). Impacts of climatic change on water and natural hazards in the Alps: can current water governance cope with future challenges? Examples from the European "ACQWA" project. *Environmental Science & Policy*, *14*(7), 734-743.

Beniston, M. (2012). Impacts of climatic change on water and associated economic activities in the Swiss Alps. *Journal of Hydrology*, *412*, 291-296.

Bindoff, N. L., Stott, P. A., AchutaRao, K. M., Allen, M. R., Gillett, N., Gutzler, D., ... & Mokhov, I. I. (2013). Detection and attribution of climate change: from global to regional.

Boé, J., Terray, L., Habets, F., & Martin, E. (2007). Statistical and dynamical downscaling of the Seine basin climate for hydro-meteorological studies. *International Journal of Climatology*, *27*(12), 1643-1655.

Carati, F. (1958). L 'impianto idroelettrico di Premadio (Sondrio).

Carenzo, M., Pellicciotti, F., Rimkus, S., & Burlando, P. (2009). Assessing the transferability and robustness of an enhanced temperature-index glacier-melt model. *Journal of Glaciology*, *55*(190), 258-274.

Castelletti, A., Pianosi, F., & Soncini-Sessa, R. (2008). Water reservoir control under economic, social and environmental constraints. *Automatica*, *44*(6), 1595-1607.

Castelletti, A., Galelli, S., Restelli, M., & Soncini-Sessa, R. (2010). Tree-based reinforcement learning for optimal water reservoir operation. Water Resources Research, 46(9).

Chen, C., Haerter, J. O., Hagemann, S., & Piani, C. (2011). On the contribution of statistical bias correction to the uncertainty in the projected hydrological cycle. *Geophysical Research Letters*, *38*(20).

Chen, J., Brissette, F. P., & Leconte, R. (2011). Uncertainty of downscaling method in quantifying the impact of climate change on hydrology. *Journal of Hydrology*, *401*(3), 190-202.

Ciarapica, L., & Todini, E. (2002). TOPKAPI: A model for the representation of the rainfall-runoff process at different scales. *Hydrological Processes*, *16*(2), 207-229.

Clarke, L., Edmonds, J., Jacoby, H., Pitcher, H., Reilly, J., & Richels, R. (2007). Scenarios of greenhouse gas emissions and atmospheric concentrations. *US Department of Energy Publications*, 6.

Clarvis, M. H., Fatichi, S., Allan, A., Fuhrer, J., Stoffel, M., Romerio, F., ... & Toreti, A. (2014). Governing and managing water resources under changing hydro-climatic contexts: The case of the upper Rhone basin. *Environmental Science & Policy*, *43*, 56-67.

Collins, M., Knutti, R., Arblaster, J., Dufresne, J. L., Fichefet, T., Friedlingstein, P., ... & Shongwe, M. (2013). Long-term climate change: projections, commitments and irreversibility.

Corripio, J. G. (2003). Vectorial algebra algorithms for calculating terrain parameters from DEMs and solar radiation modelling in mountainous terrain. *International Journal of Geographical Information Science*, *17*(1), 1-23.

Culley, S., Noble, S., Yates, A., Timbs, M., Westra, S., Maier, H. R., ... & Castelletti, A. (2016). A bottom-up approach to identifying the maximum operational adaptive capacity of water resource systems to a changing climate. *Water Resources Research*, *52*(9), 6751-6768.

Denaro, S., Anghileri, D., Giuliani, M., & Castelletti, A. (2017). Informing the operations of water reservoirs over multiple temporal scales by direct use of hydro-meteorological data. *Advances in Water Resources*, *103*, 51-63.

Déqué, M. (2007). Frequency of precipitation and temperature extremes over France in an anthropogenic scenario: Model results and statistical correction according to observed values. *Global and Planetary Change*, *57*(1), 16-26.

Dessai, S., Adger, W. N., Hulme, M., Turnpenny, J., Köhler, J., & Warren, R. (2004). Defining and experiencing dangerous climate change. *Climatic Change*, *64*(1), 11-25.

Diolaiuti, G., Bocchiola, D., D'agata, C., & Smiraglia, C. (2012). Evidence of climate change impact upon glaciers' recession within the Italian Alps. *Theoretical and Applied Climatology*, *109*(3-4), 429-445.

Diolaiuti, G., & Smiraglia, C. (2010). Changing glaciers in a changing climate: how vanishing geomorphosites have been driving deep changes in mountain landscapes and environments. *Géomorphologie: relief, processus, environnement*, *16*(2), 131-152.

Ellabban, O., Abu-Rub, H., & Blaabjerg, F. (2014). Renewable energy resources: Current status, future prospects and their enabling technology. *Renewable and Sustainable Energy Reviews*, *39*, 748-764.

Fatichi, S., Rimkus, S., Burlando, P., Bordoy, R., & Molnar, P. (2013). Elevational dependence of climate change impacts on water resources in an Alpine catchment. *Hydrology and Earth System Sciences Discussions*, *10*(3), 3743-3794.

Frei, C., Schöll, R., Fukutome, S., Schmidli, J., & Vidale, P. L. (2006). Future change of precipitation extremes in Europe: Intercomparison of scenarios from regional climate models. *Journal of Geophysical Research: Atmospheres*, *111*(D6).

Frias, M. D., Zorita, E., Fernández, J., & Rodriguez-Puebla, C. (2006). Testing statistical downscaling methods in simulated climates. *Geophysical Research Letters*, *33*(19).

Fujino, J., Nair, R., Kainuma, M., Masui, T., & Matsuoka, Y. (2006). Multi-gas mitigation analysis on stabilization scenarios using AIM global model. *The Energy Journal*, 343-353.

Fuss, S., Canadell, J. G., Peters, G. P., Tavoni, M., Andrew, R. M., Ciais, P., ... & Le Quéré, C. (2014). Betting on negative emissions. *Nature Climate Change*, *4*(10), 850-853.

Gao, X., Pal, J. S., & Giorgi, F. (2006). Projected changes in mean and extreme precipitation over the Mediterranean region from a high resolution double nested RCM simulation. *Geophysical Research Letters*, *33*(3).

Gaudard, L., Gilli, M., & Romerio, F. (2013). Climate change impacts on hydropower management. *Water resources management*, *27*(15), 5143-5156.

Gaudard, L., & Romerio, F. (2014a). Reprint of "The future of hydropower in Europe: Interconnecting climate, markets and policies". *Environmental Science & Policy*, *43*, 5-14.

Gaudard, L., Romerio, F., Dalla Valle, F., Gorret, R., Maran, S., Ravazzani, G., ... & Volonterio, M. (2014b). Climate change impacts on hydropower in the Swiss and Italian Alps. *Science of the Total Environment*, *493*, 1211-1221.

Georgakakos, K. P., & Graham, N. E. (2008). Potential benefits of seasonal inflow prediction uncertainty for reservoir release decisions. Journal of Applied Meteorology and Climatology, 47(5), 1297-1321.

Giorgi, F. (2006). Climate change hot-spots. *Geophysical research letters*, *33*(8).

Giorgi, F., Jones, C., & Asrar, G. R. (2009). Addressing climate information needs at the regional level: the CORDEX framework. *World Meteorological Organization (WMO) Bulletin*, *58*(3), 175.

Giudici, F. (2016). Advancing reservoir operation description in physically based hydrological models.

Giuliani, M., Anghileri, D., Castelletti, A., Vu, P. N., & Soncini-Sessa, R. (2016). Large storage operations under climate change: expanding uncertainties and evolving tradeoffs. *Environmental Research Letters*, *11*(3), 035009.

Gobiet, A., Kotlarski, S., Beniston, M., Heinrich, G., Rajczak, J., & Stoffel, M. (2014). 21st century climate change in the European Alps—a review. *Science of the Total Environment*, *493*, 1138-1151.

Gudmundsson, L., Bremnes, J. B., Haugen, J. E., & Engen-Skaugen, T. (2012). Downscaling RCM precipitation to the station scale using statistical transformations–a comparison of methods. *Hydrology and Earth System Sciences*, *16*(9), 3383-3390.

Haeberli, W., & Beniston, M. (1998). Climate change and its impacts on glaciers and permafrost in the Alps. *Ambio*, 258-265.

Haerter, J. O., Hagemann, S., Moseley, C., & Piani, C. (2011). Climate model bias correction and the role of timescales. *Hydrology and Earth System Sciences*, *15*(3), 1065-1079.

Hanssen-Bauer, I., & Førland, E. (2001). Verification and analysis of a climate simulation of temperature and pressure fields over Norway and Svalbard. *Climate Research*, *16*(3), 225-235.

Hartmann, D. L., Tank, A. M. K., Rusticucci, M., Alexander, L. V., Brönnimann, S., Charabi, Y. A. R., ... & Soden, B. J. (2013). Observations: atmosphere and surface. In *Climate Change 2013 the Physical Science Basis: Working Group I Contribution to the Fifth Assessment Report of the Intergovernmental Panel on Climate Change*. Cambridge University Press.

Hay, L. E., Wilby, R. L., & Leavesley, G. H. (2000). A comparison of delta change and downscaled GCM scenarios for three mountainous basins in the United States. *JAWRA Journal of the American Water Resources Association*, *36*(2), 387-397.

Hijioka, Y., Matsuoka, Y., Nishimoto, H., Masio, T., & Kainuma, M. (2008). Global GHG emission scenarios under GHG concentration stabilization targets. *Journal of Global Environment Engineering*, *13*, 97-108.

Hobbs, B. F., Chao, P. T., & Venkatesh, B. N. (1997). Using decision analysis to include climate change in water resources decision making. *Climatic Change*, *37*(1), 177-202.

Horton, P., Schaefli, B., Mezghani, A., Hingray, B., & Musy, A. (2006). Assessment of climate-change impacts on Alpine discharge regimes with climate model uncertainty. *Hydrological Processes*, *20*(10), 2091-2109.

Huss, M., Jouvet, G., Farinotti, D., & Bauder, A. (2010). Future high-mountain hydrology: a new parameterization of glacier retreat. *Hydrology and Earth System Sciences*, *14*(5), 815.

Huss, M. (2011). Present and future contribution of glacier storage change to runoff from macroscale drainage basins in Europe. *Water Resources Research*, *47*(7).

Kaser, G., Großhauser, M., & Marzeion, B. (2010). Contribution potential of glaciers to water availability in different climate regimes. *Proceedings of the National Academy of Sciences*, *107*(47), 20223-20227.

Katz, R. W., & Brown, B. G. (1992). Extreme events in a changing climate: variability is more important than averages. *Climatic change*, *21*(3), 289-302.

Katz, R. W., & Acero, J. G. (1994). Sensitivity analysis of extreme precipitation events. *International journal of climatology*, *14*(9), 985-999.

Liu, Z., & Todini, E. (2002). Towards a comprehensive physically-based rainfall-runoff model. *Hydrology and Earth System Sciences Discussions*, *6*(5), 859-881.

Liu, Z., & Todini, E. (2005). Assessing the TOPKAPI non-linear reservoir cascade approximation by means of a characteristic lines solution. *Hydrological processes*, *19*(10), 1983-2006.

Maran, S., Volonterio, M., & Gaudard, L. (2014). Climate change impacts on hydropower in an Alpine catchment. *Environmental Science & Policy*, *43*, 15-25.

Marzeion, B., Jarosch, A. H., & Hofer, M. (2012). Past and future sea-level change from the surface mass balance of glaciers. *The Cryosphere*, *6*(6), 1295.

McCarthy, J. J., Canziani, O. K., Leary, N. A., Dokken, D. J., & White, K. S. (2001). Impacts, Adaptation and vulnerability. *Third Assessment Report of the Intergovernmental panel on climate change, working Group*, *2*.

Moss, R., Babiker, W., Brinkman, S., Calvo, E., Carter, T., Edmonds, J., ... & Jones, R. N. (2008). Towards New Scenarios for the Analysis of Emissions: Climate Change, Impacts and Response Strategies. Technical Summary. Intergovernmental Panel on Climate Change, Geneva, 25 pp.

Murphy, J. (1999). An evaluation of statistical and dynamical techniques for downscaling local climate. *Journal of Climate*, *12*(8), 2256-2284.

Nandalal, K. D. W., & Bogardi, J. J. (2007). *Dynamic programming based operation of reservoirs: applicability and limits*. Cambridge university press.

Nieto, S., Dolores Frías, M., & Rodríguez-Puebla, C. (2004). Assessing two different climatic models and the NCEP–NCAR reanalysis data for the description of winter precipitation in the Iberian Peninsula. *International Journal of Climatology*, *24*(3), 361-376.

Olsson, J., Uvo, C. B., & Jinno, K. (2001). Statistical atmospheric downscaling of short-term extreme rainfall by neural networks. *Physics and Chemistry of the Earth, Part B: Hydrology, Oceans and Atmosphere*, *26*(9), 695-700.

Pachauri, R. K., Allen, M. R., Barros, V. R., Broome, J., Cramer, W., Christ, R., ... & Dubash, N. K. (2014). *Climate change 2014: synthesis report. Contribution of Working Groups I, II and III to the fifth assessment report of the Intergovernmental Panel on Climate Change* (p. 151). IPCC.

Parmesan, C., & Yohe, G. (2003). A globally coherent fingerprint of climate change impacts across natural systems. *Nature*, *421*(6918), 37.

Pellicciotti, F., Brock, B., Strasser, U., Burlando, P., Funk, M., & Corripio, J. (2005). An enhanced temperature-index glacier melt model including the shortwave radiation balance: development and testing for Haut Glacier d'Arolla, Switzerland. *Journal of Glaciology*, *51*(175), 573-587.

Piani, C., Haerter, J. O., & Coppola, E. (2010a). Statistical bias correction for daily precipitation in regional climate models over Europe. *Theoretical and Applied Climatology*, *99*(1-2), 187-192.

Piani, C., Weedon, G. P., Best, M., Gomes, S. M., Viterbo, P., Hagemann, S., & Haerter, J. O. (2010b). Statistical bias correction of global simulated daily precipitation and temperature for the application of hydrological models. *Journal of Hydrology*, *395*(3), 199-215.

Pianosi, F., & Soncini-Sessa, R. (2009). Real-time management of a multipurpose water reservoir with a heteroscedastic inflow model. *Water resources research*, *45*(10).

Priestley, C. H. B., & Taylor, R. J. (1972). On the assessment of surface heat flux and evaporation using large-scale parameters. *Monthly weather review*, *100*(2), 81-92.

Riahi, K., Grübler, A., & Nakicenovic, N. (2007). Scenarios of long-term socio-economic and environmental development under climate stabilization. *Technological Forecasting and Social Change*, *74*(7), 887-935.

Riahi, K., Rao, S., Krey, V., Cho, C., Chirkov, V., Fischer, G., ... & Rafaj, P. (2011). RCP 8.5—A scenario of comparatively high greenhouse gas emissions. *Climatic Change*, *109*(1-2), 33.

Rimkus, S. (2013). *Documentation and user guide to the hydrological model TOPKAPI-ETH*.

Schaefli, B., Hingray, B., & Musy, A. (2007). Climate change and hydropower production in the Swiss Alps: quantification of potential impacts and related modelling uncertainties. *Hydrology and Earth System Sciences Discussions*, *11*(3), 1191-1205.

Schaefli, B. (2015). Projecting hydropower production under future climates: a guide for decision-makers and modelers to interpret and design climate change impact assessments. *Wiley Interdisciplinary Reviews: Water*, *2*(4), 271-289.

Schlecht, I. and H. Weigt (2014a). "Linking Europe. The role of the Swiss electricity transmission grid until 2050." In: *Social Science Research Network*.

Schlecht, I. and H. Weigt (2014b). "Swissmod. A model of the Swiss electricity market." In: *Social Science Research Network*.

Sharma, D., Gupta, A. D., & Babel, M. S. (2007). Spatial disaggregation of bias-corrected GCM precipitation for improved hydrologic simulation: Ping River Basin, Thailand. *Hydrology and Earth System Sciences Discussions*, *11*(4), 1373-1390.

Smith, S. J., & Wigley, T. M. L. (2006). Multi-gas forcing stabilization with Minicam. *The Energy Journal*, 373-391.

Soncini-Sessa, R., Castelletti, A., and Weber, E. (2007). *Integrated and Partecipatory Water Resources Management: Theory*, volume 1A.

Thomson, A. M., Calvin, K. V., Smith, S. J., Kyle, G. P., Volke, A., Patel, P., ... & Edmonds, J. A. (2011). RCP4. 5: a pathway for stabilization of radiative forcing by 2100. *Climatic change*, *109*(1-2), 77.

Van Vliet, M. T., Wiberg, D., Leduc, S., & Riahi, K. (2016). Power-generation system vulnerability and adaptation to changes in climate and water resources. *Nature Climate Change*, *6*(4), 375-380.

Van Vuuren, D. P., Weyant, J., & de la Chesnaye, F. (2006). Multi-gas scenarios to stabilize radiative forcing. *Energy Economics*, *28*(1), 102-120.

Van Vuuren, D. P., Den Elzen, M. G., Lucas, P. L., Eickhout, B., Strengers, B. J., Van Ruijven, B., ... & van Houdt, R. (2007a). Stabilizing greenhouse gas concentrations at low levels: an assessment of reduction strategies and costs. *Climatic Change*, *81*(2), 119-159.

Van Vuuren, D. P., Edmonds, J., Kainuma, M., Riahi, K., Thomson, A., Hibbard, K., ... & Masui, T. (2011). The representative concentration pathways: an overview. *Climatic change*, *109*(1-2), 5.

Wilby, R. L., Charles, S. P., Zorita, E., Timbal, B., Whetton, P., & Mearns, L. O. (2004). Guidelines for use of climate scenarios developed from statistical downscaling methods. *Supporting material of the Intergovernmental Panel on Climate Change, available from the DDC of IPCC TGCIA*, *27*.

Wilby, R. L., & Dessai, S. (2010). Robust adaptation to climate change. *Weather*, *65*(7), 180-185.

Wilks, D. S., & Wilby, R. L. (1999). The weather generation game: a review of stochastic weather models. *Progress in physical geography*, *23*(3), 329-357.

Wise, M., Calvin, K., Thomson, A., Clarke, L., Bond-Lamberty, B., Sands, R., ... & Edmonds, J. (2009). Implications of limiting CO2 concentrations for land use and energy. *Science*, *324*(5931), 1183-1186.

Wood, A. W., Leung, L. R., Sridhar, V., & Lettenmaier, D. P. (2004). Hydrologic implications of dynamical and statistical approaches to downscaling climate model outputs. *Climatic change*, *62*(1), 189-216.

Zierl, B., & Bugmann, H. (2005). Global change impacts on hydrological processes in Alpine catchments. *Water Resources Research*, *41*(2).

Zorita, E., & Von Storch, H. (1999). The analog method as a simple statistical downscaling technique: comparison with more complicated methods. *Journal of climate*, *12*(8), 2474-2489.